GEOLOGY AND MINERALIZATION CHARACTERISTICS OF EPITHERMAL GOLD, SUWAN PROSPECT, CHANGWAT PHITSANULOK
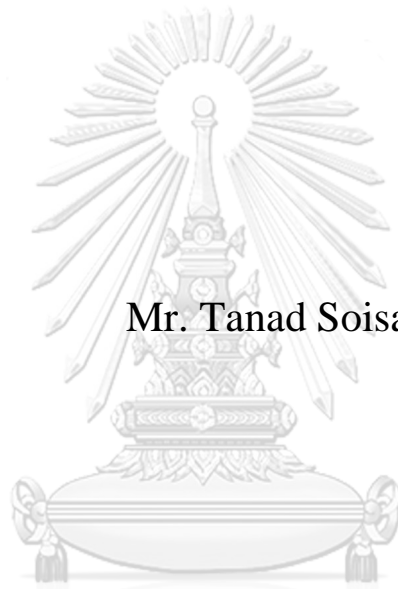
Mr. Tanad Soisa

จุฬาลงกรณ์มหาวิทยาลัย
CHULALONGKORN UNIVERSITY

A Thesis Submitted in Partial Fulfillment of the Requirements
for the Degree of Master of Science in Geology
Department of Geology
FACULTY OF SCIENCE
Chulalongkorn University
Academic Year 2019
Copyright of Chulalongkorn University

ลักษณะพิเศษทางธรณีวิทยาและการเกิดแร่ทองคำอีพิเทอร์มอล
พื้นที่ศักยภาพสุวรรณ จังหวัดพิษณุโลก

นายถนัด สร้อยซา

วิทยานิพนธ์นี้เป็นส่วนหนึ่งของการศึกษาตามหลักสูตรปริญญาวิทยาศาสตรมหาบัณฑิต
สาขาวิชาธรณีวิทยา ภาควิชาธรณีวิทยา
คณะวิทยาศาสตร์ จุฬาลงกรณ์มหาวิทยาลัย
ปีการศึกษา 2562

Thesis Title	GEOLOGY AND MINERALIZATION CHARACTERISTICS OF EPITHERMAL GOLD, SUWAN PROSPECT, CHANGWAT PHITSANULOK
By	Mr. Tanad Soisa
Field of Study	Geology
Thesis Advisor	Abhisit Salam, Ph.D.

Accepted by the FACULTY OF SCIENCE, Chulalongkorn University in Partial Fulfillment of the Requirement for the Master of Science

.... Dean of the FACULTY OF SCIENCE
(Professor POLKIT SANGVANICH, Ph.D.)

THESIS COMMITTEE

.... Chairman
(Assistant Professor VICHAI CHUTAKOSITKANON, Ph.D.)

.... Thesis Advisor
(Abhisit Salam, Ph.D.)

.... Examiner
(PITSANUPONG KANJANAPAYONT, Dr.rer.nat.)

.... External Examiner
(Takayuki Manaka, Ph.D.)

จุฬาลงกรณ์มหาวิทยาลัย
CHULALONGKORN UNIVERSITY

ถนัด สร้อยซา : ลักษณะพิเศษทางธรณีวิทยาและการเกิดแร่ทองคำอีพิเทอร์มอล พื้นที่ศักยภาพสุวรรณ จังหวัด
พิษณุโลก. (GEOLOGY AND MINERALIZATION CHARACTERISTICS
OF EPITHERMAL GOLD, SUWAN PROSPECT,
CHANGWAT PHITSANULOK) อ.ที่ปรึกษาหลัก : ดร.อภิสิทธิ์ ซาลำ

พื้นที่แหล่งสำรวจแร่ทองคำสุวรรณตั้งอยู่ทางด้านทิศตะวันตกเฉียงเหนือแหล่งแร่ทองคำชาตรี ประมาณ 6 กิโลเมตร ใน
ขอบเขตจังหวัดพิษณุโลก บริเวณภาคกลางของประเทศไทย ลักษณะการเกิดแหล่งแร่ทองคำในพื้นที่สำรวจสุวรรณ พบว่าเป็นแบบสายแร่
และสายแร่ร่างแหปรากฏในหินภูเขาไฟและหินตะกอนภูเขาไฟ ซึ่งมีอายุตอนปลายยุคเพอร์เมียนถึงตอนต้นยุคไทรแอสซิก โดยหินมีลักษณะ
เช่นเดียวกันกับหินภูเขาไฟของแหล่งแร่ทองคำชาตรี โดยสามารถอธิบายรูปแบบของชนิดการเกิดแหล่งแร่ในพื้นที่ศึกษาดังกล่าวเป็นแร่
ทองคำ-เงิน แบบอีพิเทอร์มอลชนิดมีแร่ซัลไฟด์น้อย (gold-silver epithermal low-sulfidation) ลักษณะของชนิดหินที่
เป็นแหล่งสะสมตัวของแร่ในพื้นที่ศึกษาได้แก่ หน่วยหินภูเขาไฟสีจาง (felsic volcanic rock) หน่วยหินตะกอนภูเขาไฟ
(volcanogenic sedimentary rock) และหน่วยหินแอนดีไซต์เนื้อดอก (porphyritic andesite) โดยหน่วยหินภูเขา
ไฟสีจาง ประกอบด้วย หินกรวดเหลี่ยมภูเขาไฟชนิดแร่ควอรตซ์ (quartz-rich fiamme breccia) หินกรวดเหลี่ยมภูเขาไฟชนิด
ตะกอนเศษหิน (lithic-rich fiamme breccia) และหินกรวดเหลี่ยมหินไรโอไลต์แร่ดอกเฟลสปาร์ (feldspar-phyric
rhyolite breccia) หน่วยหินตะกอนภูเขาไฟ (volcanogenic sedimentary rock) ประกอบด้วย หินทราย หินทราย
แป้ง หินโคลน หินกรวดเหลี่ยมเศษตะกอนหลายชนิด และหน่วยหินแอนดีไซต์เนื้อดอก ประกอบด้วย หินแอนดีไซต์แร่เฟลสปาร์เนื้อดอก
หินแอนดีไซต์แร่เฟลสปาร์-ฮอร์นเบลนด์เนื้อดอก หินกรวดเหลี่ยมแอนดีไซต์ ลักษณะการเกิดแหล่งแร่ในพื้นที่สุวรรณประกอบด้วย
3 กระบวนการเกิดแหล่งแร่ ได้แก่ ช่วงก่อนการเกิดแร่ (post-ore stage) ประกอบด้วยสายแร่ ควอตซ์ ไพไรต์ ช่วงการเกิดแร่
(main-ore stage) ประกอบด้วยสายแร่ ควอตซ์ คาร์บอเนต ซัลไฟด์ อิเล็กตรัม และ ช่วงหลังการเกิดแร่ (post-ore stage)
ประกอบด้วยสายแร่ ควอตซ์ คาร์บอเนต ลักษณะของกระบวนการเกิดแหล่งแร่ที่สำคัญคือช่วงการเกิดแร่ พบแร่ประกอบหลักได้แก่ ไพไรต์
สฟาเลอไรต์ คาลโคไพไรต์ กาลีนา ซึ่งแร่ประกอบหลักพวกซัลไฟด์ดังกล่าวนี้ มีความสัมพันธ์กับแร่ควอตซ์ แคลไซต์ ลักษณะของแร่
ทองคำที่พบส่วนใหญ่เกิดร่วมอยู่ในแร่ไพไรต์ ผลการศึกษาการแปรเปลี่ยนสภาพด้วยศิลาวรรณาและเครื่องมือวิเคราะห์ทางธรณีเคมีของ
กระบวนการแปรเปลี่ยนสภาพแร่ด้วยสายแร่น้ำร้อน (hydrothermal alteration) พบลักษณะขอบเขตการแปรเปลี่ยนสภาพจาก
บริเวณขอบเขตติดสายแร่น้ำร้อนตลอดจนระยะห่างจากสายแร่น้ำร้อน ได้แก่ การแปรเปลี่ยนสภาพแบบซิลิสิก (silicic alteration)
ประกอบด้วยแร่ ควอตซ์ อดูลาเรีย การแปรเปลี่ยนสภาพแบบอาร์จิลลิก (argillic alteration) ประกอบด้วยแร่ อดูลาเรีย ควอตซ์
อิลไลต์ สเมคไทต์ คาโอลิไนต์ การแปรเปลี่ยนสภาพแบบพรอไพลิติก (propylitic alteration) ประกอบด้วย คลอไรต์ แคลไซต์
และ การแปรเปลี่ยนสภาพแบบชนิดแร่ดินเหนียว (clay minerals alteration) ประกอบด้วยแร่ อิลไลต์ สเมคไทต์ คลอไรต์ คา
โอลิไนต์ จากศึกษาลักษณะทางธรณีวิทยา รูปแบบสายแร่กระบวนการเกิดแร่ รวมถึงกระบวนการแปรเปลี่ยนสภาพแร่ ซึ่งสามารถเทียบเคียง
ลักษณะการเกิดแหล่งแร่พื้นที่ศึกษาสุวรรณพบว่ามีลักษณะรูปแบบการเกิดแหล่งแร่คล้ายกับแหล่งแร่ทองคำชาตรี

สาขาวิชา   ธรณีวิทยา   ลายมือชื่อนิสิต ....

ปีการศึกษา   2562   ลายมือชื่อ อ.ที่ปรึกษาหลัก ....

6072053823 : MAJOR GEOLOGY
KEYWORD: Suwan Prospect epithermal gold-silver volcanic unit
        Tanad Soisa : GEOLOGY AND MINERALIZATION CHARACTERISTICS OF EPITHERMAL   GOLD,   SUWAN PROSPECT, CHANGWAT PHITSANULOK. Advisor: Abhisit Salam, Ph.D.

      The Suwan prospect is located about 6 km northwest of the Chatree gold mine in Phitsanulok province, central Thailand. Gold-silver mineralization occurs as veins and stockworks hosted in volcaniclastic and volcanogenic-sedimentary rocks of Late Permian-Early Triassic age which is classified as a low sulfidation epithermal deposit base on mineralization texture, alteration pattern and sulfide mineral assemblages. From top to bottom, the hosted volcanic succession can be divided into 3 units, namely 1) Felsic volcanic unit (Unit 1), 2) Volcanogenic-sedimentary unit (Unit 2), and 3) Porphyritic andesite unit (Unit 3). Unit 1 consists predominantly of quartz-rich fiamme breccia, lithic-rich fiamme breccia and feldspar-phyric rhyolite breccia. The volcanogenic-sedimentary unit (Unit 2) consists of fine to coarse-grained sandstone, sandy-matrix polymictic breccia, polymictic intermediate-felsic breccia, mudstone and limestone lenses. Unit 3 comprises plagioclase-phyric andesite, plagioclase-hornblende-phyric andesite and monomictic andesitic breccia. At least 3 stages of mineralization have been identified namely, 1) pre-gold stage; quartz-pyrite vein (stage 1), 2) main gold stage; quartz-carbonate-sulfides-electrum vein (stage 2), and 3) post-gold stage; quartz-carbonate vein (stage 3). In the main gold stage (stage 2), pyrite is a major sulfide mineral with minor amount of sphalerite, chalcopyrite and galena. These sulfide minerals are closely associated with quartz, calcite and major gangue minerals of stage 2. Gold mainly occurs as inclusions in pyrite and EPMA analysis confirms that it forms as electrum. On the basis of petrographic observation and X-Ray Diffraction Analyzes (XRD), the hydrothermal alteration at the Suwan prospect can be divided into four zones. From proximal to distal to the ore zone, they are 1) Silicic zone (quartz-adularia), 2) Argillic zone (adularia-quartz-illite-smectite-kaolinite), 3) Propylitic zone (chlorite-calcite) and 4) Clay minerals (illite-smectite-chlorite-kaolinite). Based on geological information such as mineralogy, vein textures, and hydrothermal alteration, the Suwan prospect could be classified as low sulfidation epithermal gold-silver deposit similar to the well known Chatree deposit.

Field of Study:	Geology	Student's Signature	....
Academic Year:	2019	Advisor's Signature	....

ACKNOWLEDGEMENTS

TABLE OF CONTENTS

Page

LIST OF TABLE

LIST OF FIGURE

CHAPTER 1

INTRODUCTION

1.1 Background

Thailand has a long history of gold exploration and production. According to Craw and Khin Zaw (2011) , gold occurrences, prospects and deposits distribute from the north to the south of the country. In addition, several gold mining concessions reported before 1981 including Toh Moh in the south and French mine in southeastern part are among important historic gold mines in the country. Recently, the largest modern gold mine has been operated by Akara Resources Public Company since 2001 located in central Thailand. Another gold mine is Phu Thap Fah gold skarn deposit located in Loei province in northeastern Thailand. In Thailand, majority of mineral deposits are confined to Loei Fold Belt (LFB), where Phu Thap Fah gold skarn and Chatree gold-silver epithermal style are located. Other small deposit and occurrences include, Khao Phanom Pha gold skarn and Khao Lek iron-copper skarn and Khao Thap Kwai iron skarn. In Sukhothai Fold Belt (SFB), only gold occurrences have been reported and gold is commonly associated with antimony and fluorite (e.g. Bo Thong prospect in southeastern Thailand; Paipana, 2014).

Precious metals (e.g. gold and silver), iron and copper make up a significant amount of metalliferous minerals found in Thailand. Although gold, silver, iron and copper productions have played a significant role in the mining industry, very few mines remain in production. The largest gold deposit in Thailand is Chatree gold-silver mine in Phichit-Phetchabun provincial bordering area which is classified as low sulfidation epithermal gold-silver deposits. Some gold prospects around Chatree deposit have been preliminarily proved to have high potential to contain economic resources. For Chatree deposit, several studies have been undertaken in which Cumming (2004) focused on volcanic stratigraphy and petrochemistry. Salam (2013) emphasized on several fields including volcanic stratigraphy and facies architecture, and geochronology and petrochemistry. Furthermore, Salam (2013) also studied in fields such as mineralization, and hydrothermal alterations including stable and

radiogenic isotopes. Other preliminary studies are geotectonic and geochronology of volcanic-plutonic rocks in Loei-Phetchabun Fold Belt (Khositanont et al., 2013), petrochemical characteristic of igneous rocks in Phetchabun area (Kamvong et al., 2006) and relationship between Cu-Mo mineralization and epithermal Au-Ag in Chatree deposit (Tangwattananukul & Ishiyama, 2017). However, no study has been undertaken at Suwan prospect prior to this study. This study will further understand of a similar style of deposit which is hosted in volcanic rocks but may have some distinctive characteristics.

1.2 Location

The Suwan Prospect is located about 8 kilometers, northwest of Chatree gold-silver deposit and approximately 60 kilometers southwest of Phitsanulok Province or about 320 kilometers north of Bangkok (Fig. 1.1). It is located on the boundaries between Phitsanulok, Phichit, and Phetchabun provinces. The area is generally flat area mostly used for agricultural and farmland (Fig.1.2).

1.3 Objective

The main objectives for this study are as follows:

- To determine the relationship between geological characteristic and mineralization processes.
- To classify chemical composition of mineral occurrences and modeling of mineral deposits.

1.4 Methodology

The writer of this content undertook extensive research to cover the objectives of this thesis. The methodology of study is divided into 3 parts comprising field investigation, laboratory study and data analysis. The summary of all methodologies are the following paragraphs.
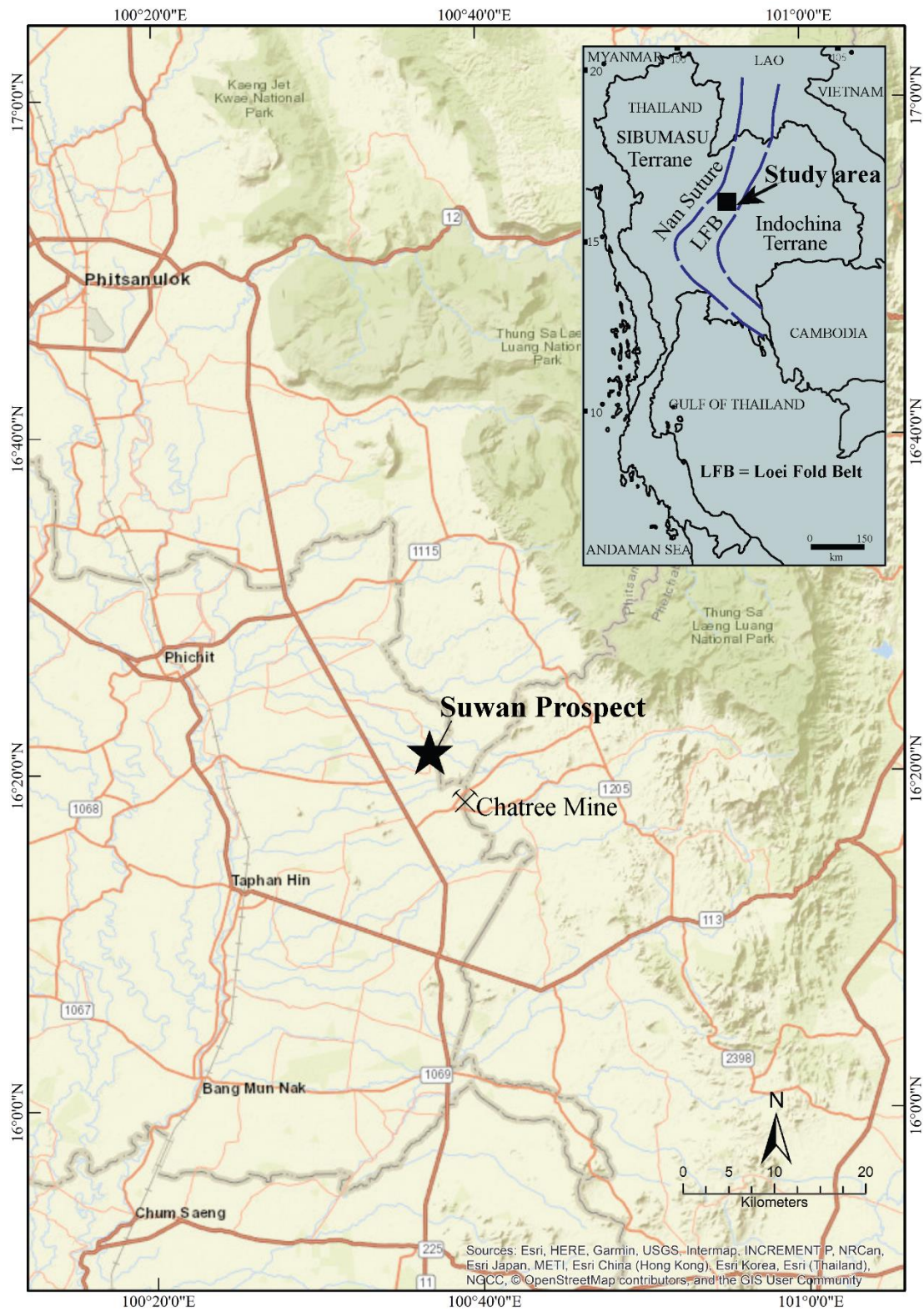
Fig. 1.1 Map showing the location of the Suwan Prospect and Chatree mine.

Fig. 1.2 Topographic map of Suwan Prospect, Chatree Mine and Khao Panompha deposit (modified from google satellite, 2019).

1.4.1 Field investigation

Field works were conducted in two seasons, first field work undertaken in October (2017) and second one is January (2018). This study was mainly based on diamond drill cores samples from the selected cross section total of nine drill holes (DDH4065, DDH4066, DDH4067, DDH4069, DDH4080, DDH4102, DDH4119, DDH4138 and DDH4139). Diamond drill cores used in this study were provided by the Akara Resources Public Company. Logging of drill cores has focused on host volcaniclastics sequence in term of lithology, volcanic facies, veins paragenesis, mineralization, and alteration. Representative samples were collected for further laboratory works particularly on volcanic petrographic study, ore petrography, and advanced geochemistry analyses including whole rock geochemistry (e.g. major oxides, trace elements and rare earth elements), and electron probe micro-analyzer (EPMA).

1.4.2 Laboratory study

In this study, six different laboratory methods have been carried out including petrographic study, ore petrographic investigation, X-ray diffraction (XRD), K-

feldspar staining, electron probe microanalysis (EPMA), and inductive coupled plasma mass spectrometry (ICP-MS).

Petrographic study

Prior to petrographic study, all collected diamond drill cores samples were detailed examined and described. All together (89 samples) have been prepared for petrographic study in which (36 samples) thin sections for confirmation of rocks types and facies determination and another 25 thin sections were prepared for hydrothermal alteration study. Twenty-four ore samples were prepared for polish mounts and polish thin sections for ore petrographic investigation.

Petrographic and ore petrographic studies were conducted using transmitted light and reflected light microscope at the Department of Geology, Faculty of Science, Chulalongkorn University. Study has been focused on identifying silicate and ore mineral assemblages and textures, and their relationships. In addition, this study was also emphasized on hydrothermally altered mineral assemblage for classifying and defining styles of hydrothermal alteration prior to X-Ray Diffraction analyses. For an unidentified sulfide mineral, EPMA were utilized to confirm its composition and mineral species. Ore petrographic study was also used to determine mineral assemblage in defining veins paragenesis (mineralization stages).

Electron Probe Microanalysis (EPMA)

In this study, the electron probe microanalysis (EPMA) was carried out at Department of Geology, Faculty of Science, Chulalongkorn University. This analysis was used to determine the composition of some petrographic identified minerals including unidentified minerals. The instrument used for the microanalysis is a JXA 8100, working at XRF-WDS. These samples for identification were supported by polished and polished-thin sections. The elements selected for analyzing are S, As, Fe, Sb, Cd, Pb, Ni, Cu, Mo, Mn, V and Zn.

X-Ray Diffraction (XRD)

Following petrographic study, representative hydrothermal altered wall rock samples were crushed bowdlerized for further confirmation of alteration mineralogy

using X-Ray Diffraction (XRD) instrument stored at the Department of Geology, Faculty of Science, Chulalongkorn University. Prior to analysis, samples were treated followed the procedure and process described by U. S. Geological Survey (USGS). Samples were prepared as air-dried, glycolate oriented and heated. The X-ray diffractometer is model D8 Advance, Bruker AXS, 40 kV and 30 mA. The conditions for determination are 2 thetas 5-50 degree with increment 0.02 degree with a scan speed of 2 degrees per minute. Programs used Diffract plus#1 software of the Bruker Analytical X-ray System and interpreted by the Eva program.

The alteration assemblage of clay minerals in epithermal deposits is important, with several zones of activity from hydrothermal veins. Clay mineral studies are systematic in zones that have been checked to analyze any activity and mineral assemblages. The clay minerals analyzed by X-ray diffraction (XRD) which have an oriented technique to identify clay types in petrographic study. This study separated clay minerals by oriented technique, following the methodology documented by Poppe et al., (2002).

XRD analysis was used to determine the peak of mineral assemblages in separated samples within the oriented technique. For each sample analyzed, the similarly 2Ө diffractograms peak of materials was used to compare the peak by the Eva Program for classification and interpretation of materials. For example, in adularia peaks which is present, the 2Ө peak ~13.5° and overlap of plagioclase adularia at ~23.5°.

The rock samples for XRD analysis were analyzed for powder specimens from drill core slabs using a rock grinding machine. The use of clay minerals is applied to reduce quartz amounts in the powder samples, which can interfere in the detection of other minerals. Sodium hexametaphosphate $((NaPO_3)_6)$ is used with each powder sample by mixing with distilled water in a beaker and leaving it for 24 hours. Subsequently, the liquid in each beaker was stirred gently and dropped on a glass plate until it dried out. These dry powder samples were analyzed for X-ray diffraction patterns in the laboratory at Chulalongkorn University. The diffraction started from 5° to 50° with an increment of 0.02° with the scan speed at 1 sec/step. These samples were then added to ethylene glycol for 24 hours then analyzed along with the first

configurations. They were then heated to 550 °C for 24 hours then for detection clay minerals.

K-feldspar staining

Hydrothermal alteration of K-feldspar is an important component in the alteration assemblage at Suwan Prospect. But, the characteristic texture of alterations was difficult to identify for mineral compositions. Staining of rock samples was done to identify K-feldspar and determine the relationships between alteration and hydrothermal vein conditions. The staining method was described by Norman (1974) as a result of stained estimate K-feldspar volume percent in a photograph of each sample.

The studies of K-feldspar are important in determining how hydrothermal potassium feldspar changes and mineralization assemblage. This method has identified hydrothermal potassium as an adularia that can be used to detect the amount of mineralization. However, identification of potassium feldspar is difficult during core logging which uses staining to check the textural relationships in vein systems. The staining is undertaken from the drill core sample, following the methodology presented by (Norman, 1974). These stained 13 samples of drill slabs to interpret the alteration styles within the study area. Finally, the staining was conducted to estimate K-feldspar volume percentages in photographs of each sample, using image analysis software ENVI 5.3. The color of K-feldspar is checked for quantities of secondary K-feldspar levels to classify percentages of the colored images.

The K-feldspar staining technique was applied to estimate the percentage of mineral composition in photographs of each sample using ENVI 5.3 and ArcGIS software. During this step, photographs of stained rock slap surfaces were firstly taken by digital camera with the highest pixel resolution (23.4 MP), and then saved to JPG image format with 100% quality. Thereafter, these photographs were imported into ENVI 5.3 software, then, Region of Interest (ROI) or training areas of six categories of minerals included K-feldspar, albite, plagioclase, calcite, quartz and mafic minerals and opaque minerals, were selected to represent of each mineral. Next step, based on ROI or selected training areas, supervised classification tool of ENVI 5.3 software was applied to classify the zones of each mineral. Next step, six mineral zones from

supervised classification were converted to shape file for ArcGIS software; each color represents a different mineral. Finally, the quantification of each mineral percentage is calculated based on an area of each mineral and total area of six mineral zones and displays in percentage values.

X-ray fluorescence (XRF)

Whole-rock oxides and trace element analysis of all samples were carried out using XRF at the Department of Mineral Resources (DMR) and the Australian Laboratory Service (ALS). This method provided major oxide quantities useful for exploration for analysis that included SiO_2, TiO_2, Al_2O_3, Fe_2O_3, MnO, MgO, CaO, Na_2O, K_2O, and P_2O_3. These results were added to a classification diagram using GCDkit software.

Inductively Coupled Plasma Mass Spectrometry (ICP-MS)

Whole-rock geochemical analyses were done for the total seven sample, including porphyritic andesite, monomictic andesite breccia and rhyolitic rock at various depths. This method was undertaken for major (Si, Ti, Al, Fe, Mn, Mg, Ca, Na, K, P and S) and Trace (Rb, Sr, Cr, Cu, Ba, Ba, Bi, Sn, Zr, Mo, Nb, V, Zn, Ni, Pb, Th, Sc, U and Y) elements analyzing by ICP-MS at Australian Laboratory Service (ALS). This technique additionally analyzed for rare earth elements (REE: La, Ce, Pr, Nd, Sm, Eu, Gd, Tb, Dy, Ho, Er, Tm, Yb and Lu). The samples for this analysis was carefully selected from the least altered sample from drill core samples. The concentration of elements were analyzed on a GCDkit software (Janousek et. al., 2006) to interpret whole-rock geochemical data for contemporary scientific term.

1.5 Thesis structure

As an overview, the thesis is divided into the following Chapters:

Chapter I: documents the aim and objective of the research, the location, methodology, and literature review of the study area.

Chapter II: includes the regional tectonics, regional geology and regional structure relating to mineralization in this project.

Chapter III: focuses on the detail of deposits geology at Suwan Prospect, including descriptions of the lithology, stratigraphic unit, and geochemistry.

Chapter IV: documents the detailed paragenesis, mineralization stages, hydrothermal vein, geochemical signature including ores, gangues mineral assemblage, geochemical characteristics, including alteration study, alteration styles, and the epithermal system at Suwan Prospect.

Chapter V: summarizes the results of this research and the implication for the characterization of epithermal deposits at Suwan Prospect.

CHAPTER 2
REGIONAL GEOLOGY

2.1 Introduction

   This chapter reviews tectonic setting, volcanic rocks and regional geology. In addition, reviewing also includes major ores deposits in LFB particularly epithermal, porphyry and skarn deposits. There are significant constraints on the metallogenic and tectonic evolution of Southeast Asia's mainland.

2.2 Tectonic setting

   Thailand and its neighboring countries are located in two major tectonic terranes, Shan-Thai and Indochina (Bunopas, 1981). The Shan-Thai terrane covers an area of northern Thailand and eastern Myanmar extending to southern Thailand, Peninsular Malaysia to Sumatra and it is later also known as SIBUMASU particularly when included peninsular Malaysia and Sumatra (Metcalfe, 1984). In between the two terranes lies the Sukhothai Arc in which formerly known as Sukhothai Fold Belt-SFB (Bunopas, 1981)on the eastern edge of Shan-Thai terrane. The Loei Fold Belt-LFB which is on the western edge of Indochina terrane, a volcano-plutonic zone extends from central Laos through Loei, Phetchabun and Sra Kaeo in southeast Thailand and to the west of Cambodia (Fig. 2.1). Barr and Macdonald (1991) have proposed the Inthanon zone in between Shan-Thai and Sukhothai Arc (Fig. 2.1). They interpreted as representing Paleo-Tethyan oceanic rocks, pre-Devonian basement rocks, Late Triassic, Early Jurassic S-type granitoids, and gneissic rocks. Several workers also agree and further described the characteristics of Paleo-Tethyan rocks consisting of pelagic Carboniferous-Permian seamount-type carbonate rocks associated with basaltic rocks, Middle Devonian-Meddle Triassic radiolarian chert, and mélange-type rocks (Caridroit et al., 1992; Ueno, 1999; Ueno et al., 2010). Inthanon zone (Hara et al., 2013). The Shan-Thai and Indochina terranes are believed to have rifted from north of Australia (Gondwana), during the Carboniferous period, and collided together in the late Permian or early Triassic (Bunopas, 1994).

Jungyusuk and Khositanont (1992) proposed 5 volcanic provinces (Fig. 2.1) namely, 1) Loei volcanic province, 2) Prae-Lampang volcanic provinces, 3) Loei-Phetchabun-Ko Chang volcanic provinces, 4) Chiangkhong-Pong-Lampang-Tak volcanic provinces and 5) Lam Narai volcanic province. Additional volcanic belts were proposed by Panjasawatwong et al. (2006) namely, 1) Chiang Rai-Chiang Mai, 2) Chiangkhong-Lampang-Tak volcanic belt and 3) Loei-Phetchabun-Nakhon Nayok volcanic belt.

2.3 Mineral deposits

The LFB is the most important for metalliferous mineral deposits such as base (e.g., copper and iron) and precious (e.g., gold and silver) metals (Fig. 2.2) which are related to magmatic rocks both volcanic and plutonic rocks (Khin Zaw et al., 2009) especially the magmatic rocks of Late Permian to Late Triassic age (Khin Zaw et al., 2007). After the discovery of Chatree epithermal gold-silver deposit in central Thailand, the LFB became one the attractive targets for mineral exploration in mainland SE Asia (Table 2.1). Some deposits located in the LFB are Phu Thap Fah (Au skarn in Loei province), Phu Lon (Cu-Au skarn in Nong Khai province), Khao Phanom Pha (Au skarn in Phichit province) (Fig. 2.2). High potential deposits include PUT1 and PUT2 in Loei province. Phu Kham Cu-Au skarn and Ban Houayxai Au-Ag epithermal in Laos are still debatable whether they in LFB or Throung Son Fold Belt (Fig. 2.2). Crow & Khin Zaw (2011) summarized importance distribution of mineral deposits in LFB (Table 2.1; Fig. 2.2) and also provided their style of mineralization.

It has been found that gold-silver, copper, and iron were related to volcanic and plutonic rocks. Gold-copper deposits occur in several localities along Loei-Phetchabun-Ko Chang volcanic belt which consists of skarn and epithermal deposit types. The well-known deposits were found at Phu Kham, Phu Lon, Phu Thap Fah, Phu Thep, Khao Phanom Pha, Khao Lek, Chatree and French Mine areas. In summary, gold-silver found as porphyry, skarn and epithermal deposits are commonly associated with intrusive and volcanic rocks and are generally confined to structural control and tectonic setting. However, there are two type mineralization zones close to the study area. The one " Chatree deposit" is epithermal gold-silver (quartz-carbonate-adularia-sulfide veins) while the other "Khao Phanom Pha" gold bearing quartz-

muscovite-chlorite-sulfide vein (Salam et al., 2014). These hosted rocks are volcanic, volcaniclastic and volcanic sedimentary rocks (Salam, 2013).
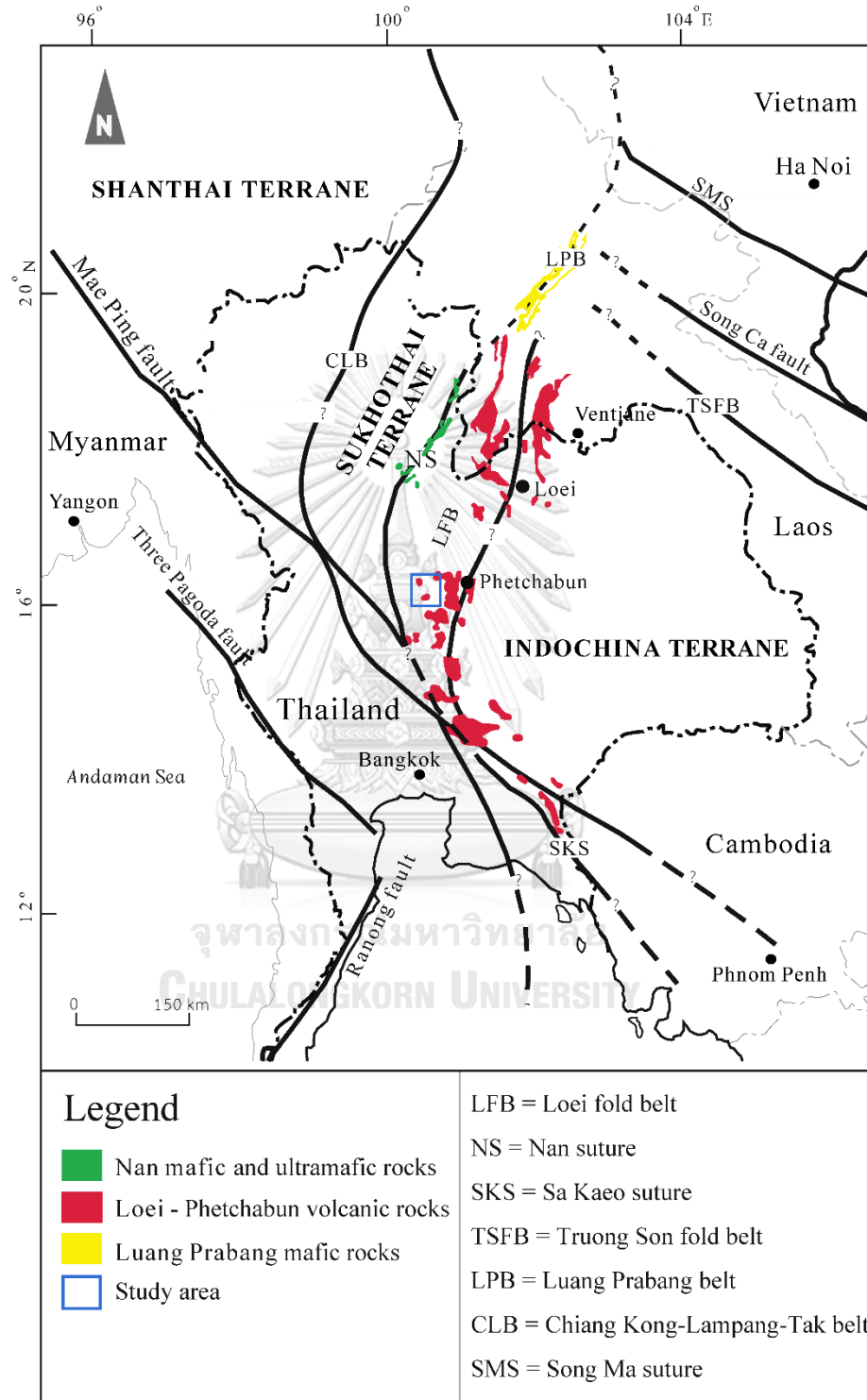
Fig. 2.1 Tectonic plate and major suture of Thailand (Bunopas & Vella, 1983; Jungyusuk & Khositanont, 1992; Charusiri et al., 2002; Panjasawatwong et al., 2006).
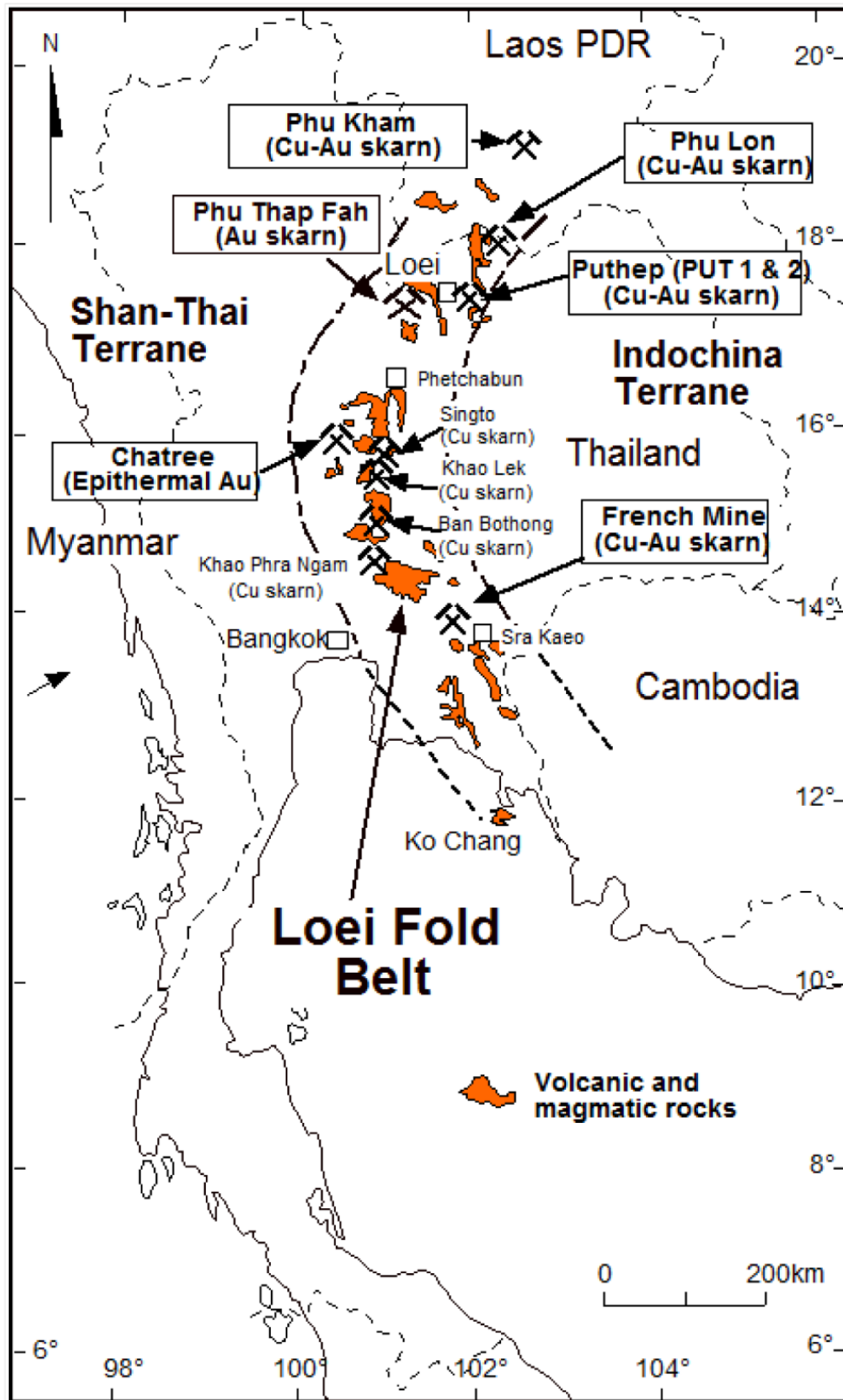
Fig. 2.2 Mineral deposits location along the Loei-Phetchabun-Ko Chang volcanic Belt, Thailand (Khin Zaw et al., 2009).

Table 2.1 Major mineral deposits occurring along the Loei Fold Belt in Thailand: After Khin Zaw et al., (2007, 2009, 2014)

Deposits (coordinate)	Host rock (age)	Intrusion (age)	Ore mineralogy	Alteration type	Resources /reserve	Reference
Skarn						
Phu Lon (18° 12'N, 102° 08'E)	Volcaniclastic rock and limestone (Early Carboniferous)	Diorite and quartz monzonite (Early to Middle Triassic	Chalcopyrite, pyrite, magnetite, gold	Potassic, phyllic, propylitic, skarn	5.4 Mt@ 2.4% Cu, 0.64 g/t Au (resource)	Sittithaworn et al., (1993), Kamvong et al., (2005), Khin zaw et al., (2007)
PUT-1 (Phu Thep) (17° 28'N, 101° 52'E)	Siliciclastic and limestone (Carboniferous)	Diorite and quartz monzonite porphyry (Early to Middle Triassic)	Chalcopyrite, pyrite, magnetite	Potassic, phyllic, propylitic, skarn	160 Mt@ 0.53% Cu, 0.09 g/t Au (resource)	Kamvong et al., (2006)
PUT-2 (17°26'N, 101° 46'E)	Siliciclastic and limestone (Carboniferous)	Diorite and quartz monzonite porphyry (Early to Middle Triassic)	Chalcopyrite, pyrite, magnetite	Potassic, phyllic, propylitic, skarn	36.4 Mt@ 0.43% Cu (resource)	Kamvong et al., (2006), Khositanont (2008)
Phu Thap Pah (17° 56'N, 101° 40'E)	Siliciclastic and limestone (Permian)	Granodiorite (Early Triassic)	Chalcopyrite, pyrrhotite, native gold, bismuth, telluride	Skarn (prograde and retrograde)	0.75 Mt@ 7.97g/t Au (resource)	Khin Zaw et al., (2007)
Khao Phanom Pha (16° 18'N, 100° 33'E)	Volcaniclastic rocks (Late Permian)	No known intrusion	Pyrrhotite, pyrite, chalcopyrite, galena, native gold, electrum	Chlorite, muscovite	No data	Khositanont (2008), Crossing (2004)
French Mine (13° 57'N, 101° 49'E)	Volcaniclastic rocks and limestone (Late Permian)	Granodiorite (Early Triassic)	Chalcopyrite, pyrite, molybdenite	Skarn (prograde and retrograde)	No data	Muller (1999)
Khao Lek (15° 56'N, 100° 46'E)	Volcaniclastic rocks and limestone	Biotite-hornblende granodiorite (Late Permian to Early Triassic)	Magnetite, pyrite, chalcopyrite, gold	Skarn (prograde and retrograde)	No data	Khin Zaw et al., (2007), Khositanont (2008)
Epithermal						
Chatree (16° 17'N, 100° 39'E)	Volcaniclastic and epiclastic rocks (Late Permian)	Hornblende andesite intrusion (Middle Triassic)	Pyrite, sphalerite, galena, chalcopyrite, electrum, argentite	Silicic, argillic, propylitic	81 Mt@ 1.2 g/t Au, 10 g/t Ag (resource)	Salam (2007, 2008), Diemer and Diemer (1999)
Wang Yai (16° 22'N, 100° 38'E)	Volcaniclastic (Late Permian) and rhyolite (Late Carboniferous)	Diorite (Late Triassic)	Electrum, argentite, chalcopyrite, galena, sphalerite	Silicic, phyllic, propylitic	No data	De Little (2005)

Ban Houayxai deposit

Ban Houayxai Au-Ag deposit located in the southern part of the Phu Bia Contract Area and at northern of Lao PDR within the Truong Son Fold Belt (TSFB), northern Lao PDR. The deposit has a mineral resource 76 Mt at 0.82 g/t Au and 7.0 g/t Ag. It is the third largest gold deposit in the Indochina region. This deposit is hosted in early Permian volcano-sedimentary unit (Manaka et al., 2014) which is a part of a Late Carboniferous-Early Permian (310-270 Ma). The Au-Ag mineralization at Ban Houayxai was dated by K-Ar and Ar-Ar technique of adularias from the feldspar-phyric andesite yielded early Permian age. (Manaka et al., 2014). The mineralization at Ban Houayxai occurs as veins, veinlets and minor breccias. The main gold mineralization is characterized as quartz-carbonate-sulfides-electrum. Most sulfides are pyrite, sphalerite, galena and minor chalcopyrite and stephanite. Quartz and carbonate are major gangue mineral with minor of sericite and chlorite. Gold mainly form as electrum in association with sulfide minerals.

Phu Kham deposit

The Phu Kham is copper-gold skarns deposit is located at TSFB and hosted in late Carboniferous to early Permian volcaniclastic rock and siliclastic rocks, calcareous shale and carbonate rocks which related to the oxidized Triassic I-type intrusions (Backhouse, 2004; Tate, 2005; Khin Zaw, Meffre, et al., 2009; Khin Zaw et al., 2011). These alteration assemblages are composed of; (1) biotite + magnetite ± K-feldspar; (2) sericite-quartz-pyrite ± epidote; (3) epidote-calcite-quartz + chlorite; and (4) muscovite-pyrophyllite-quartz. The skarn alteration related to garnet (proximal zone) and garnet-epidote (distal zone) of mineral assemblages. The Phu Kham copper-gold deposit has resources 192Mt at 0.62 % Cu, 0.24 g/t Au (Tate, 2005; Khin Zaw et al., 2009) .

Phu Lon deposit

Phu Lon is identified as copper-gold skarn deposit hosted in volcanogenic sedimentary units and limestone in the Devonian (Kamvong et al., 2006). It is located at the northernmost portion of the LFB within the Loei volcanic-plutonic belt (Kamvong et al., 2006) of Nong Khai province. This deposit has resource of 5.4 Mt at

2.4 % Cu and 0.64 g/t Au. The mineralization is occurred as the calc-silicate mineral assemblages: (1) Pre-ore stage; garnet + tremolite + calcite + quartz ± vesuvianite ± magnetite ± sulfides; (2) Ore-skarn stage; garnet + clinopyroxene + magnetite, and epidote + actinolite + chalcopyrite + pyrite ± calcite ± quartz ± tremolite; and (3) Post-ore stage; calcite + quartz + chlorite + sericite ± epidote ± actinolite (Kamvong et al., 2006).

Phu Thap Fah deposit

Phu Thap Fah is gold skarn deposit that is hosted in the Permian sedimentary sequence consisting of crystalline limestone and siltstone. The mineralization is intruded by Triassic granodiorite and microdiorite dikes (Khin Zaw et al., 2007). This deposit constitutes mineral resource (measured and indicated) 407,000 tonnes at 3.54 g/t Au (Khin Zaw et al., 2011). The prograde skarn is characterized by the present of andraditic garnet-cliopyroxene skarn, whereas retrograde skarn is characterized by amphiboles, epidote, chlorite, carbonate and quartz assemblage. Gold occurs as electrum, and gold-bismuth-telluride. Most of gold is confined to the massive pyrrhotite-pyrite-chalcopyrite in the retrograde zone (Khin Zaw et al., 2011).

Phu Thep deposit

Phu Thep prospect (PUT1 and PUT2) is located at central of Loei province within LFB. Both areas are identified as porphyry-related Fe-Cu-Au skarn deposits (Khin Zaw et al., 2011). These prospects occur as fractures filling or veins which present on the centered of the two dioritic and granodioritic intrusions. Phu Thep deposits are hosted in Carboniferous sedimentary rocks (Wang Saphung Formation) including siltstone, limestone and sandstone. According to Khin Zaw et al. (2011), the PUT1 is known as Phu Hin Lek Fia which has resource of 183 Mt at 0.5% Cu and 0.13 g/t Au. LA ICP-MS U-Pb zircon age dating of the intrusive rock (diorite/monzodiorite) was dated to have an age of 242.4 ± 1.3 Ma (Middle Triassic) and Ar-Ar dating of two biotite samples using laser ablation revealed ages of 248 ± 2 Ma and 247 ± 6 Ma respectively. Dating of mineralization of PUT1 using Re-Os method of molybdenite obtained an age between the zircon and biotite ages at 245 ±

0.9 Ma, indicating that the mineralization and intrusion appear to have occurred between 248-242 Ma (Khin Zaw et al., 2014).

Khao Phanom Pha deposit

The Khao Phanom Pha deposit is located about 8 km west of Chatree deposit, Phichit province. The mineralization is hosted in volcaniclastic rocks including polymictic andesite, polymictic rhyolite, and fine-grained diorite intrusion. The mineralization is characterized by quartz-sulfide-gold veins that identified as a skarn type deposit (Salam, 2013; Khin Zaw et al., 2014). Ore zone occurs at the contact between endoskarn (diorite intrusion) and exoskarn (volcaniclastic rocks). The age of host volcaniclastic is inferred Late Permian to Early Triassic which is probably similar to Chatree host volcanic sequence. The Ar-Ar dating of muscovite from gold bearing vein obtained the age of 250 ± 1 Ma (Salam, 2013).

Chatree deposit

The Chatree deposit is located between Phichit and Phetchabun Provincial bordering area, central Thailand. The Chatree deposit is an epithermal low-sulfidation gold-silver that occurs as veins, stockwork and minor breccias hosted by volcanic and volcanogenic sedimentary facies (Salam et al., 2014). The host volcanic sequence was dated using LA ICP-MS U-Pb zircon age dating technique yielded Late Permian to Early Triassic ages (Salam et al., 2014). These rocks have been two volcanic suits and formed immediately after the beginning of subduction and probably created a new island arc by a mixed volcano-plutonic magmatism at Permo-Triassic boundary (Salam et al., 2014). The major structures are fault and shear zones in N-S, NE-SW and NW-SE directions. The mineralization at Chatree deposit was formed around the Permian-Triassic age which is indicated on the basis of adularia crystals dating (250 Ma) by Salam et al. (2008). Major mineralization is characterized by colloform-crustiform banded quartz ± carbonate ± chlorite ± adularia - sulfide - electrum veins. The adularia-sericite-carbonate-quartz epithermal veins, breccias and stockworks in which the mineralization occurs in volcanic breccias and the sedimentary sequence, is associated with a dextral shear zone that is superimposed on the former volcanic centers (Diemar & Diemar, 1999; Cumming et al., 2008; Crow & Khin Zaw, 2011).

Gold-silver mainly occurs as an electrum that presented free grains and associated with quartz, carbonate, chlorite minerals and mostly inclusions in pyrite. The Chatree has 10 million ounces of gold resources (Salam, 2013).

Khao Lek deposit

Khao Lek iron-copper skarn deposit is located at Amphoe Nong Bua, Changwat Nakhon Sawan. It is hosted in Permian Limestone of Tak Fa Formation and Late Permian to Early Triassic volcaniclastic rocks (Andrianarimanana, 2016). The hosted volcaniclastic rocks are ranging in composition from basaltic andesite to basalt consisting of tuff, lapilli tuff and breccia. Skarn at Khao Lek is classified as a calcic skarn type characterized by well developed garnet zone particularly in limestone protolith but poorly developed of pyroxene zone with an exception in endoskarn. The iron-copper mineralization is confined to endoskarn of 3 to 5 meters overprinting diorite intrusive body striking ENE-WNW, which could be intruded along fault zone. The mineralization is characterized by massive magnetite containing chalcopyrite-pyrite veinlets and patches. Retrograde skarn is well developed particularly in hangingwall volcanic rocks. The retrograde skarn is characterized by quartz-amphibole-chlorite-calcite veins/veinlets.

French Mine deposit

Khin Zaw et al. (2014) reported the French Mine gold skarn deposit located at the Kabin Buri district in eastern Thailand, is hosted in volcaniclastic and interbedded limestone. The host sequence was intruded by Late Triassic granodiorite (U-Pb zircon 203 ± 8 Ma; Khin Zaw et al., 2014). The drill hole investigation has presented a low-grade deposit, 16.8 g/t Au. The characterization of French Mine skarn has been classified four paragenetic stages of mineralization which consisted of prograde stage by garnet-pyroxene $\pm$ albite $\pm$ biotite and gold-bearing stage by pyroxene – garnet – wollastonite $\pm$ vesuvianite $\pm$ quartz.

2.4 Regional geology of Suwan Prospect

The Suwan Prospect covers area in the Phitsanulok, Phichit and Phetchabun Province that comprises of several rock units ranging in ages of Carboniferous to Mesozoic (Fig. 2.3).

2.4.1 Carboniferous rocks

The Carboniferous rocks are in the eastern to southern part of the area, which consist of volcanogenic rhyolitic siltstone, sandstone, shale, chert and minor limestone (Salam, 2013; Salam et al., 2014). Chonglakmani et al. (1983) presented Carboniferous - Lower Permian rocks in western part of Chon Daen area are shale and limestone units which were consisted of Khao Pun limestone, Khao Pun shale and siltstone, Ban Khao Nam Sap limestone, Khao Cha Ngok limestone, Khao Noi shale and sandstone and Ban Kuti Phra limestone. It is suggested that they are the depositional environments from subaerial to shallow marine and normal sea water to water tuning brackish. The Carboniferous unit is classified into volcanogenic sedimentary rocks dominant of Dan Lan Hoi Formation and limestone dominant unit of Wang Saphung Formation, which is widely distributed in the eastern and the southern trending areas. This unit mainly consists of laminated siltstone, sandstone, minor conglomerate and limestone (Salam, 2013). It occurs as thin-bedded and intercalated with dark-gray limestone lens occurring as small hills and low relief area and low angle dipping. The age this unit was analyzed from rhyolite siltstone at Wang Pong District using LA-ICP MS U-Pb zircon age technique and obtained an age of 327 ± 7 Ma (Khin Zaw et al., 2007). Rhyolite breccia and rhyolite from Khao Sai and Wang Yai, the southern part of the studied area have been reported to have 323 ± 5 Ma and 321 ± 7 Ma (Khin Zaw et al., 2007). The Carboniferous unit is overlain by a thick limestone formation of Middle Permian age and defined by basal conglomerate, siltstone, and shale at the lower part of the unit (Salam, 2013).
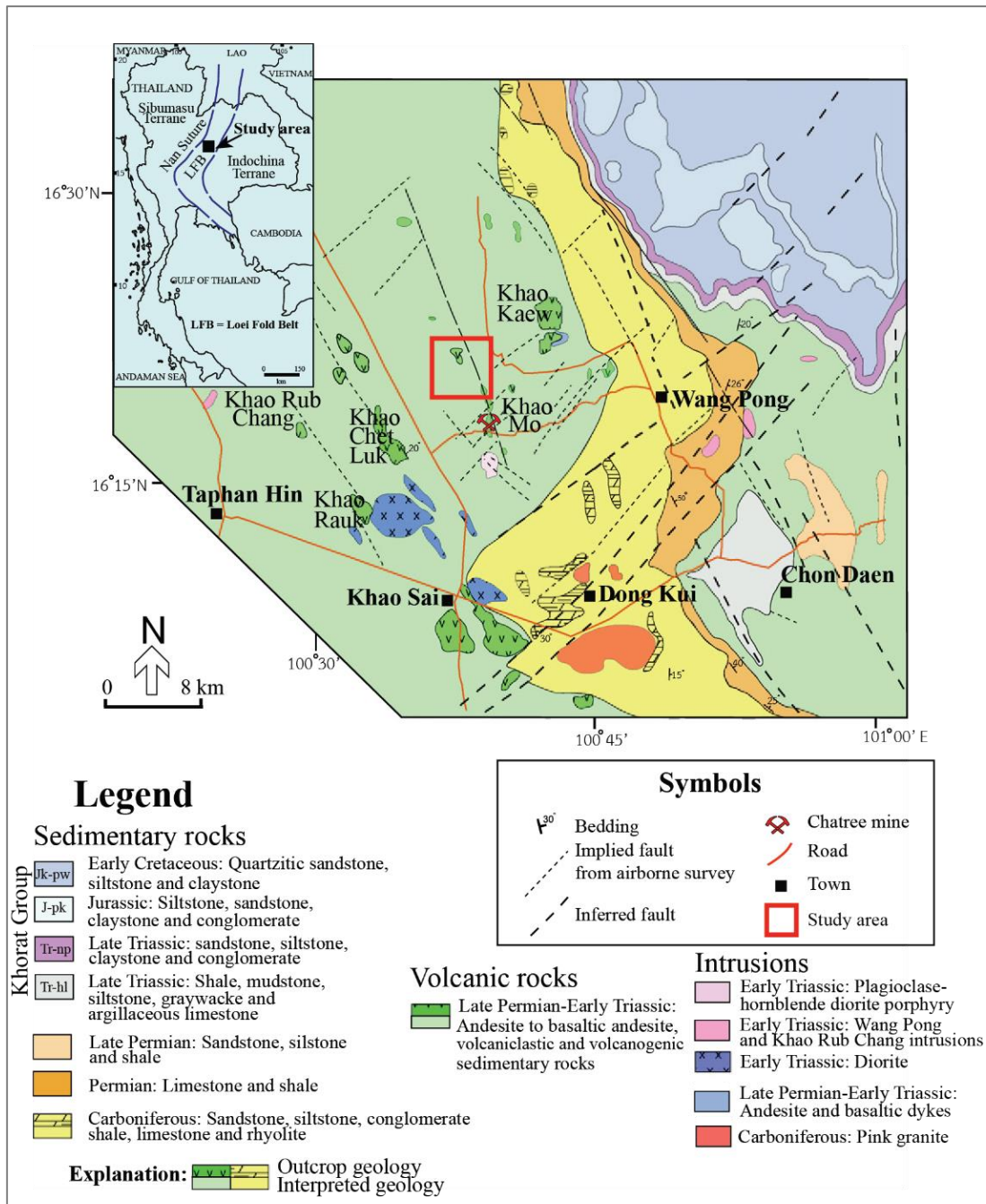
Fig. 2.3 Map showing regional scale geology of Suwan Prospect, modified from Salam et al. (2014)

2.4.2 Permian rocks

The Permian rocks consist of limestone, dolomitic limestone, chert sandstone, siltstone and shale (Fig. 2.4). In general, Lower to Middle Permian age consists thin-bedded chert and fine-grained clastic sedimentary rocks with intercalated thin-bedded limestone (Department of Mineral Resources, 2014). Middle to Upper Permian age

formed, clastic sedimentary rocks and pyroclastic such as shale, sandstone and andesitic tuff which are interbedded of thin layers and lenses of limestone (Salam, 2013). The Permian rocks are widely distributed in Thailand and it is also known as Saraburi Group by DMR (1999) at Saraburi Province in Central Thailand. This unit overlays the Carboniferous sedimentary unit and is typically composed of limestone. The common index fossils are fusulinids and brachiopod (Hinthong, 1981).

Fig. 2.4 Photographs of Permian limestone (Location: 693671E/1799323N UTM-wgs1984). **A.** Bedded limestone outcrop by pitting which highly weathered. **B.** Chert nodule presented in thin-bedded limestone and **C.** Chert nodule in limestone bedded, size range 5-10 cm

According to the geological map of Thailand (Department of Mineral Resource, 2013), the Permian limestone of Saraburi Group overlies Carboniferous sedimentary rocks. At southwest of Wang Pong, the base of Permian limestone is characterized by conglomerate and sandstone. This unit comprises thick-bedded to massive, fossiliferous limestone interbedded with thin shale, siltstone and chert which is

present north-south of strikes and easting of dips direction at south of Wang Pong District. The Permian sequence in this area commonly consists of siliciclastic and carbonates deposited in the various environments ranging from marginal marine to shallow marine, slope and basin center (Chonglakmani et al., 1983).

The Permian rocks are bounded in the east to southeast by N-S trending which contained sandstone, siltstone, shale and limestone. This unit crops out at Khao Noi, 3 km south of Ban Tha Kham (the road from Chon Daen to Taphan Hin), and is composed of calcareous shale, siltstone and subordinate sandstone (Chonglakmani et al., 1983). They are high weathered and have an abundant of brachiopods, crinoids, bryozoan and sponge. The distribution of Khao Noi shale and sandstone are exposed on the northwest trending and parallel with Permian limestone.

2.4.3 Volcanic rocks

The stratigraphic divisions of volcanic rock in study area were defined from field mapping and core logging of Chatree mine project succession that classified into four main units (Cumming et al., 2008; Salam, 2013; Salam et al., 2014). The Middle Permian to Lower Triassic volcanic sequence that hosts the Chatree deposit is bounded to the east and southeast by N-S trending basement high which contains Carboniferous volcanic sedimentary rock and Lower Permian limestone of the Saraburi Group.

Plagioclase-hornblende-phyric basaltic andesite

According to Salam et al. (2014), the lowest stratigraphic unit of the Chatree volcanic complex comprises of plagioclase-hornblende-phyric basaltic andesite, plagioclase-phyric andesite, monomictic andesitic breccia, mudstone-matrix monomictic andesitic breccia, fiamme breccia and minor carbonaceous mudstone. Minor coherent basalt and monomictic basaltic breccia are locally present in this unit. Basaltic and plagioclase-phyric andesite dykes are common and cross-cut the whole succession. The lower contact of this unit was exposed at Wang Yai deposit 15 km to the east of Chatree and overlies Carboniferous rhyolite. This unit is presented at southeast of Khao Sai, about 15 km south of Chatree area which is mainly exposed by coherent plagioclase-phyric andesite and monomictic andesite breccia facies.

Polymictic mafic-intermediate breccia

This unit mainly consists polymictic mafic-intermediate breccia interbedded or intercalated with thin intervals of monomictic plagioclase-phyric and/or plagioclase-hornblende-phyric basaltic andesite breccia. The contact with the underlying unit is gradational. This unit is well exposed in the Chatree mine, southeast of Khao Sai Township as well as west of the Chatree mine where it is mainly represented by polymictic mafic-intermediate breccia and minor monomictic plagioclase-phyric and/or plagioclase-hornblende-phyric basaltic andesite breccia.

Fig. 2.5 Volcanic sandstone (location: behind the Wang Pong Subdistrict Municipality Office station, 691571E/1807283N UTM-wgs1984). **A.** Bedding of volcanogenic sedimentary rocks which shows fault cross-cutting sequences, **B.** Thin layers of lithic-rich volcanic sandstone and volcanic siltstone and **C.** Photograph showing lamination of volcanic sandstone.

Volcanogenic sedimentary rocks

This unit is mainly represented by volcanogenic sedimentary facies and includes laminated siltstone, carbonaceous mudstone, sandstone, quartz-rich fiamme breccia, sand-matrix polymictic breccia and feldspar-phyric rhyolite (Fig. 2.5). The sand-matrix polymictic breccia is mainly restricted to the lower part of the succession, overlying the mafic-intermediate polymictic breccia. Sandstone occurs in the upper part of the unit and commonly contains fiamme. In the western and southern parts of Chatree, this unit also includes plagioclase-phyric basalt, plagioclase-phyric andesite and monomictic andesite breccia overlain by volcanogenic sedimentary facies association including laminated siltstone, sandstone, and sand-matrix polymictic breccia and mudstone-matrix polymictic breccia which is overlain by fiamme breccia.

Fiamme breccia

The uppermost of volcanogenic sedimentary unit consists of lithic-rich fiamme breccia interbedded with fiamme-rich sandstone and thin beds of accretionary lapilli-rich siltstone and polymictic mud-matrix breccia. This unit overlies the polymictic mafic-intermediate breccia.

The fiamme are interpreted as deformed pumice clasts which have an elongate shape and bedding-parallel alignment. These have been compacted and contained vesicles and flattening textures (C. Gifkins et al., 2002; McPhie & Allen, 2003; Salam, 2013).

According to Salam (2013), the volcanic stratigraphy and facies architecture in study area are andesite-dominated facies, found earliest event in the central part that is followed by deposition of mafic-intermediate polymictic breccia facies association. Subsequently followed by the deposition of volcanogenic sedimentary facies association which is mainly distribution in northern part of the area. The latest event represented by the emplacement of rhyolite facies (e.g., fiamme breccia facies association).

2.4.4 Mesozoic rocks

The Mesozoic rocks occur in northeastern part of study area that is known as redbeds of Khorat Group (Fig. 2.3). Most of the rock units are sandstone, siltstone and

conglomerate which are developed in the Triassic basins and isolated half-grabens (Chonglakmani & Sattayarak, 1978) . The lower part of unit comprised mainly of basal conglomerate with predominant of Permian limestone which unconformably on the eroded Permian rocks (Sattayarak et al., 1989). The middle to upper units consist of thick sequence or mega-sequences of siliciclastic redbeds of Khorat Group. The distribution of continental redbeds of Early Triassic age is reported in some marginal basins in the west and in the north (Hahn, 1982). In addition, those rocks are widely ranged in ages from Early Triassic to Cretaceous (Chonglakmani & Sattayarak, 1978; Hahn, 1982; Sattayarak, 1983; Meesook et al., 2002).

The Khorat Group comprises redbed sequence which consists of six formations. These are from bottom to top: Nam Phong, Phu Kradung, Phra Wihan, Sao Khua, Phu Phan and Khok Kruat Formations (Racey et al., 1994). The Khorat Group were deposited in and intracontinental basin as a sequence of predominantly lacustrine, fluvial and floodplain dominated sediments. This sequence is at least 4 km thick and extended into Laos, Cambodia, Vietnam and Southwestern China (Heggemann et al., 1994; Racey et al., 1994).

2.4.5 Plutonic rocks

The plutonic rocks were previously reported by Salam (2013). The plutonic rocks are poorly exposed in Chatree district, and only small isolated outcrops were found with exception at Wang Pong where the rocks are mapped in Department of Mineral resources (1976). Petrography, geochronology and geochemistry have been undertaken (e.g. Kamvong et al., 2006; Khin Zaw et al., 2007; Salam et al., 2014). The plutonic rocks of Dong Khui, Khao Rub Chang, Wang Pong, Khao Chet Lok, Chatree mine (N-prospect) and Singto prospect are briefly described below:

Dong Khui granite

Dong Khui granite is typically pink colored, medium-grained equigranular texture (Fig. 2.6A and 2.6B). This rock crops out in the undulating topography at Dong Khui sub-district in Chon Daen district (Fig. 2.3). A similar granite was identified in drill-hole (rotary air blast-RAB) in the south of Dong Khui area (Fig. 2.3; Salam et al., 2014). The granitic rock at Dong Khui formed as small stocks and

produced narrow contact metamorphism in country rock which metamorphosed to marble and calc-silicate rocks (Salam et al., 2013). Petrology study revealed the rock contains mainly K-feldspar, quartz, plagioclase, hornblende, and trace of opaque minerals. The granitic rock of Dong Khui area have been dated at 310±8 Ma (LA-ICP-MS zircon U-Pb age; Khin Zaw et al., 2007; Salam et al., 2014).

Fig. 2.6 Lithological characteristics of Carboniferous granite at Dong Khui (Salam, 2013). **A.** Outcrop of pink medium-grained biotite granite close to quarry in Dong Khui and **B.** Hand specimen of medium-grained pink granite showing equigranular texture comprising of quartz, feldspar and biotite crystals.

Khao Rub Chang granite

Based on Salam et al., (2014), Khao Rub Chang granite occurs beside the main road (Taphan Hin-Phichit) in the northwest of Chatree deposit and about 15 km south of Phichit Provincial Capital (Fig. 2.7A and 2.7B). The rock composes of medium to coarse-grained, quartz, feldspar, biotite as well as muscovite and is typically pinkish to grey in color. The granite is crosscut by pink to orange aplite dykes that are, in turn, and cut by dark basaltic dykes.

Wang Pong intrusive rock

The Wang Pong intrusive rock is in the northeast of Wang Pong Town (Figs. 2.8A, 2.8B, 2.8C and 2.9A and 2.9B). The rocks consist of biotite granite and granodiorite with minor gabbro. The biotite granite is characterized by medium to coarse-grained, equigranularity textures, containing mainly quartz, K-feldspar and plagioclase as well as biotite and hornblende. Trace amounts of apatite, ilmenite and magnetite also are present. Granodiorite consists of plagioclase with the subordinate amount of K-feldspar and quartz. Mafic minerals typically include pyroxene,

hornblende, and biotite. LA-ICPMS zircon U-Pb dating of granodiorite shows an age of 249.2±4.4 Ma (Salam, 2013).

Fig. 2.7 Lithological characteristics of Late Triassic(?) granite at Khao Rub Chang, Phichit Province, from Salam (2013). **A.** Pink biotite-muscovite granite is cross-cut by aplite (pink) dyke that is in turn cut by basaltic dyke (black), about 1 km northeast of Khao Rub Chang and **B.** Hand specimen of medium-grained pink granite showing equigranular texture comprising of quartz, feldspar, biotite and minor muscovite crystals.

Khao Chet Lok diorite intrusion

The Khao Chet Lok diorite intrusions are cropped out at Khao Chet Lok, Khao Ruak and further to the northwest and southeast of Khao Sai. The diorite is commonly present in as xenoliths of post-mineralization basaltic dykes at the Chatree deposit area. These diorite xenoliths have been dated to be 245.9±5.6 Ma by LA-ICPMS zircon U-Pb age (Salam, 2013).

N-prospect intrusion

N-prospect granodiorite is located about 1 km south of the Chatree mine (CH pit). The main body of intrusion is identified as plagioclase-hornblende diorite porphyry, containing coarse-grained feldspar phenocrysts. Second generation is classified as plagioclase-phyric andesitic and is typically characterized by finer-grained containing feldspar phenocrysts (Salam, 2013). The plagioclase-phyric andesite cross-cuts the plagioclase-hornblende diorite porphyry. Geochronological data support the cross-cutting relations as LA-ICPMS zircon U-Pb ages yielded 238±5 Ma and 243±5 Ma for younger and older phase intrusions. The molybdenite Re/Os age of 244±1 Ma has been obtained from the porphyry-like Cu-Mo

mineralization hosted in the plagioclase-hornblende diorite porphyry intrusion (Salam, 2013).
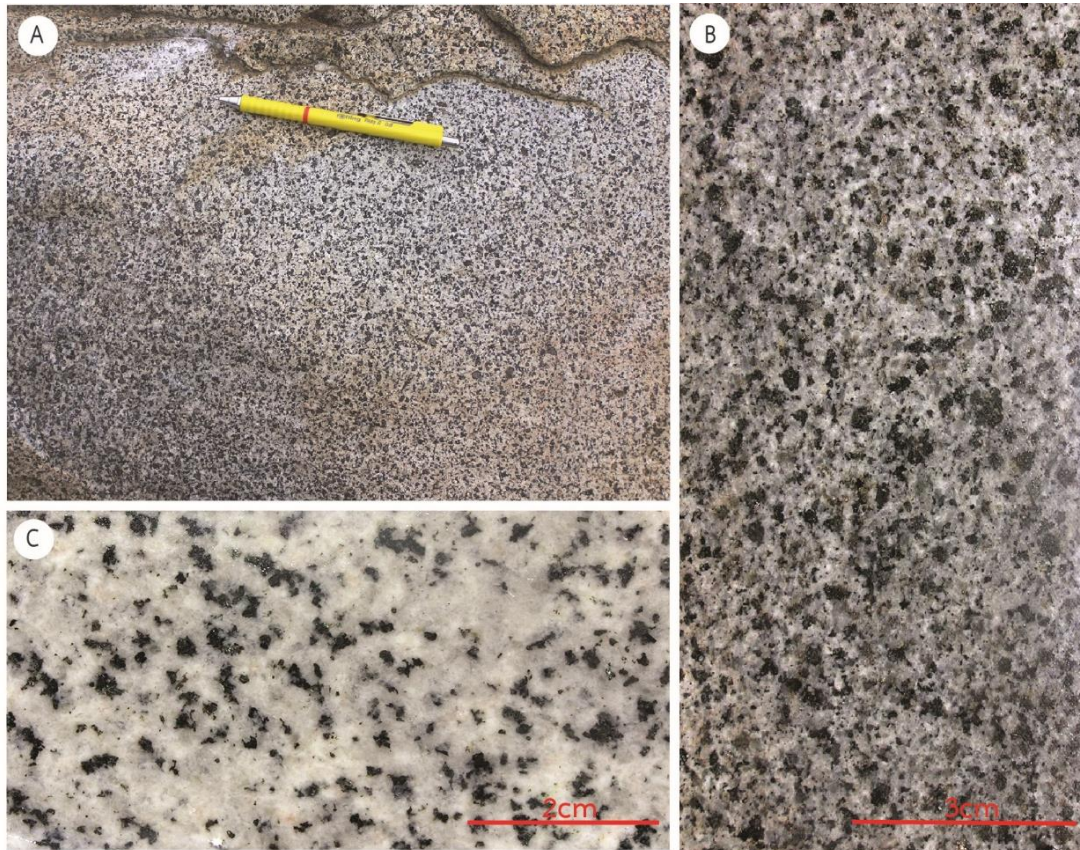
Fig. 2.8 Photographs of the Wang Pong intrusive in the northeast of the study area, from Salam (2013). **A.** Outcrop of Wang Pong granite. **B.** A hand specimen of granite sample showing dominants of felsic minerals with minor mafic minerals; and **C.** A hand specimen of granodiorite sample.
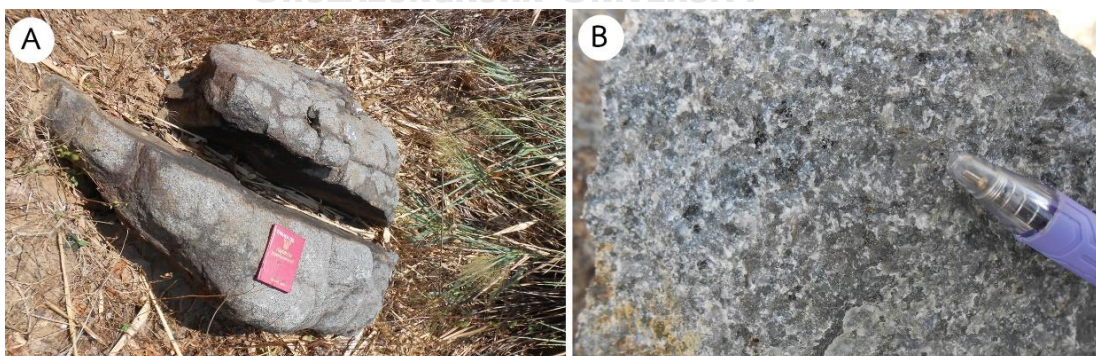
Fig. 2.9 Photographs of Wang Pong diorite (location: 701417E/1807222N, UTM-WGS 1984). **A.** Outcrop of slightly weathered diorite; and **B.** A close-up of outcrop in Figure A, medium to coarse grained diorite composed of plagioclase, hornblende and minor felsic minerals.

2.5 Regional structures

The major structures in Loei-Phetchabun Fold Belt are extended from north to south that have resulted from the collision of the Shan-Thai and Indochina terranes (Bunopas & Vella, 1983). Both the Shan-Thai and Indochina terranes contain Early to Late Paleozoic clastic sedimentary rocks, platform carbonates which have been overlain by Triassic volcanic and intruded by Triassic and Cretaceous granites. The nature of the collision of these terranes is subduction between two terranes and the effect is preserved as N-S and NW-SE trending fault zones. Uplifting, rotation and extension shown in NNE-SSW trending fault zones were in Cenozoic occurred (Bunopas & Vella, 1983; Bunopas, 1994; James & Cumming, 2007). Most structural trending in the region is intersected by NE-SW faults direction that is associated with granodiorite intrusions emplaced during pre-postdate of mineralization (James & Cumming, 2007). The intrusive rocks in the Middle Triassic (Salam, 2013) were mainly diorite (plagioclase-hornblende porphyry) and andesite dykes (calc-alkaline). According to Salam (2013), the mineralization was initiated along the NW-SE of arc parallel structural, which produced the development of dilation on the N-S to NNE-SSW and NE-SE structures.

The interpretation of an airborne magnetic map (Tulyatid, 2001) was conducted to understand fault/fracture and intrusions. The aeromagnetic datasets used for this study were the Phetchabun survey and portions of surveys A-4N and A-6 (DMR, 1989) . The interpretation of magnetic map consists of the identification of three main elements: (1) zones of common magnetic character; (2) fault; and (3) intrusive bodies (Fig. 2.10). Separating magnetic character into different zones is based on the amplitude, grid shading and texture of the magnetic anomalies. The texture of magnetic color grid shading can be described by coherence, roundness, linearity, symmetry, wavelength and strike length. The correlation of these interpreted geophysical signatures with the geological map of the study area was made. The geological structure in studied area can be delineated magnetic maps by recognizing linear boundaries between areas of different magnetic levels. The significant relief and texture have been interpreted to magnetic bodies, lineament, rock forming and minerals composition in host rock.
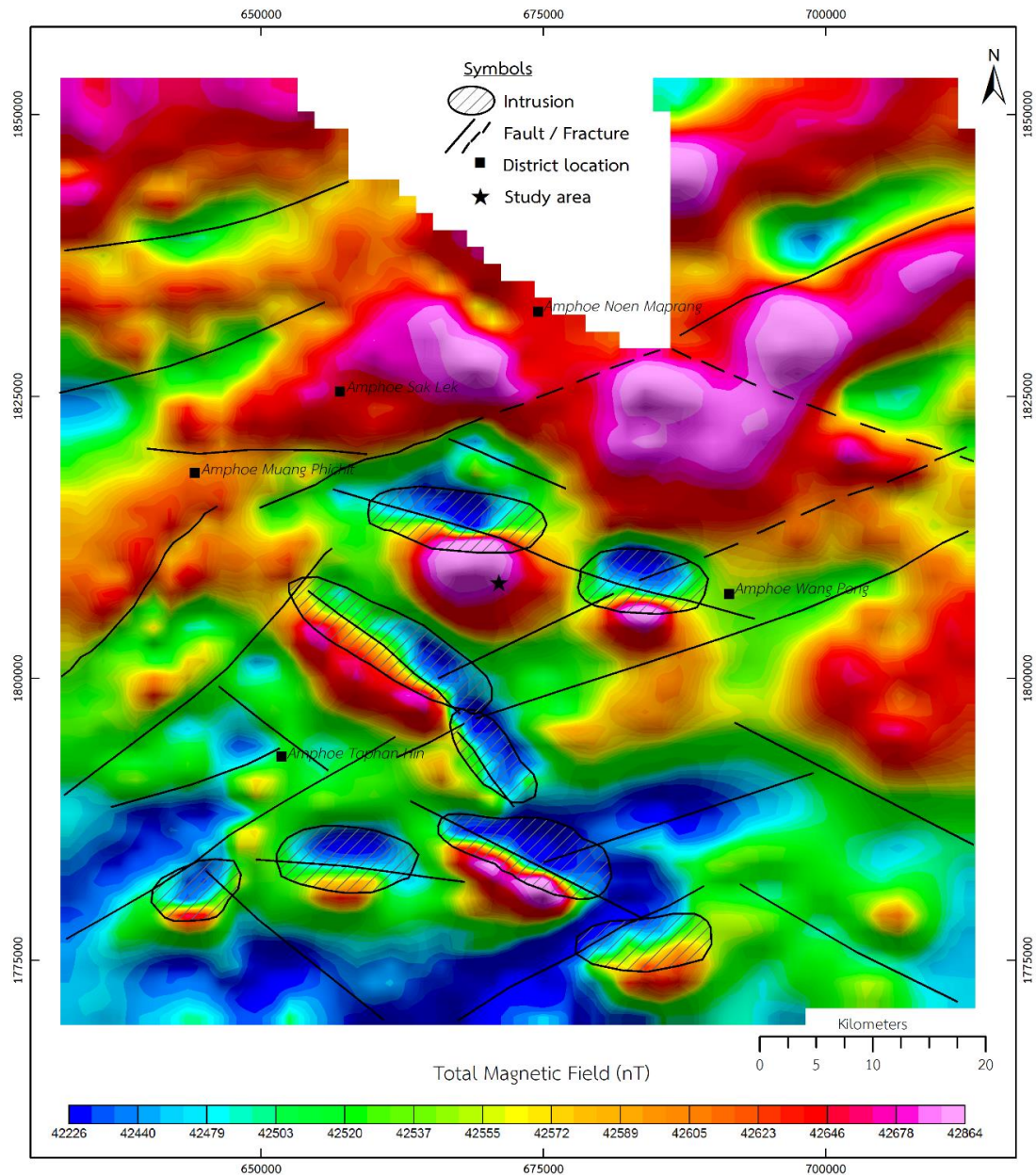
Fig. 2.10 The Airborne magnetic interpretation map (Modified from DMR, 1989)

     The anomaly of airborne magnetic features may be caused by hydrothermal mineralization within a fault being intruded with magnetic material, such as diorite. In general, magnetic character along the Phitsanulok-Phichit-Phetchabun province can be characterized as complex. They have been derived mainly from volcanic units which are mostly flat-lying and several cases are the result of typical superimposed layers of several composition. Structurally, the study area is complex with several fault directions being interpreted from the magnetic data. Mostly, the directions of faults are NE-SW and NW-SE as shown in Figure 2.10. A family of faults which is

roughly at N35°E and is observed mainly along the eastern edge of the research area (Wisedsind et al., 1994). In the north-northeastern and south-southwestern field, the magnetic map shows the magnetic anomaly which is interpreted to be intrusive bodies. In this case intrusive signatures were recognized as a circular or elliptical area of either high amplitude for the intermediate to basic rocks.

CHAPTER 3
VOLCANIC STRATIGRAPHY, FACIES AND GEOCHEMISTRY

3.1 Introduction

This chapter presents the deposit geology, stratigraphy and petrography of the Suwan Prospect. The geological studies described from diamond drill core logging present the correlation between the stratigraphic columns. Most of stratigraphic units show the variety of lithology and volcanic textures. It generally consists of altered rocks that preserve their depositional characteristics. The analysis and interpretation of rock units allow to define the depositional environment which can represent the host epithermal gold-silver mineralized systems.

3.2 Background geology of Suwan Prospect

The identification of lithofacies and facies associations are diverse and laterally discontinuous in texture, mineralogy and composition. The description of the rock units of Suwan Prospect is derived from field studies and nine drill cores logging that details stratigraphy and lithology of the depositional environment in the study area. The number of drill holes consisted of DDH4065, DDH4067, DDH4066, DDH4069, DDH4080, DDH4102, DDH4119, DDH4138 and DDH4139 (Fig. 3.1). The drill hole data were supported by Akara Resources company limited. The classification of facies and volcanic architecture was based on petrographic study which can be divided into three main units including phyric andesite unit, volcanogenic sedimentary unit and felsic volcanic unit.

The focus of study of volcanic rocks was to describe volcanic stratigraphy, volcanic facies, petrographic studies and geochemical analysis and follow the nomenclature of McPhie et al. (1993) to describe these rocks. The information on the units has been simply determined from drill core logging and field investigation. On a local scale, rock units in Suwan Prospect are covered by thick layers of unconsolidated sediments and unexposed on the surface.

3.3 Volcanic stratigraphy

The volcanic facies are associated with coherent (non-fragmental facies) autoclastic, epiclastic and pyroclastic facies. These facies included porphyritic andesite facies association, monomictic andesite breccia facies association, volcaniclastic sedimentary facies association, fiamme breccia facies association, and feldspar-phyric rhyolite facies association. The result of drill core logging revealed the bottom of volcanic stratigraphy is porphyry andesite unit that has been covered by the volcanogenic sedimentary rocks. The lower volcanogenic sedimentary rocks are commonly polymictic felsic-intermediate-mafic breccias.

Fig. 3.1 Google image showing drill holes location of the Suwan Prospect.

It typically occurred stratigraphically beneath the volcanogenic sedimentary rocks of the middle unit at the Suwan Prospect that included volcanic siltstone, volcanic sandstone, mudstone, limestone and polymictic intermediate-felsic breccias. While the upper sequences are mostly pyroclastic volcanic rocks such as monomictic

rhyolite breccia, lithic-rich fiamme breccia, quartz-rich fiamme breccias and feldspar-phyric rhyolite breccia that are presented as a felsic volcanic sequence.

The Suwan Prospect volcanic sequences presented complex stratigraphic division. The identification of district scale is obscure because of the paucity of bedding, facing data and the general lack of extensive marker layers. The thickness of stratigraphic layer in the Suwan Prospect is approximately 200 m. There are three main stratigraphic units (Fig. 3.2, 3.3, 3.4 and 3.5). The lithostratigraphic units are porphyritic andesite unit (Unit 3), volcanogenic sedimentary unit (Unit 2) and felsic volcanic unit (Unit 1). The stratigraphic units are presented from the bottom to the top.

Porphyritic andesite unit (Unit 3): This stratigraphic unit consists of coherent plagioclase-hornblende-phyric andesite, monomictic andesite breccia and minor plagioclase-phyric andesite (Fig. 3.2, 3.3, 3.4 and 3.5). The lower contact of this unit has not been discovered in the Suwan area. The drill core samples of this unit are well recovered and mainly represented as coherent plagioclase-hornblende-phyric andesite and monomictic andesite breccia facies. The coherency is commonly observed at the inter-layering of monomictic andesite breccia.

Volcanogenic sedimentary unit (Unit2): This unit mainly comprises volcanogenic sedimentary facies association with the presence of laminated siltstone, sandstone, mudstone, limestone, polymictic intermediate-felsic breccia and sand-matrix polymictic breccia (Fig. 3.2). The thickness of volcanogenic sedimentary unit varies from 10 m to 80 m. The unit is overlain by Unit 1 (Felsic volcanic unit). The volcanic siltstone and volcanic sandstone are commonly presented in the middle parts of this unit and are typically laminated. The polymictic intermediate-felsic breccia and sand-matrix breccia are mainly found at lower part of this unit.

Felsic volcanic unit (Unit 1): This unit mainly consists of quartz-rich fiamme breccia, monomictic feldspar-phyric rhyolite breccia, lithic-rich fiamme breccia and rhyolitic rock (Fig. 3.2). The thickness of this unit varies from 10 m to 50 m. This unit overlays the polymictic intermediate-felsic breccia of Unit 2.

	Unit's name and facies components	Unit No.
0.5 2 8 32 64 (mm) 0 Alluvium sediments Feldspar-phyric rhyolite Quartz-rich fiamme breccia 50 Lithic-rich fiamme breccia	**Felsic volcanic unit** Lithic-rich fiamme breccia Quartz-rich fiamme breccia Feldspar-phyic rhyolite and monomictic feldspar-phyric rhyolite breccia	Unit 1
Polymictic intermediate-felsic breccia Mudstone 100 Polymictic breccia and sand-matrix polymictic breccia Polymictic intermediate-felsic breccia Volcanic sandstone Volcanic siltstone Mudstone 150	**Volcanogenic sedimentary unit** Volcanogenic sedimentary rocks siltstone, sandstone (cross-laminated) and mudstone Polymictic breccia and sand-matrix polymictic breccia Polymictic intermediate-felsic breccia	Unit 2
Plagioclase-phyric andesite Monomictic plagioclase-phyric andesite breccia Monomictic plagioclase-hornblende-phyric andesite breccia Plagioclase-hornblende-phyric andesite 200 Plagioclase-phyric andesite	**Porphyritic andesite unit** Plagioclase-phyric andesite Monomictic plagioclase-phyric andesite breccia Plagioclase-hornblende-phyric andesite Monomictic plagioclase-hornblende-phyric andesite breccia	Unit 3

Fig. 3.2 Summary of stratigraphic column of volcanic sequence at the Suwan Prospect central Thailand.
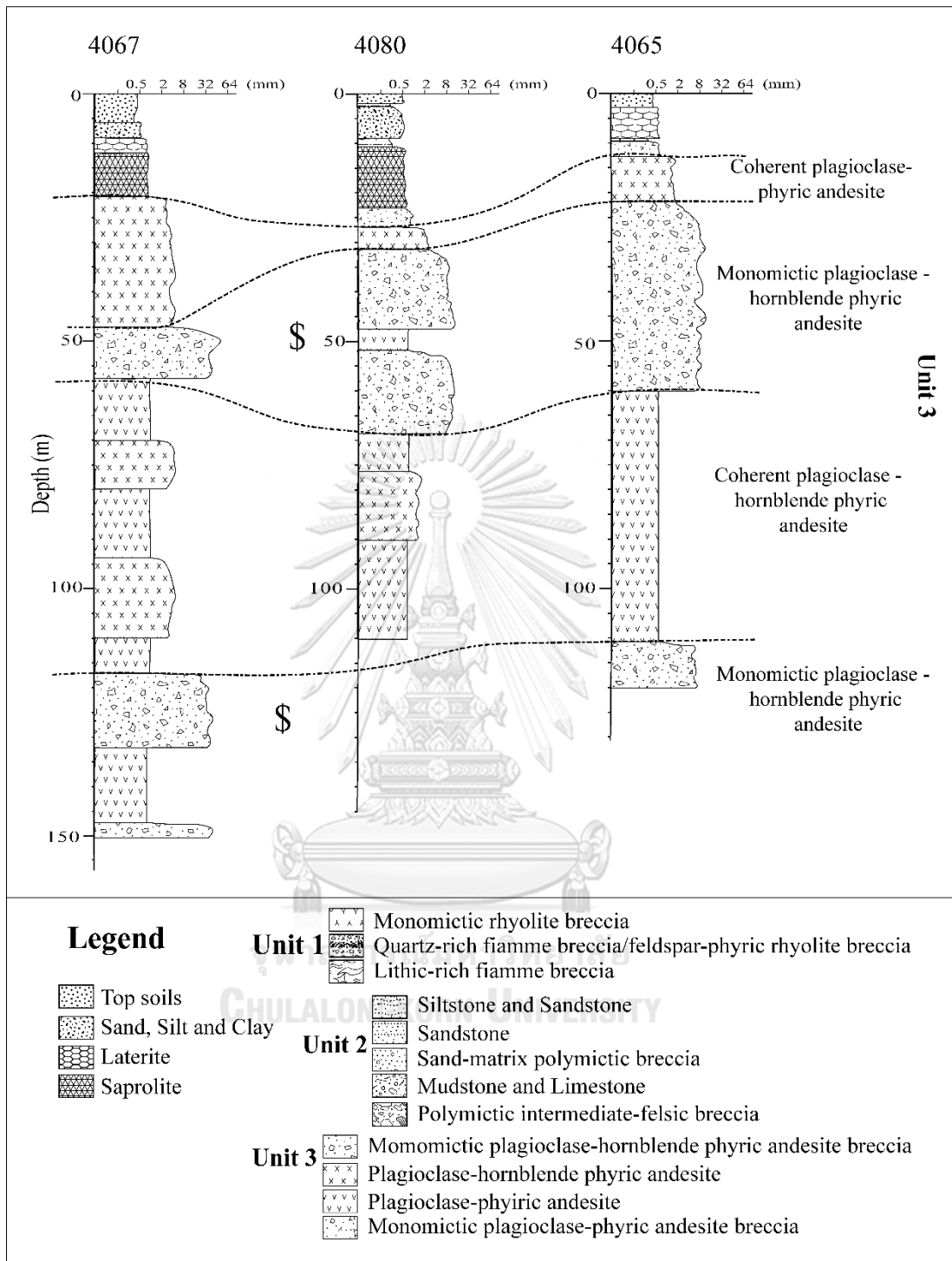
Fig. 3.3 East-west stratigraphic correlation at the southern part of Suwan Prospect including diamond drill holes No. DDH4067, DDH4080 and DDH4065.
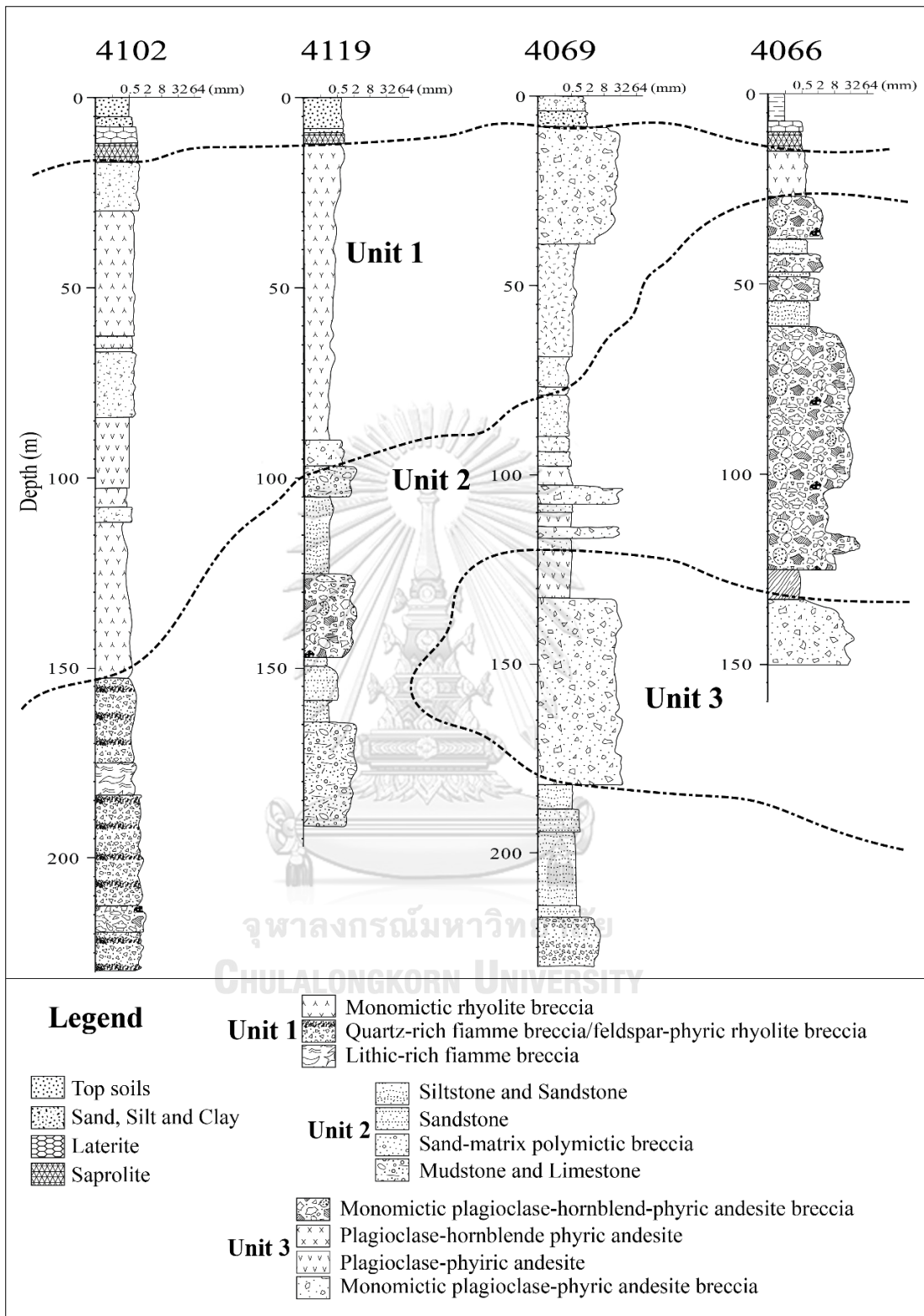
Fig. 3.4 East-west stratigraphic correlation at the central part of Suwan Prospect including diamond drill holes No. DDH4102, DDH4119, DDH4069 and DDH4066.
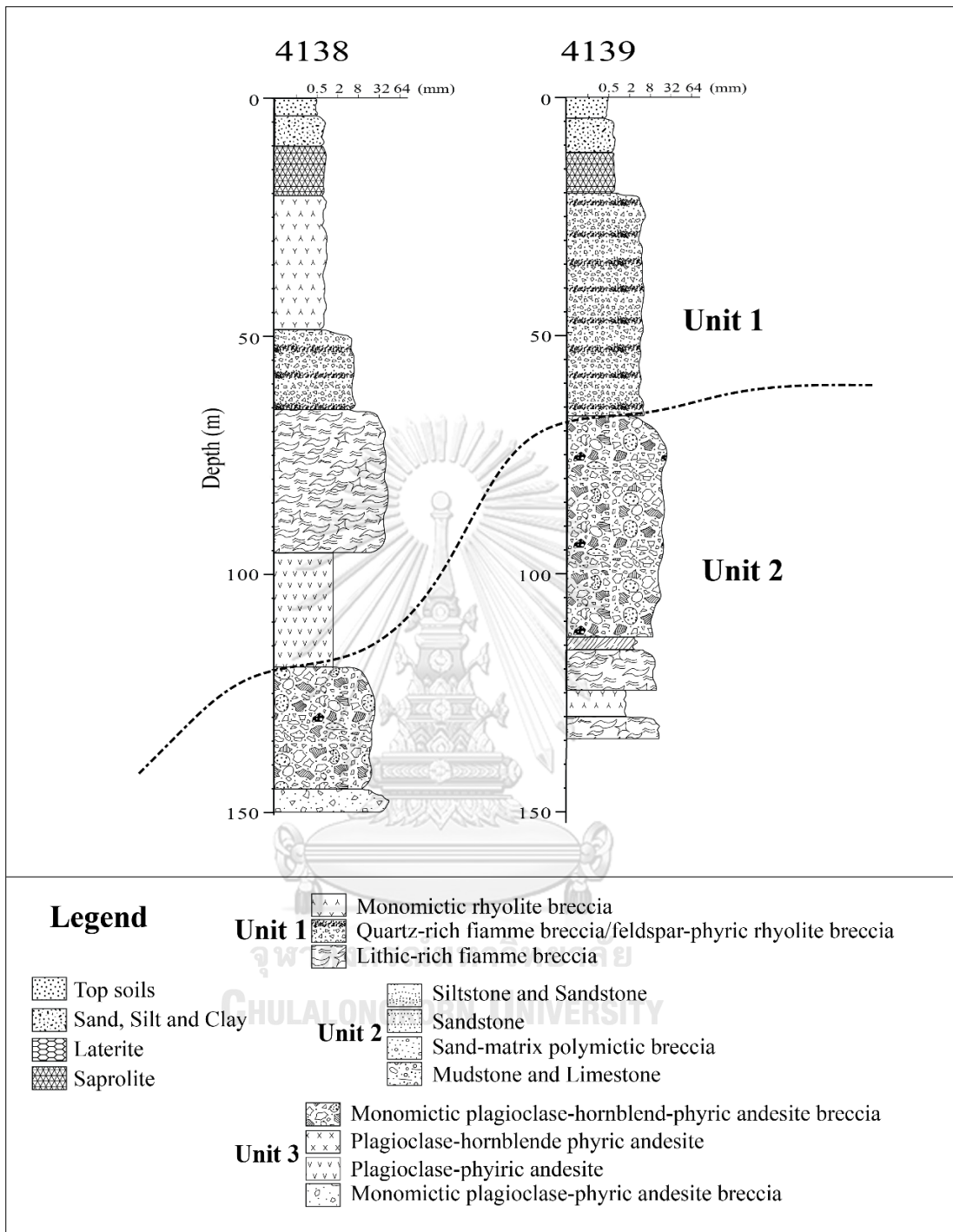
Fig. 3.5 North-south stratigraphic correlation at the northern part of Suwan Prospect including diamond drill holes No. DDH4138 and DDH4139.

3.4 Volcanic facies association

Study of volcanic facies is attempted to understand the environment of deposition of volcanic rock sequences. This study could be supported study of Chatree host sequence undertaken by Cumming (2004) and Salam (2013).

3.4.1 Porphyritic andesite facies association

This facies association consist of two facies namely, 1) Plagioclase-hornblende-phyric andesite facies and 2) Plagioclase-phyric andesite facies. Details will be given below:

Plagioclase-hornblende-phyric andesite facies

Most of core recovering is slightly fresh, greenish black to greenish gray, hornblende - plagioclase ± pyroxene ± pyrite with groundmass of feldspar and quartz (Fig. 3.6). The intermediate composition of the sample has been confirmed by XRF analysis for SiO_2 and alkaline content. It associates with several phenocrysts, including two or three crystal types. These are commonly patched in microcrystalline groundmass that dominated by altered minerals such as chlorite, calcite and clay minerals. The thickness of this facie is unexplored. However, it can be determined by correlating several drill holes, and it is estimated to have not less than 50 m thick. The upper contact is graded with monomictic andesite breccias, basaltic andesite and polymictic breccias. The plagioclase-hornblende-phyric andesite are euhedral plagioclase and hornblende phenocrysts with groundmass of plagioclase, pyroxene and amphibole.

The composition of plagioclase-hornblende-phyric andesite is commonly plagioclase-hornblende-phenocryst. The phenocrysts range from 10-40 vol. %, mostly < 5 mm in diameter, and are predominantly hornblende with plagioclase and mafic minerals. The phenocryst of hornblende and plagioclase are medium to coarse grained and subhedral to euhedral. Some clasts of hornblende and plagioclase feldspar are altered to secondary minerals such as albite, chlorite, smectite or illite. The fine-grained groundmass generally comprises fine-grained feldspar and mafic minerals which are illustrated to be very fine grained under microscopic of altered minerals from hydrothermal alteration. Some of altered hornblende-plagioclase porphyritic

andesites are associated with the monomictic andesite breccia and polymictic andesite breccia facies. In other hand, some analyses were performed on the altered rocks, and they generally reflect the transformation minerals that will be described in the Chapter IV of alteration mineralogy.

Plagioclase-phyric andesitic facies

This facie was comprised green to dark gray, light green to dark grayish green of porphyritic andesite. Phenocrysts are predominantly coarse to extremely coarse-grained feldspar (20-40%) and mafic minerals (10-30%). This plagioclase-phyric andesite has fine-grained groundmass that comprised predominantly of feldspars. The phenocrysts are average 1-2 mm in size whereas the mafic minerals are finer grained. The plagioclase occurs mostly as irregular to euhedral form phenocrysts with up to 3 mm in size. Many of the plagioclase are microscopically displayed to have simple twinning and crystal zonation. The groundmass is also altered differently. Some strongly altered samples have a silicified groundmass made up of fine crystalline quartz and calcite pseudomorphs replaced plagioclase.
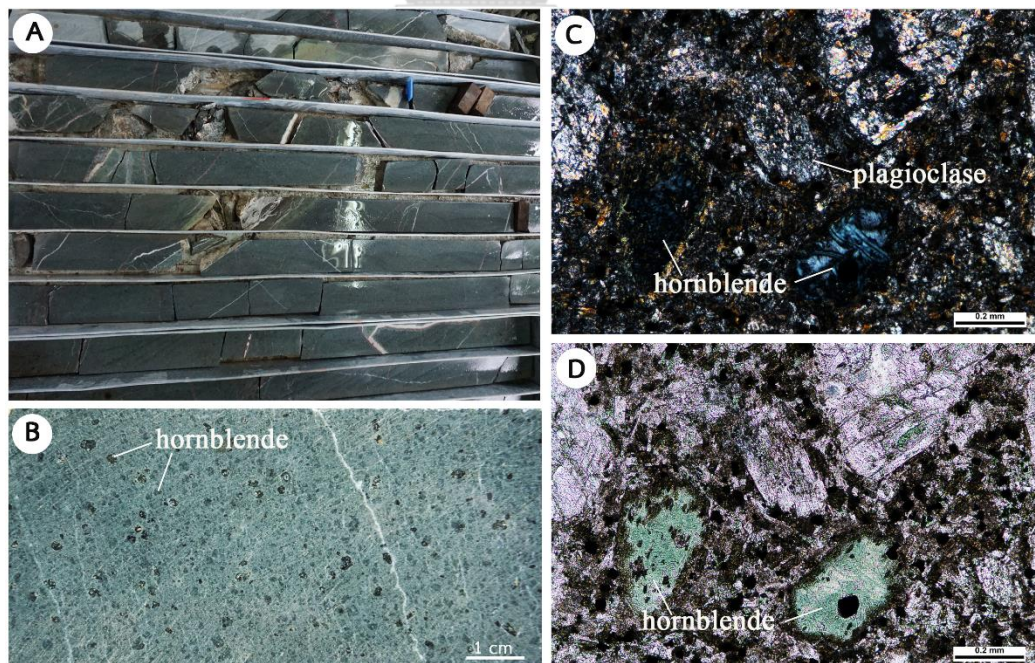
Fig. 3.6 Characteristics of plagioclase-hornblende-phyric andesite. **A.** Photograph of diamond drill core showing andesite containing some quartz-calcite veins/veinlets. **B.** Photograph close up view of porphyritic andesite showing phenocrysts of hornblende. **C.** and **D.** Photomicrograph showing plagioclase and hornblende phenocrysts in cross nicol and plane polarize respectively (sample No. 4080-75.00m).

3.4.2 Monomictic andesite breccia facies association

This facies association consists of three facies, namely 1) monomictic plagioclase-hornblende-phyric andesite breccia facies, and 2) monomictic plagioclase-phyric andesite breccia, and 3) monomictic hornblende-phyric andesite breccia.

Monomictic plagioclase-hornblende-phyric andesitic breccia facies

The monomictic plagioclase-hornblende-phyric andesitic breccias commonly show the jigsaw-fit clasts of porphyritic andesite (Fig. 3.7) which are same composition in coherent units. Clasts are typically range 0.5 to 5.0 cm, with angular to sub-rounded and mud to sand matrix. These units are defined as autoclastic of coherent with the surficial of lava flow formation. Intervals of the monomictic andesite breccia facies are up to 5-40 m thick and have gradational contact with volcanic sandstone and stratified porphyritic andesite. The monomictic andesite breccia is composed of plagioclase-hornblende-phyric clasts, green-hornblende-phyric clast and feldspar crystals fragments in a matrix and cemented by calcite and quartz wall shards. There are three different monomictic clast populations: plagioclase-phyric, hornblende-phyric and plagioclase-hornblende-phyric clasts.

Monomictic plagioclase-phyric andesite breccia facies

This facie frequently presented greenish-brown, orange-greenish gray and greenish-gray. Clasts are predominantly sub-angular to sub-rounded and range in size from 1 to 5 cm. The facie is relatively poorly sorted. Clast types consist only of plagioclase-phyric andesite and altered andesitic rocks. The poorly sorted and clast-supported sequence is generally massive layered and discontinuous bedding. The matrix is composed of fine grained (1-2 mm) andesitic materials and rock fragments. Facie thickness is highly variable although it is generally 2 to 20 m thick.

Monomictic hornblende-phyric andesitic breccia facies

Hornblende-phyric clasts are phenocrysts-rich, consisting 15-20%, 1-3 mm of hornblende phenocrysts. Clasts of hornblende-phyric andesite are pale green and pale dark pink and are between 0.5 mm to 7 cm in length. These clasts are variably compacted and presented angular to sub-rounded of shape. The primary hornblende-

phyric andesite is composed of hornblende-plagioclase phenocrysts and microcrystalline groundmass. Altered clasts are commonly illite, sericite, feldspar, chlorite, calcite and quartz. Hornblende- phyric clasts are pale light-green and also similar minerals compositing with plagioclase-hornblende-phyric facies. The presence of breccia clast is consisted of hornblende and plagioclase 10-20%, 1-3 mm phenocrysts in groundmass of fine-grained to micro-crystalline.
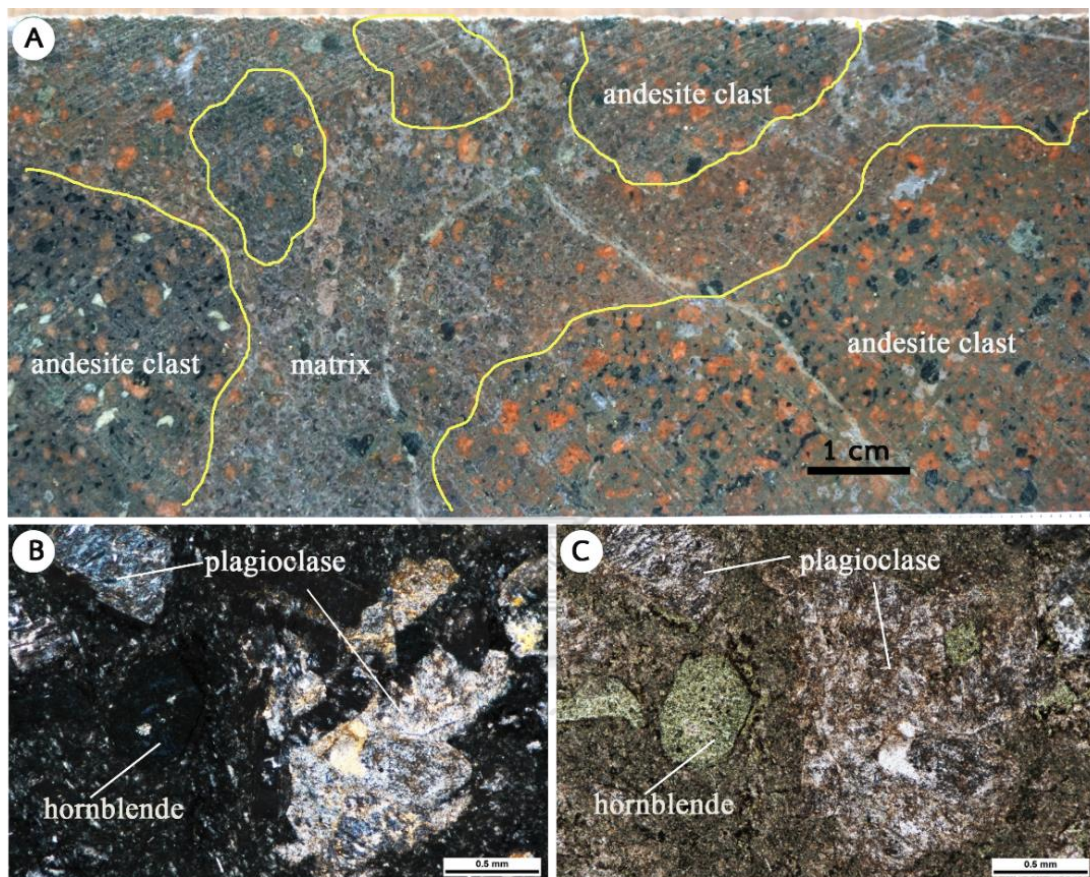
Fig. 3.7 Photographs showing monomictic plagioclase-hornblende-phyric andesite breccia **A.** Photograph showing diamond drillcore of plagioclase-hornblende-phyric andesite breccia (sample No. 4067-57.00m). **B.** Photomicrograph showing plagioclase and hornblende (now partly altered to chlorite) phenocrysts with fine-grained chlorite rich groundmass (cross nicol). and **C.** Photomicrograph showing altered hornblende plagioclase (plain polarized light).

3.4.3 Volcanogenic sedimentary facies association

This facies association has four facies namely, 1) Mudstone-limestone facies, 2) Laminated fine-grained sandstone facies, 3) Sand-matrix polymictic breccia facies, and 4) Polymictic intermediate-felsic breccia facies.

Mudstone facies

The volcanogenic sedimentary rocks in the facies are mostly siltstone, sandstone, mudstone and limestone which are thick layers. Carbonate rocks consist of fossiliferous-breccias and mudstone that are dark-gray and pale brown and composed of skeletal fragments of molluse, crinoid stems and minor mud and lithic clasts within quartz-rich volcanic siltstone/sandstone thin layers (Fig. 3.8).
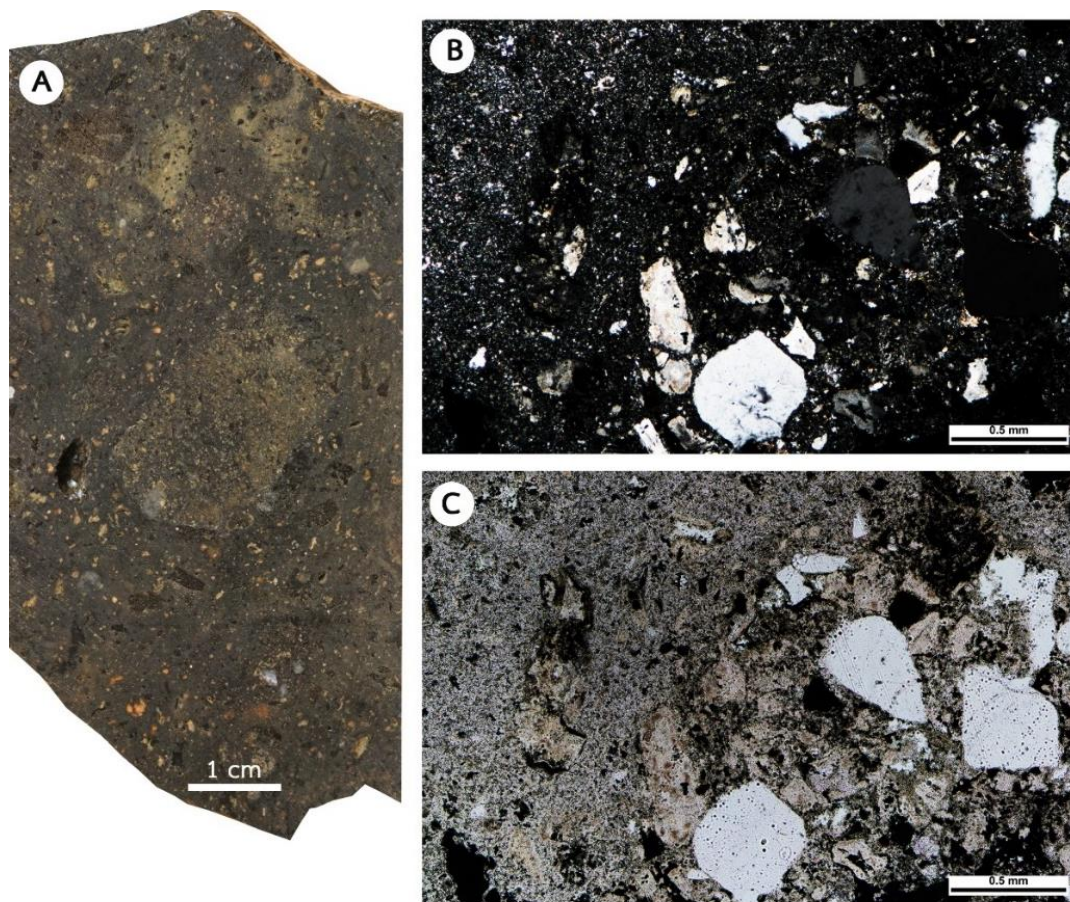
Fig. 3.8 Characteristics of mudstone **A.** Photograph of diamond drillcore of mudstone (sample No. 4069-159.00m) grayish brown containing some sand and pebble-size fragments. **B.** Photomicrograph of mudstone with some angular to sub-angular lithic clasts of quartz and rock fragments (cross nicol) and **C.** Photomicrograph of the same position as in figure B under plain polarized light confirmed the larger fragments are within sand-size rock fragments.

Carbonate-mudstone-matrix breccia occurs as clastic rocks or fragments which are corals, brachiopods in dark-gray mudstone and grayish-brown limestone. This unit is well presented in drill hole number DDH4119. These facies average 15 m in

thickness (10 - 25 m) and can be traced in drill core for 140 m and 170 m. Contacts are typically sharp and irregular or planar, although several upper contacts are unconformity with coherent andesitic basalt. Limestone and mudstone facies overlie or occur within facies of siltstone and sandstone or polymictic breccias. Generally, these facies are texturally less altered and occur in adjacent of laminated sandstone and siltstone. Limestone consists of white and purple carbonate clasts (0.3 - 1.5 cm) in yellowish brown matrix. One of samples also constrains clast to matrix supported and are poorly sorted and jigsaw-fit fossiliferous clasts. Local domains of carbonate clasts are angular to sub-rounded in shape.

Laminated fine-grained sandstone facies

The fine-grained sandstone facies is commonly associated with polymictic intermediate-felsic breccia and sand-matrix polymictic breccia (Fig. 3.9). The beds of this facie contain gradational contacts. Intervals of this facies are typically less than 10 m. Beds of this facies are thin to very thick (0.5-10 m), internal diffusely stratified, massive or normal graded/reversely graded, cross laminated and lateral sharped. Single layers consist of poorly to moderate sorted, grain-supported, laminated siltstone and sandstone typically composed of felsic rocks and crystal clasts. Clasts range from 1 mm to 2.5 mm and are generally sub-angular to sub-rounded. Basal contact of layers is sharp or gradational of sandstone.

Sand-matrix polymictic breccias facies

This facie typically shown brownish-orange, yellowish-gray and light-gray colors (Fig. 3.10). Generally, matrixes are consisted of very coarse sand (0.5-2 mm) to pebble (1-2 cm) grained and poor sorted, which are dominated in andesite, rhyolite, sandstone, siltstone and mudstone rock fragments. The clast shapes are typically sub-angular to sub-rounded, whereas matrix grains are sub-rounded. Composition of clasts is variable and includes andesite, rhyolite, volcaniclastic sandstone and quartz clasts. The facie in bottom sequence shows laminated siltstone/sandstone with sharp contact by normal graded bedding and shearing zone at the downwards. The upper part of this facie, contacts to felsic volcanic rocks (Unit 1) and coherent phyric andesite.
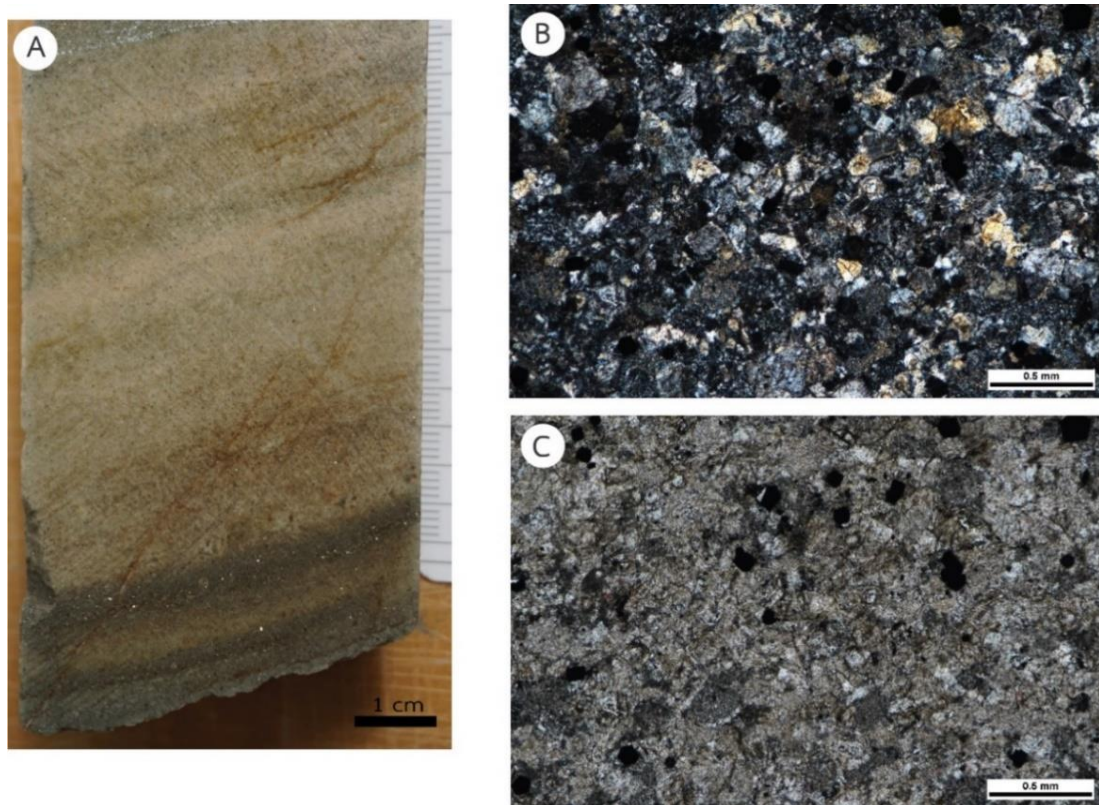
Fig. 3.9 Characteristics of laminated fine-grained sandstone, **A.** Photograph of diamond drillcore sample (No. 4066-39.00m) showing lamination made up of fine to very fine sand with mafic minerals rich layers, **B.** Photomicrograph showing quartz, feldspar and opaques minerals of fine-grained sandstone (cross nicol), and **C.** Some of alteration minerals are light green which is chlorite and opaques are pyrite (plain polarized light).

Polymictic intermediate-felsic breccias facies

The polymictic breccias are shown in figure 3.11. They are mainly clast-supported aggregates of angular to sub-rounded, poorly sorted and moderate altered matrix that contains plagioclase-quartz crystals and rock fragments. The polymictic breccia is sharp contacts, massive bodies, normally graded and siltstone/sandstone tops. Beddings are 5-65 m range of thick and commonly sharp at lower contacts. Clasts types are mainly of sandstone, siltstone, mudstone, quartz crystals, rhyolite and andesite/basalt. Clasts average less than 5 cm in size but can be up to 15 cm in diameter. The clasts are typically randomly oriented and locally jigsaw-fit textures. The most clasts are pebbly to cobble and sub-angular to sub-rounded with moderately altered. Some large (>10 cm) siltstone, mudstone, andesite and basalt clasts are altered and have zoned rims. Mafic clasts are commonly andesite and basalt that are partly altered to chlorite and clay minerals. Lithic clasts have been altered to chlorite,

illite, sericite, calcite and feldspar. The chlorite-sericite-illite lithic rich clasts contain plagioclase crystals and commonly have a chlorite-sericite-pyrite alteration.
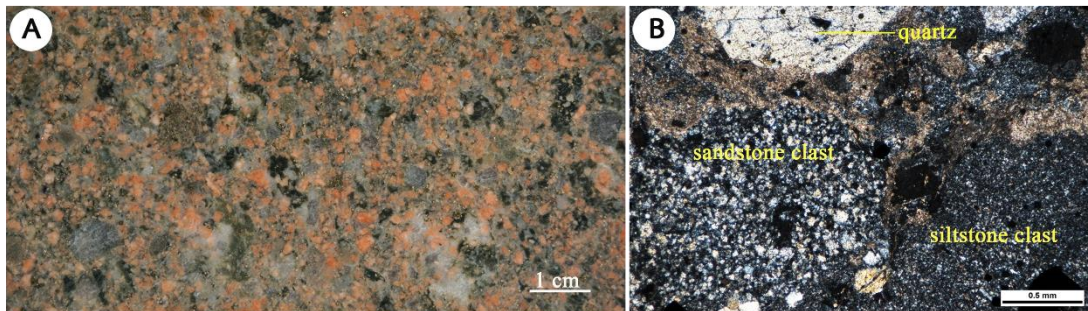
Fig. 3.10 Photographs showing sand-matrix polymictic breccia sample No. 4066-87.50m, **A.** Diamond drillcore sample of polymictic breccia and highly altered that showing reddish-pink color of altered minerals and **B.** Photomicrograph showing sandstone, siltstone and quartz clast in mud and sand matrix (cross nicol).
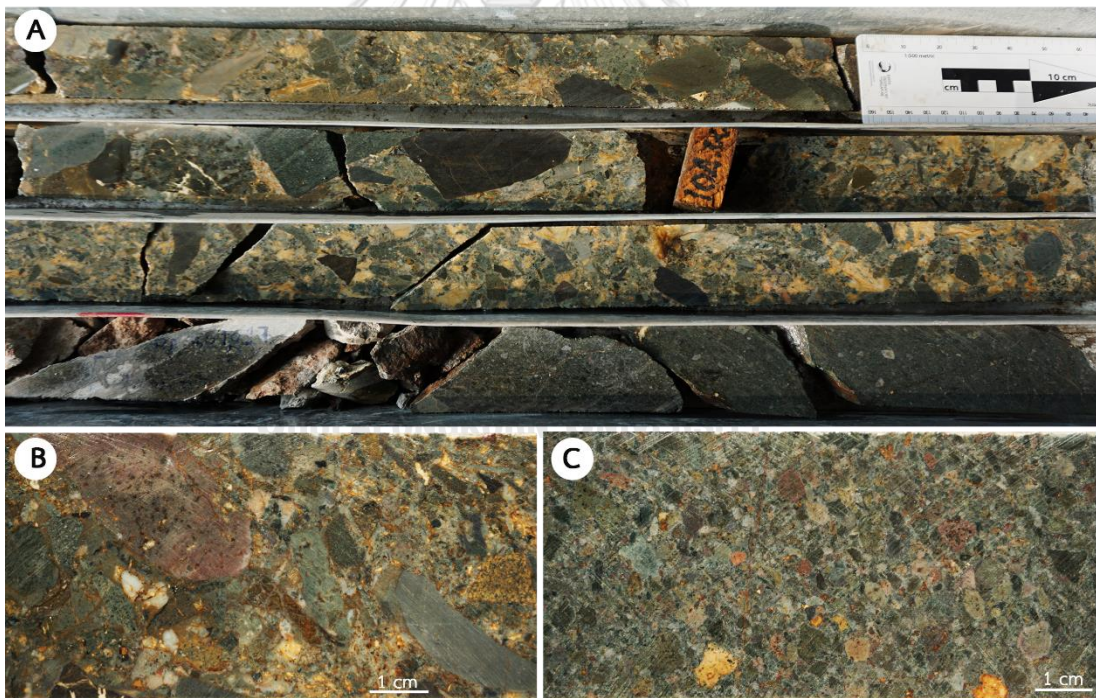
Fig. 3.11 **A.** Photographs showing diamond drill core sample polymictic intermediate-felsic breccia facie of sample No. 4139-104.30m, **B.** Close up of polymictic breccia that presenting clast-supported of andesite, basalt, felsic, siltstone and mudstone clasts with jigsaw-fit texture (sample No. 4139-104.30m), and **C.** Polymictic breccia lithic-rich, clast-supported consisted of sedimentary rock, felsic and mafic clasts in which clast rim zones are altered (sample No. 4139-67.50m).

3.4.4 Fiamme breccia facies association

This facies association is made up of 1) Feldspar-phyric rhyolite facies, 2) Quartz-rich fiamme breccia facies and 3) Lithic-rich fiamme breccia facies.

Feldspar-phyric rhyolite facies

This facies association is commonly occurred in the drill hole 4102, 4138 and 4139. Intervals of facies association are occurred as discontinuous sequences that vary in thickness from 1 m to 100 m and have coherent facies, breccia facies and tuffaceous facies. Coherent facies are typically massive, flow-banded, or brecciated and may have pyroclastic or pumiceous margins. The breccia facies are typically monomictic quartz-rich breccia and inclusion of rhyolitic rock and pyroclastic rocks. The rhyolite facie is typically massive, crystal-rich and may have monomictic feldspar-phyric rhyolite breccia and quartz-rich fiamme breccia. Lithologic and textural characteristics of rhyolite units are generally flow banded and massive layers that have commonly quartz-feldspar porphyritic components. Interval of rhyolite in Suwan Prospect varies from 5 to 75 m in thickness, and there are conformable with bedding in the layered feldspar-rich fiamme breccia. Most of altered rhyolite composed of quartz-felspar and alteration minerals which are composed of quartz-chlorite-calcite-sericite. Whereas the tuffaceous formations are clastic rich. Flow-banding of feldspar-phyric rhyolitic rock typically occurs as massive layers and alternating brownish-green quartz-feldspar rich bands and grayish-green chlorite ± illite/sericite in the groundmass (Fig. 3.12).

The optical studies of rhyolitic rock samples suggest apparent textural features within the rhyolite and rhyolitic-tuff samples, including widespread spherulites, amygdule, euhedral to subhedral phenocrysts, microcrystalline groundmass and replacement by alteration minerals. This facie is characterized by 5-20% of phenocryst, evenly distribution, euhedral, 1-3 mm of quartz and plagioclase phenocrysts in a very fine-grained groundmass of quartz-feldspar ± chlorite ± sericite ± calcite ± clay minerals. The feldspar phenocrysts are variably altered to chlorite, illite/sericite, albite, calcite, epidote and microcrystalline quartz. Some quartz-feldspar ± illite/sericite ± chlorite textures contain relic of perlite. Some rhyolite facies are feldspar-phyric containing 5%, 3 mm feldspar phenocrysts in fine-grained

groundmass of feldspar-quartz-illite/sericite. Groundmass texture in flow-banding rhyolite may include amygdales, microcrystalline quartz-feldspar, spherulite and combination of quartz, chlorite, illite/sericite and carbonate. Some spherulites have been altered to chlorite, calcite and clay minerals in which the original amygdule textures are defined by thin radius of chlorite, sericite and calcite. The microcrystalline mosaic of quartz, feldspar, sericite, chlorite and carbonate typically separates spherulite.
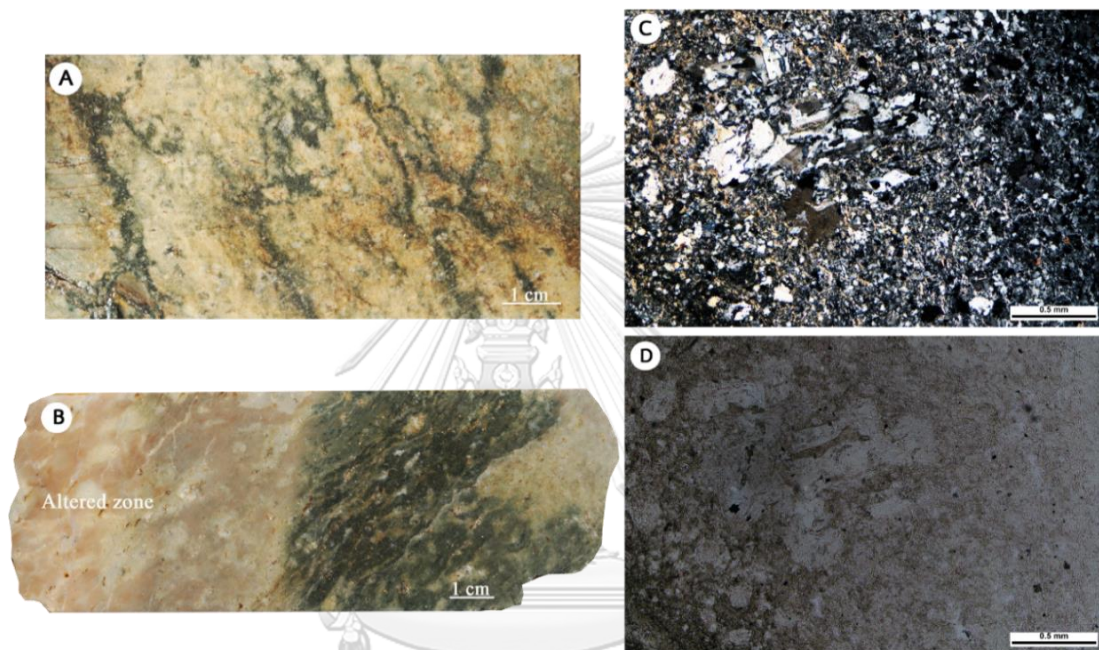
Fig. 3.12 Drill core samples of feldspar-phyric rhyolite (sample No, 4138-68.80m), **A.** Photograph showing banded of chlorite (green) with light-white color of feldspar porphyry crystals, **B.** Yellowish brown and greenish banding of altered minerals with light white of quartz-feldspar phenocrysts texture and presenting pink color of altered zone, **C.** Photomicrograph showing microcrystalline quartz-feldspar of groundmass and clay minerals by alteration (cross nicol), and **D.** Photomicrograph showing microcrystalline colorless of quartz and feldspar with chlorite (green) and opaque minerals (black) (plain polarized light).

Quartz-rich fiamme breccia facies

This facie shows massive graded bedding, fine to coarse grained, porphyritic and amygdaloidal. This rock is commonly found as a porphyritic texture on the hand specimens by diamond drill cores. Quartz-rich fiamme breccia formation is made up of massive graded units fining upward to laminated, rhyolitic clasts. The upper of the facie is commonly feldspar-phyric rhyolite facies. The bottom commonly contains lithic-rich fiamme breccias facies. From the top of this facies, the dominant lithology is poorly sorted grayish green or yellowish gray of the quartz-rich fiamme breccias.

There are also subordinate horizons of volcanogenic clastic. Locally, the dominant lithology is pale pink to brownish gray, matrix-supported, mostly monomictic and quartz-rich with one subordinate interval of clast-supported monomictic quartz-feldspar rhyolite breccia. The clast size averages from granule to pebbles and angular to subangular of shapes. In general, under the microscopic, the texture is featured by large of crystal fragments of quartz, feldspar and opaque minerals. The size of crystal fragments varies from 2 mm to 5 mm (Fig. 3.13). This texture shows clast-rich and fine-grained groundmass. This fiamme breccia is characterized by quartz and feldspar crystal clasts which are presented in K-feldspar staining technique. However, the phenocrysts of crystal clast are shown as amygdule and vesicular forming. Most of them have an angular shape with altered to secondary mineral such as chlorite, illite/sericite and clay minerals.
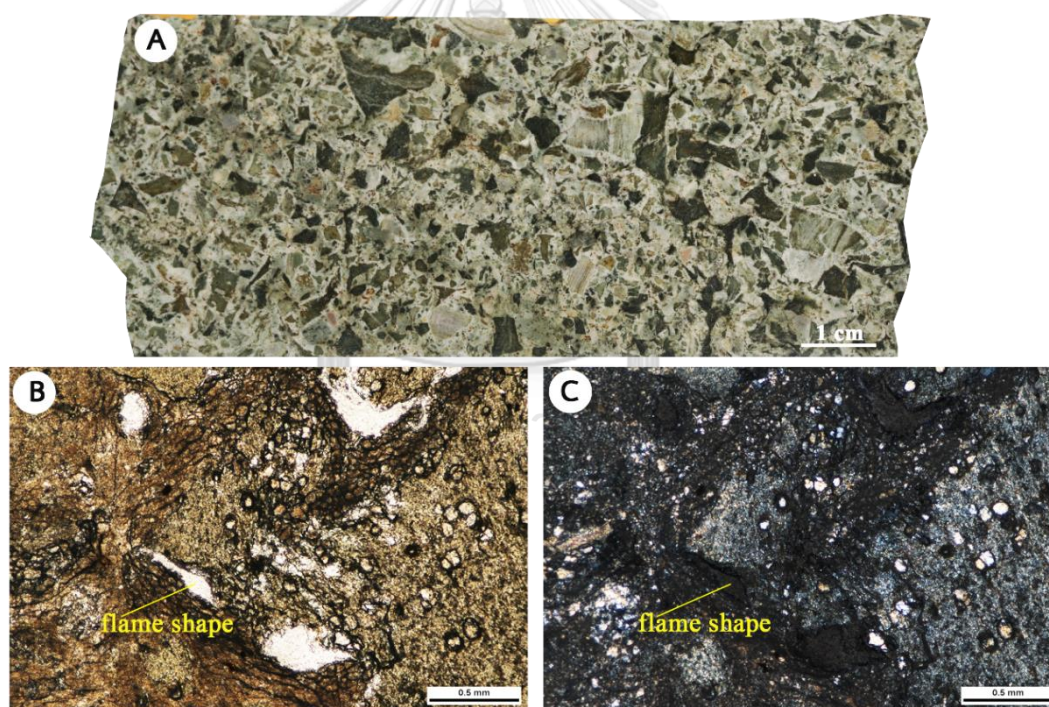
Fig. 3.13 Quartz-rich fiamme breccia (sample No. 4138-53.30m) **A.** Photograph showing angular shape of pumice clasts, poorly sorted and moderate compaction and defined to autoclastic texture. **B.** Anhedral to subhedral of quartz (cross nicol) and **C.** Flame texture of quartz and lithic rich fragments showing jigsaw-fit texture (plain polarized light).

Lithic-rich fiamme breccia facies

The lithic-rich facies are up to 30 m in thickness and have gradational contact with rhyolite facies. Rocks in the facies comprise pumice and lithic clasts in a wide

range of grain sizes (fine ash to pebble) (Fig. 3.14). The characteristics of fiamme texture are flattened of glass shards, elongate crystals and welded pyroclastic flow deposits. The rocks in study area are generally angular in clasts shape, poor-sorted, matrix-supported, massive stratified and dominantly quartz clasts. The fiamme breccia unit is composed of plagioclase-phyric, flame pumice clasts (30-50%), quartz-plagioclase crystal fragments (5-30%), vesicular volcanic lithic clasts (5-10%) and volcanic lithic clasts (20-50%). The lithic clasts are angular or elongate shape with mosaic textures. They are enclosed in pale gray-creamy quartz-feldspar-altered boundaries that are product of hydrothermal alteration. The proportion of clasts have been varied considerably in intervals from sand to pebble in size. Locally, groups of lithic clasts have fine-grained matrix, jigsaw-fit texture, parallel flame or glassy lenses, tube vesicles of clasts and feldspar-phyric scattered among clasts. The glassy lenses clasts are flame-like shapes in welded pumice breccia that are called fiamme breccias.
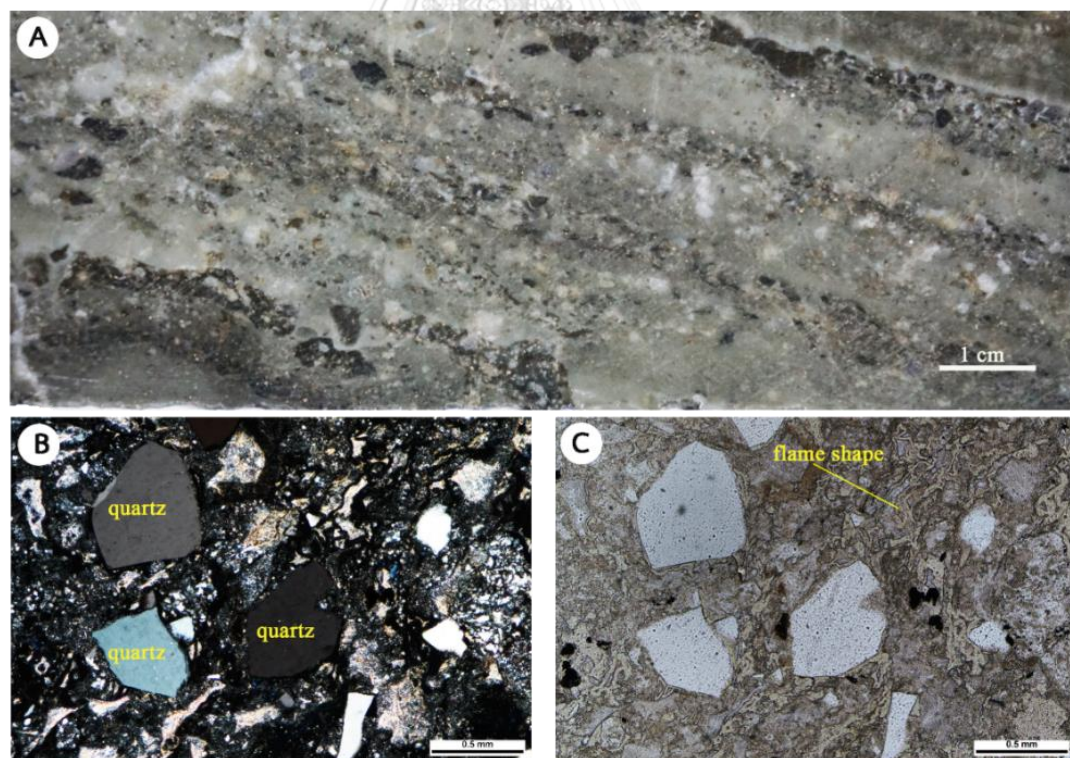
Fig. 3.14 Lithic-rich fiamme breccia, **A.** Photograph showing drill core slab sample of altered lithic-rich fiamme breccia (sample No. 4066-140.70m), **B.** Photomicrograph of lithic clast of plagioclase, quartz and altered of minerals with microcrystalline groundmass texture (cross nicol), and **C.** Photomicrograph of crystal clasts and groundmass which shows flame like shape textures of fiamme breccia (plain polarized light).

The fiamme breccias have wide variety of shapes. They have flame-like, brush-like, bow-tie, irregular branching, wedge and blocky (Gifkins et al., 2005). Some fiamme breccias are commonly interconnected, aligned parallel, laminated bedding and have random orientations. Locally, fiamme breccias are deformed and composed of green-pale gray feldspar-phyric clasts. The crystal fragments and matrix (shard and feldspar crystal fragments, 2 mm - 5 mm) are silicified and compacted. The distribution and contact relationships among the stratified pumice breccia and fiamme breccias are complex. Commonly there is a gradational contact from rhyolite facies at bottom.

3.5 Geochemistry

The geochemistry of rock classification is usually used for identification of geochemical indicator of the element compositions. For examples, elemental analyses, distribution and concentration of major oxides and trace element are used to defined type of rocks. This section will report the whole-rock major oxides, trace and rare earth element geochemical data plots.

3.5.1 Major elements geochemistry

The total of 18 samples representing coherent lava and monomictic breccia samples have been analyzed using X-ray fluorescence (XRF) analysis method. The XRF analyses have been undertaken at the Department of Mineral Resource (DMR). These samples were chosen carefully of fresh and less altered rock and the result of whole rock major oxides is presented in Table 3.1.

The host volcanic rocks from the Suwan prospect were classified based on their SiO_2 content although rocks of older ages referred to the Chatree volcanic host sequence that has ages of 258 to 250 Ma (Salam et al., 2014). The Suwan hosted volcanic sequences also believed to have similar age could also been altered to certain level. Hence, the data from this study were plotted to verify their degree of hydrothermal alteration affecting on volcanic rocks was evaluated in parts using the diagram of Madeisky (1996). The diagram suggests that most of the Suwan volcanic rocks have molar (K + Na + 2Ca)/Al (1 is unaltered rocks; Booden et al., 2010). Whole rock major element concentrations of representative volcanic rocks are

presented in Table 3.1 and calculating to molar in Appendix C. Diagram of the K/Al vs. (K+Na+2Ca)/Al molar ratios (Madeisky & Stanley, 1993; Madeisky, 1996) is typically used to evaluated K-metasomatism and mass transfer in related to hydrothermal alteration minerals from whole-rock geochemical data. In this diagram (Fig. 3.15), fresh rocks will usually plot on or near to plagioclase K-feldspar and Ca-gain line. This diagram shows that the most altered rocks from the study area display between albite/plagioclase and K-Na, Ca-loss with interlayered illite-smectite, whereas slightly altered rocks plot to the right of that zone. The line slop 1 that extends from the origin to 1,1 represents rocks that contain no Ca or Na (Warren et al., 2007). Along this line, the data plot has only one sample of plagioclase-phyric andesite locate close to the interlayered illite-smectite zone. The molar value of K/Al is 0.02 to 0.27 that contain K-Na with Ca-loss and trending to smectite and kaolinite-chlorite phases. The molar value of (K+Na+2Ca)/Al is 0.31 to 1.81 which represents the range near plagioclase-albite-K-feldspar of fresh rocks. Most of all molar data are typically plotted on the albite-plagioclase area of fresh rock. The result given in Table 3.1 reveals that major oxides (SiO_2) of Suwan volcanic rocks have SiO2 contents ranging from 44.7 to 65.6 wt.% which falls within basalt to basaltic andesite. The corrected major elements (Fig. 3.16) are compared to a plot of SiO_2 against Na_2O+K_2O, which is used for geochemical classification of volcanic rocks.

Table 3.1 The XRF geochemistry of least altered volcanic rocks of Suwan prospect.

Sample No.	4066-87.30	4067-27.60	4067-39.50	4067-71.50	4067-75.60	4067-128.00	4080-53.60	4080-57.80	4080-88.50
Rock types	MFR	PAD	MPHA	PAD	PHA	PHA	PHA	PHA	PAD
P_2O_3	0.07	0.12	0.07	0.11	0.13	0.07	0.11	0.09	0.11
SiO_2	65.78	54.97	57.52	44.72	52.19	49.73	53.02	45.18	50.76
Al_2O_3	11.64	17.22	11.67	16.21	15.30	15.23	15.99	18.07	17.89
MnO	0.16	0.51	0.39	0.33	0.34	0.20	0.26	0.40	0.23
Fe_2O_3	3.68	8.71	8.55	7.78	7.01	7.29	7.83	7.21	9.31
Na_2O	1.15	0.70	0.10	1.58	0.81	1.42	1.00	0.10	5.00
CaO	4.80	0.26	4.51	8.38	6.06	13.27	6.49	7.40	7.36
MgO	1.99	3.99	3.92	4.53	3.22	2.23	2.20	3.31	3.07
TiO_2	0.28	0.54	0.37	0.48	0.47	0.34	0.50	0.46	0.53
K_2O	4.07	6.90	3.55	6.87	7.71	1.94	3.42	5.04	0.89
LOI	5.50	8.43	8.04	5.77	6.90	8.03	12.27	4.34	2.03
H_2O	0.23	0.36	0.35	0.21	0.22	0.26	0.20	0.21	0.21
Total	99.35	102.71	99.04	96.97	100.36	100.01	103.29	91.81	97.39

Abbreviation: HAD = Hornblende-phyric andesite, PHA = Plagioclase-hornblende-phyric andesite, ADD = Andesite dyke, PAD = Plagioclase-phyric andesite, MFR = Monomictic-feldspar-phyric rhyolite breccia, MPHA = Plagioclase-hornblende-phyric andesite breccia.

Table 3.1 (cont.)

Sample No.	4065-98.20	4067-112.70	4080-48.30	4080-75.00	4080-99.00	4080-97.00	4080-108.00	4069-125.50	4069-141.80
Rock types	HAD	PHA	PHA	HAD	PHA	PHA	PHA	ADD	PAD
P_2O_3	0.12	0.06	0.11	0.11	0.12	0.10	0.07	0.56	0.07
SiO_2	52.02	50.89	50.13	51.69	51.82	56.81	46.86	50.51	51.57
Al_2O_3	19.52	17.60	19.41	19.95	19.78	16.63	18.55	14.06	17.62
MnO	0.16	0.27	0.17	0.18	0.17	0.11	0.53	0.24	0.23
Fe_2O_3	9.27	8.61	9.32	9.41	9.46	7.73	8.89	13.17	6.37
Na_2O	2.55	4.55	2.24	2.75	2.74	2.59	2.18	3.71	2.42
CaO	9.10	5.29	3.92	6.79	8.16	9.31	7.58	7.06	5.49
MgO	3.33	6.21	5.05	3.66	3.32	2.26	5.77	3.73	3.76
TiO_2	0.58	0.36	0.58	0.59	0.59	0.47	0.39	2.94	0.36
K_2O	0.95	1.64	2.80	2.11	1.31	0.53	2.35	0.90	4.48
LOI	3.93	5.84	2.40	2.17	3.07	6.11	2.67	2.68	6.78
H_2O	0.41	0.22	0.17	0.20	0.20	0.19	0.19	0.20	0.40
Total	101.92	101.53	96.30	99.61	100.72	102.84	96.01	99.74	99.53

Abbreviation: HAD = Hornblende-phyric andesite, PHA = Plagioclase-hornblende-phyric andesite, ADD = Andesite dyke, PAD = Plagioclase-phyric andesite, MFR = Monomictic-feldspar-phyric rhyolite breccia, MPHA = Plagioclase-hornblende-phyric andesite breccia.

○ Plagioclase-phyric andesite
△ Plagioclase-hornblende-phyric andesite
+ Hornblende-phyric andesite
× Monomictic plagioclase-hornblende-phyric andesite breccia
□ Monomictic feldspar-phyric rhyolite breccia
▽ Post-mineralization dyke
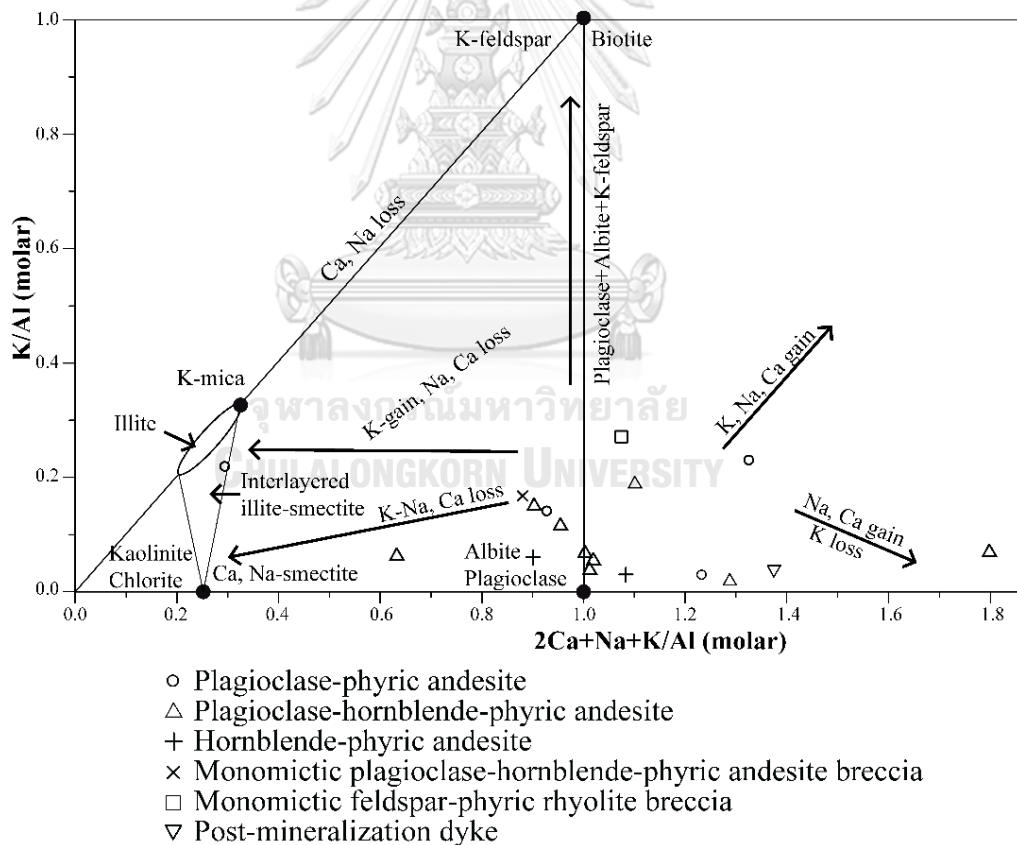
Fig. 3.15 Molar K/Al vs molar (K+Na+2Ca)/Al (Madeisky, 1996; Warren et al., 2007). In this diagram, the alteration minerals kaolinite, illite and adularia plot on a boundary zone. Unaltered andesitic volcanic rocks typically have molar (K+Na+2Ca)/Al values, which is partly observed for the Suwan Prospect volcanic rock. Most of the Suwan Prospect rocks have molar (K=Na+2Ca)/Al>0.8 to 1.4 considered to be the least altered rocks.

The TAS diagram (Le Bas et al., 1989) has been used to classify both host volcanic and post-mineralized dyke and it shows most samples were classified as intermediate to mafic rocks (Fig. 3.16) with exception of one sample was plotted in the field of felsic composition. Most rocks have variable concentration of Na_2O and K_2O (average $Na_2O/K_2O \approx 1.9$ wt.%). The total alkali-silica diagram (TAS) proposed by (Le Bas et al., 1989) is one of the most useful classification schemes available for volcanic rock. Based on diagram (Fig. 3.16), the composition of volcanic rocks from Suwan prospect were classified as andesite and rhyolite. Further confirms the petrographic investigation.
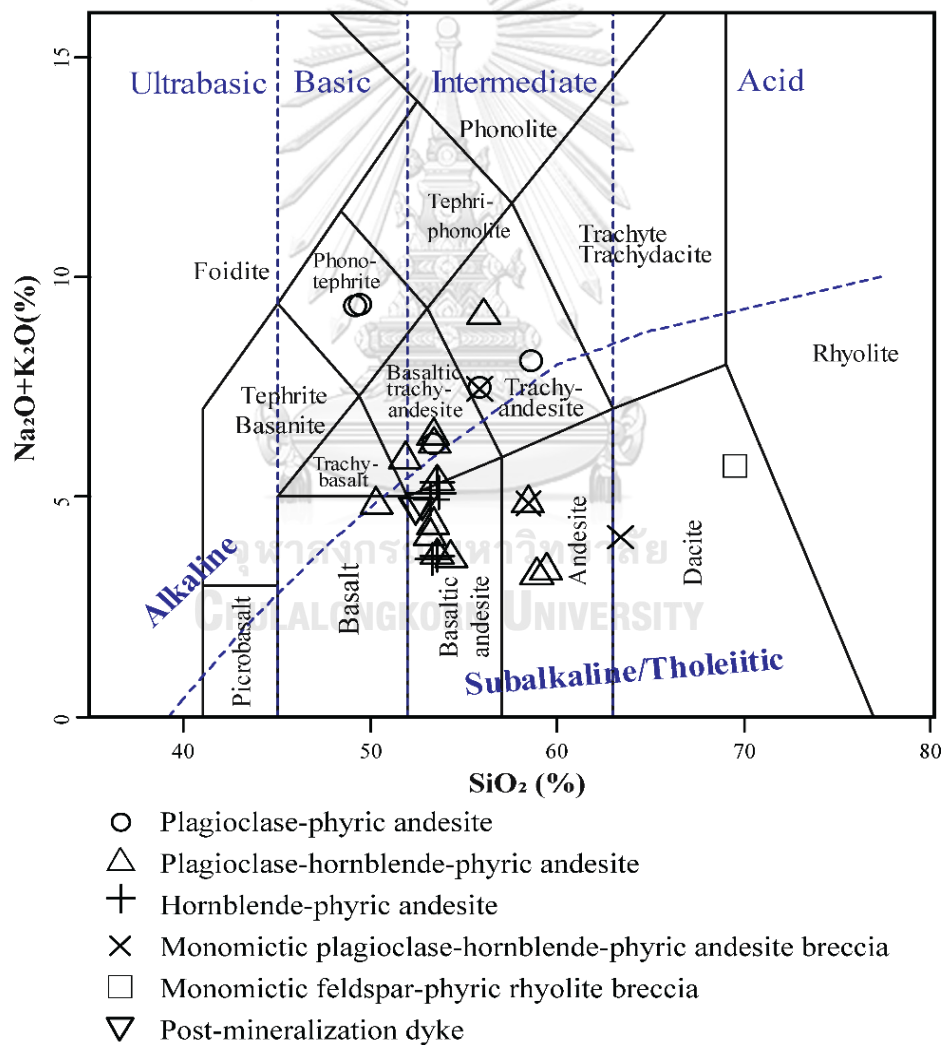
Fig. 3.16 Diagram of total alkaline vs. silica (TAS) with subdivision of the alkaline and sub-alkaline/tholeiitic (Le Bas et al., 1989).
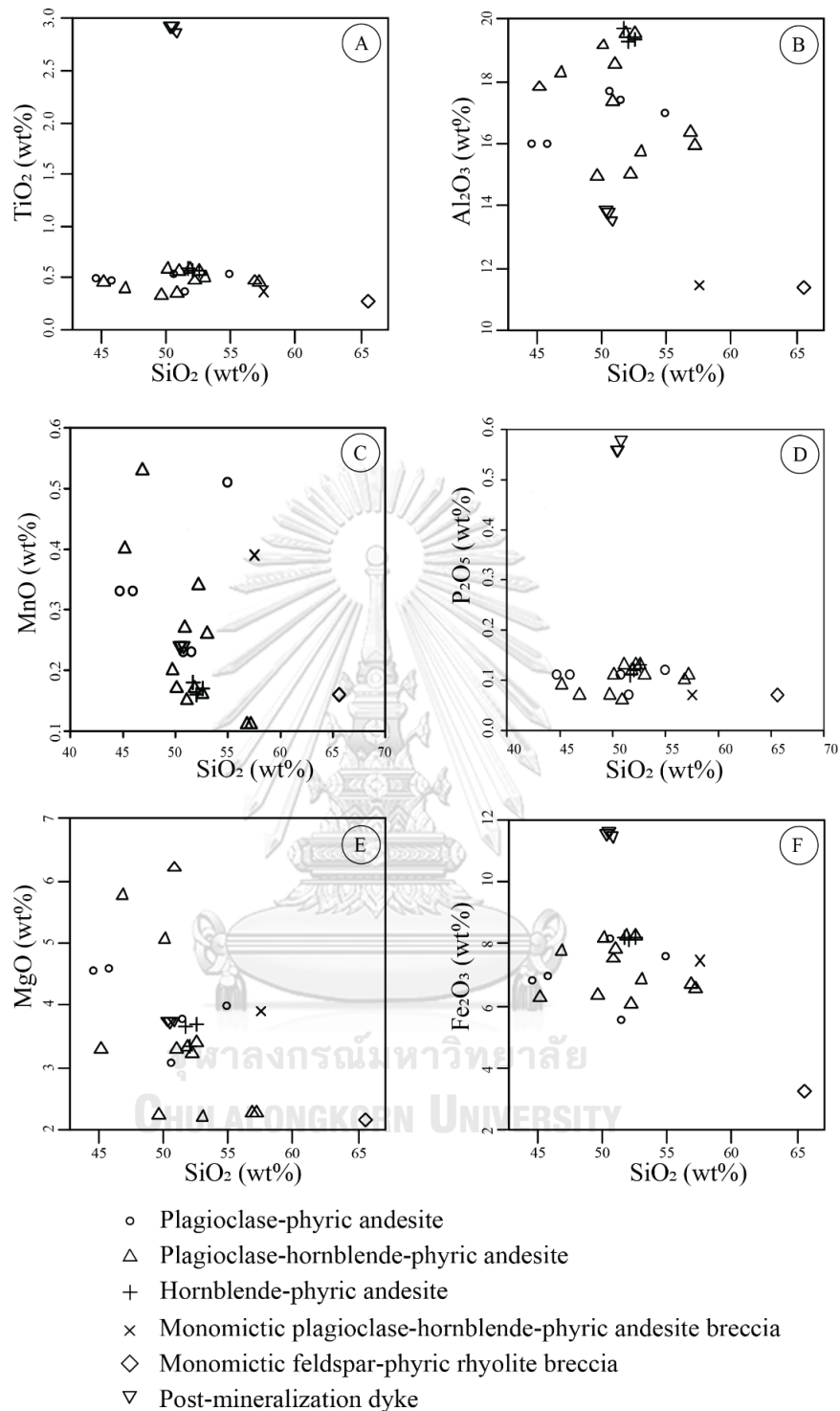
Fig. 3.17 Major element binary diagram plotted as function of SiO_2 for the host volcanic rocks and post-mineralization dykes. **A.** TiO_2 vs. SiO_2 showing low Ti values and relatively high Ti for andesite dyke, **B.** Al_2O_3 vs. SiO_2 showing high Al values for porphyritic andesite, **C.** MnO vs. SiO_2 showing slightly low Mn values and relatively high for porphyritic andesite, **D.** P_2O_5 vs. SiO_2 showing low P in host volcanics and high in dykes, **E.** MgO vs SiO_2 showing trends similar to Figure. C. and **F.** Fe_2O_3 vs. SiO_2 showing low Fe values and high Fe in dykes.

Bivariate plots for major elements versus SiO_2 (Fig. 3.17) showing low concentration of TiO_2 and P_2O_5 (Figs. 3.17 A and D) with an exception of post-mineralized andesite dyke which displays very high TiO_2 and P_2O_5 and Fe_2O_3 (Figs. 3.17 A, D and F). For hornblende-phyric andesite is high in Al_2O_3, low in MnO and similar for other major oxides. The rest of groups including plagioclase-phyric andesite, plagioclase-hornblende-phyric andesite, monomictic-plagioclase-hornblende-phyric andesite breccia and monomictic-feldspar-phyric rhyolitic breccia have similarities for most of major oxides.

For the AFM diagram (Fig. 3.18), these rocks are typically illustrated on the calc-alkaline series and some dispersion on tholeiite series. In order to classify also the kind of magma from these rock types. The geochemical compositions were plotted in AFM diagram (Irvine & Baragar, 1971). Within the mafic group (SiO_2 <52%) AFM diagram have found two different series, which are earlier classified by the petrographic studied. These major elements of volcanic rocks classification plots on the MgO-Fe_2O_3-(Na_2O+K_2O) diagram are mostly apparent on calc-alkaline series. Some of plagioclase-hornblende-phyric andesite, hornblende-phyric andesite and late dyke andesite have a tholeiite series position.
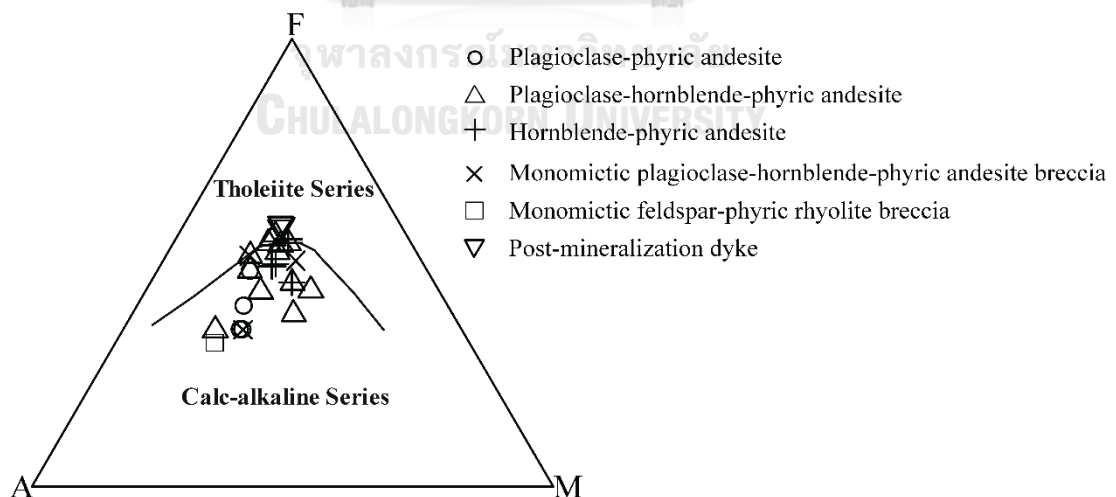
Fig. 3.18 AFM diagram (Irvine & Baragar, 1971), showing the calc-alkaline and tholeiite series of Suwan Prospect.

3.5.2 Trace element geochemistry

The result for low abundant trace and rare earth elements are shown in Table 3.2. The binary plots of these trace elements versus SiO_2 concentration show that large ion lithophile elements (LILE) such as Ba, Rb, Sr and V (Fig. 3.19). These elements have been mobilized by hydrothermal process. Whereas, Sr and V are present a trend of low values with increasing SiO_2 concentration. The diagram of Ba and Rb are present mostly low values, but high concentrations for plagioclase-phyric-andesite and monomictic-feldspar-phyric-rhyolitic-breccia. The high field strength elements (HFSE) such as Nb, Y, Ce and Zr (Fig. 3.19) have low concentration for all host volcanic rocks. However, HFSE shows high value for post-mineralized andesite dyke. Diagram of Zr/TiO_2 vs. Nb/Y (Fig. 3.20 A; Winchester and Floyd, 1977) for the Suwan host volcanic rocks and post-mineralization dykes suggested that rocks of various groups were classified as basaltic andesite and to basalt.

The high field strength elements (HFSE: Zr, Ti, Nb) which are believed to be immobile during hydrothermal processes (Pearce, 1980) for the Suwan host volcanic rocks and post-mineralization dykes reveals that mostly rocks have low Zr and Ti of island arc boundary but has single plots on the within-plate lavas of post mineralization dyke. Plot of Ti against Zr (Fig. 3.20B) presents the post-mineralization dykes has tholeiite series and basaltic-andesite unit.

3.5.3 REE geochemistry and multi element spider diagrams

REE elements variation in the volcanic host rocks and post-mineralization from study area are explained by Sample/REE primitive mantle (Boynton, 1984), Sample/OIB (Sun & McDonough, 1989) and Sample/Chondrites diagrams (Thompson, 1982). These diagrams are present on figure 3.21 and can be described into three magmatic suites of the variable REE concentration.

Suite 1 contains low Ti, P, Zr and Y (Fig. 3.21B and C) with high LREE which represented to monomictic feldspar-phyric rhyolite breccia or felsic volcanic rock of unit 1.

Suite 2 contains slightly high HREE with low LREE (Fig. 3.21A, B and C). Suit 2 is porphyritic andesite unit (unit 3) including plagioclase-hornblende-phyric andesite and monomictic basalt-andesite breccia.

Suite 3 contains very high LREE and HREE with very low Rb, Ba, Sr and Cs (Fig. 3.21B and C) which represented to alkaline metal elements. This suite is post-mineralization dykes in the study area.

Table 3.2 Abundance of trace and REE composition (in ppm) determined by ICP-MS analysis of least altered Suwan Prospect host volcanic rocks.

Sample No.	4069-125.50	4080-97.00	4065-98.30	4080-75.00	4080-99.00	4067-71.50	4066-87.30
Rock types	ADD	PHA	PHA	HAD	PHA	PAD	MFR
V	327.000	261.000	335.000	318.000	308.000	247.000	81.000
W	103.000	376.000	163.000	77.000	111.000	1.000	2.000
Y	48.200	9.300	12.000	12.000	11.900	9.800	10.200
Yb	4.480	1.040	1.320	1.380	1.310	1.040	1.020
Zr	207.00	19.000	27.000	25.000	24.000	20.000	31.000
Ba	88.20	50.40	171.50	362.00	184.00	1250.00	1200.00
Ce	37.300	5.700	8.000	7.200	7.200	4.800	8.100
Cr	10.000	10.000	20.000	20.000	10.000	30.000	90.000
Cs	0.030	0.250	0.240	0.520	0.530	0.110	0.860
Dy	8.210	1.580	2.140	2.090	1.980	1.670	1.510
Er	5.000	1.080	1.370	1.230	1.330	1.050	1.010
Eu	2.530	0.490	0.600	0.600	0.600	0.400	0.460
Ga	23.000	20.300	18.500	19.800	19.800	15.800	9.900
Gd	8.560	1.520	1.880	1.830	1.730	1.510	1.480
Hf	5.100	0.700	0.900	0.800	0.800	0.700	1.000
Ho	1.730	0.340	0.460	0.430	0.450	0.360	0.350
La	14.400	2.400	3.900	3.100	3.000	1.800	4.000
Lu	0.670	0.160	0.220	0.210	0.200	0.170	0.170
Nb	7.600	0.600	0.700	0.600	0.600	0.500	0.700
Nd	26.300	4.400	5.700	5.600	5.400	3.900	5.300
Pr	5.420	0.840	1.150	1.050	1.030	0.730	1.070
Rb	8.50	8.70	11.20	29.00	18.50	78.70	57.10
Sm	7.320	1.220	1.580	1.730	1.560	1.260	1.300
Sn	4.000	4.000	1.000	2.000	2.000	2.000	3.000
Sr	172.00	424.00	498.00	702.00	517.00	248.00	130.00
Ta	0.700	0.700	0.300	0.100	0.200	<0.1	<0.1
Tb	1.370	0.240	0.330	0.310	0.320	0.260	0.240
Th	1.620	0.170	0.260	0.240	0.230	0.180	0.440
Tm	0.710	0.140	0.200	0.190	0.180	0.160	0.160
U	0.550	0.070	0.110	0.100	0.080	0.070	0.150

Abbreviation: HAD = Hornblende-phyric andesite, PHA = Plagioclase-hornblende-phyric andesite, ADD = Andesite dyke, PAD = Plagioclase-phyric andesite, MFR = Monomictic-feldspar-phyric rhyolite breccia, MPHA = Plagioclase-hornblende-phyric andesite breccia.
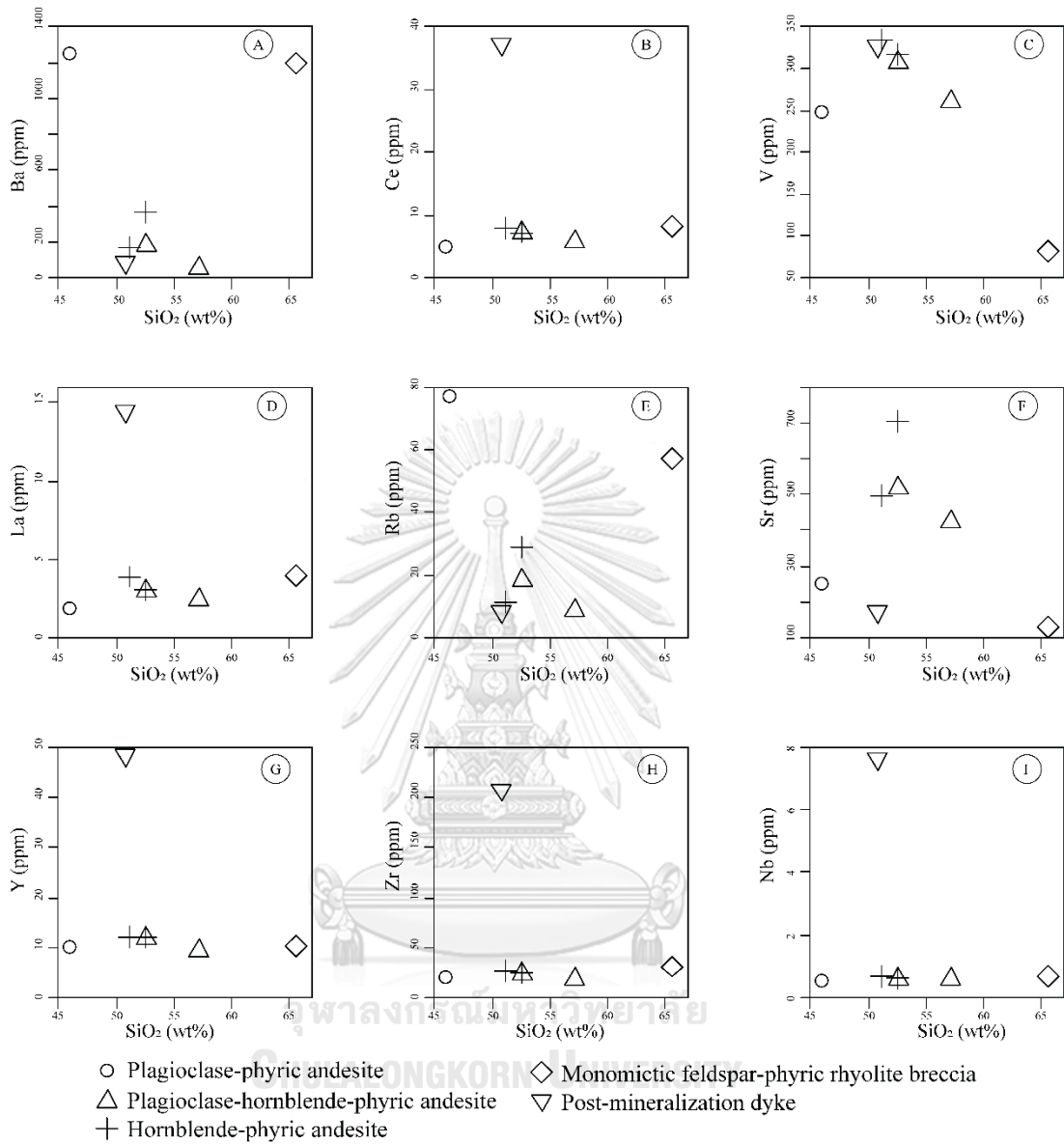
Fig. 3.19 Selected high field strength elements (HFSE), trace element and large ion lithophile elements (LILE) plotted against SiO$_2$ for host volcanic rocks at Suwan Prospect. **A.** Ba vs SiO$_2$ showing mostly low Ba and high for monomictic rhyolite breccia, **B.** Ce vs SiO$_2$ showing high values for volcanic dykes, **C.** V vs SiO$_2$ showing mostly high values and low value only monomictic rhyolite breccia, **D.** La vs SiO$_2$ showing mostly low La values and high for dykes, **E.** Rb vs SiO$_2$ showing mostly low Rb value and high monomictic rhyolite breccia, **F.** Sr vs SiO$_2$ showing dispersion low to high Sr values, **G.** Y vs SiO$_2$ showing low Y values and high for dyke, **H.** Zr vs SiO$_2$ showing low Zr values and high for dyke and **I.** Nb vs SiO$_2$ showing low Nb values and high for volcanic from dyke.
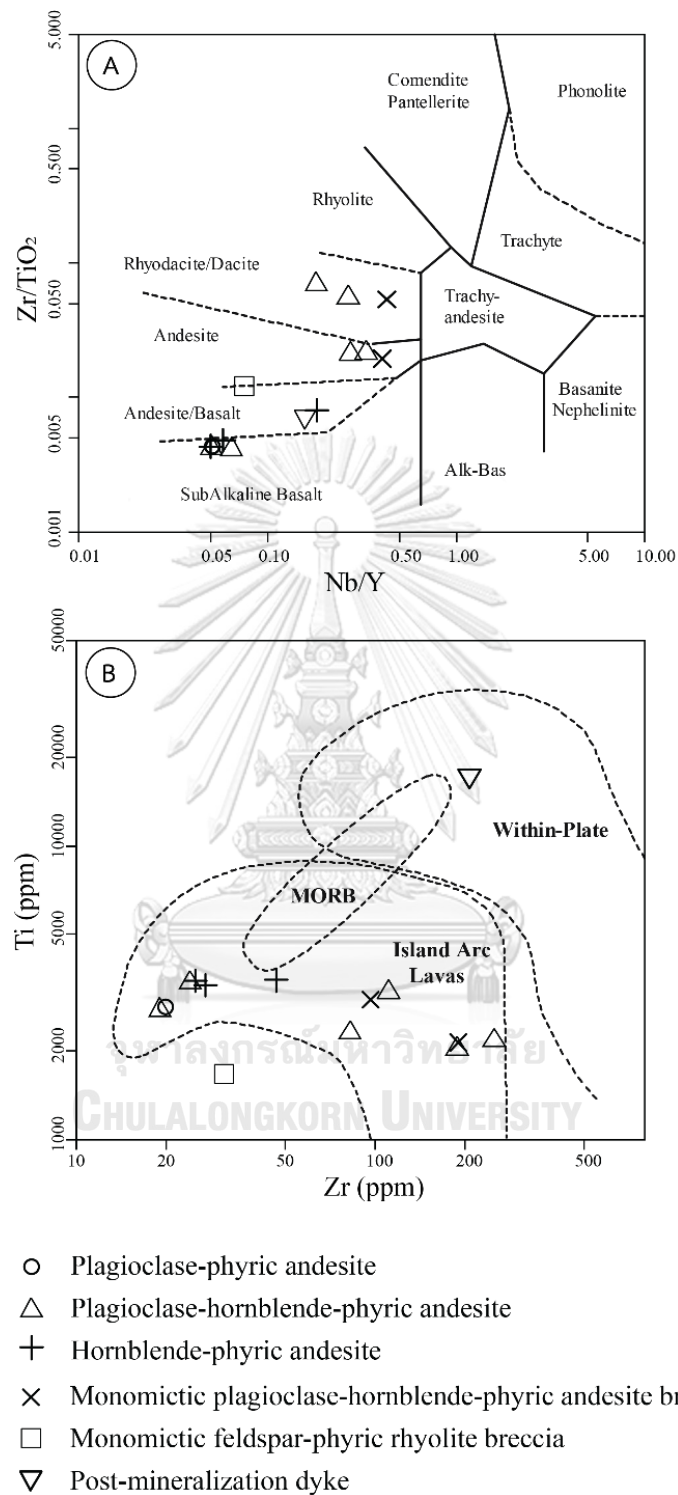
Fig. 3.20 **A.** Nb/Y and Zr/TiO₂ diagram for Suwan Prospect volcanic host rocks after (Winchester & Floyd, 1977) and **B.** Plot of Ti vs. Zr the fields of island arc lavas, within-plate lavas for different tectonic setting after (Pearce & Norry, 1979).

- ○ Plagioclase-phyric andesite
- △ Plagioclase-hornblende-phyric andesite
- + Hornblende-phyric andesite
- × Monomictic plagioclase-hornblende-phyric andesite breccia
- ◇ Monomictic feldspar-phyric rhyolite breccia
- ▽ Post-mineralization dyke
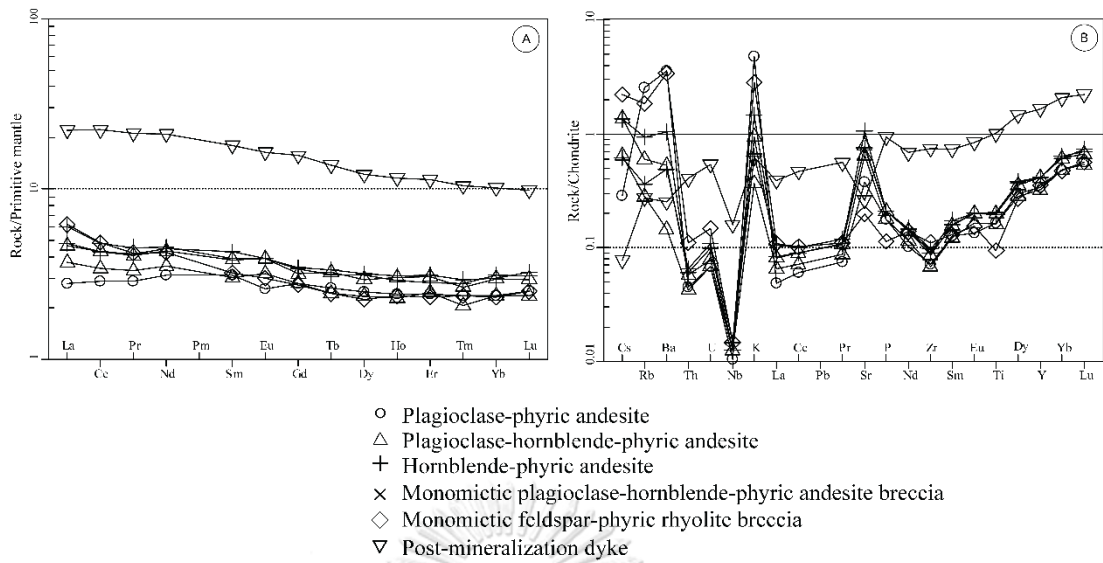
Fig. 3.21 **A.** Primitive mantle-normalized REE patterns of host volcanic rocks and post-mineralization dykes from Suwan Prospect (after McDonough and Sun, 1995) and **B.** Chondrite-normalized spider diagram (after Sun and McDonough, 1989).

CHAPTER 4
MINERALIZATION AND ALTERATION

4.1 Introduction

This chapter documents characteristics of mineralization, mineral paragenesis, mineral assemblages and hydrothermal alteration of gold-silver epithermal deposit at Suwan prospect.

4.2 Mineralization

Gold-silver mineralization at Suwan prospect occurs as veins, veinlets and minor breccia hosted in volcaniclastic rocks (details in Chapter 3). Core logging data reveal that major quartz veins at this prospect strike northwest-southeast, which is similar general strike of main structures at the Chatree deposit. Based on cross cutting relationships, veins mineral assemblages, and textural features at least three mineralization stages have been recognized namely I) pre-ore stage, II) ore stage (main gold stage), and III) post gold stage. Figure 4.1 shows veins and mineral parageneses.

Stage I: Pre-ore stage is characterized by quartz that occurs majority as silicification. The alteration assemblages are minor and trace of chalcedony, quartz, adularia, illite, chlorite, epidote and calcite. Although the ore minerals rarely occur in this stage, it is the evidence of early mineralization in the study area. Gold and silver have been associated with trace elements, which resulted in geochemistry of hydrothermal fluids and alteration styles of hosted rocks. Ores distributions may also be complex, such as chalcopyrite $\pm$ sphalerite $\pm$ galena $\pm$ electrum $\pm$ pyrite, these can be important in epithermal systems. The gold and silver distribution in Suwan Prospect were known critical environments in main-ore stage in the form of electrum. The main-ore stage included sulfide, gangues and alteration minerals, which are typically characterized material relationships in gold and silver deposits. This main stage has related to principal alteration zones, presenting silicic, argillic, propylitic and clay minerals from proximal to distal zone of the altered rocks. The major ore

minerals are pyrite, chalcopyrite, galena, sphalerite and electrum which are minor in pre-stage and post-stage of mineralization. Post-ore stage was characterized by carbonate ± quartz veins and rare pyrite with slightly altered host rocks. Late stage veins cross cutting all stages are commonly barren and absence of sulfides.

4.3 Paragenesis and characteristics of mineralization stages

The paragenetic sequence of mineralization at Suwan Prospect is relatively simple (Table 4.1) compared to those of Chatree deposit previously studied by many workers (Cumming et al., 2008; Salam, 2013; Salam et al., 2014).

Based on cross cutting relationships, veins mineral assemblages, and textural features at least three mineralization stages have been recognized namely, I) pre-ore stage, II) ore stage (main gold stage), and III) post gold stage. Figure 4.1 shows veins paragenesis sequence, and mineral paragenesis.

Table 4.1 Diagram showing generalized paragenesis of mineralization and alteration assemblages of the Suwan Prospect.

Ore stages / Minerals	Pre-gold Stage (I)	Gold Stage (II)	Post-gold Stage (III)
	Early --→ Late		
Ores			
pyrite			
chalcopyrite			
galena			
sphalerite			
arsenopyrite			
electrum			
Gangues			
quartz			
chalcedonic-quartz			
chlorite			
calcite			

Alteration mineralogy associated with Gold Stage (II)
quartz
adularia
illite/smectite
chlorite
calcite
kaolinite

▬▬▬ Major   ▪▪▪▪ Minor   ------ Trace

4.3.1 Pre-gold stage

Pre-gold stage is characterized by small quartz veins/veinlets, and minor stockworks consisting of almost quartz (Fig. 4.1). Quartz forms as microcrystalline and occasionally as very fine-grained. It has been observed mainly as crosscut veins in porphyritic andesite and volcanogenic sedimentary rock units. Several types of zoning are present in breccias of fault zones. These zones were strongly altered and cemented with silicic fluids and they formed quartz ± pyrite of the hydrothermal breccia. The hydrothermal breccias composed mostly of silica phases, adularia and pyrite. They form matrix-support zones along hydrothermal fluid channel that have commonly angular clasts from 1 cm to 10 cm in diameter. The breccias localities comprise silicified texture that is generally filled with microcrystalline to euhedral quartz, pyrite and rare sulfide minerals (Fig. 4.1).
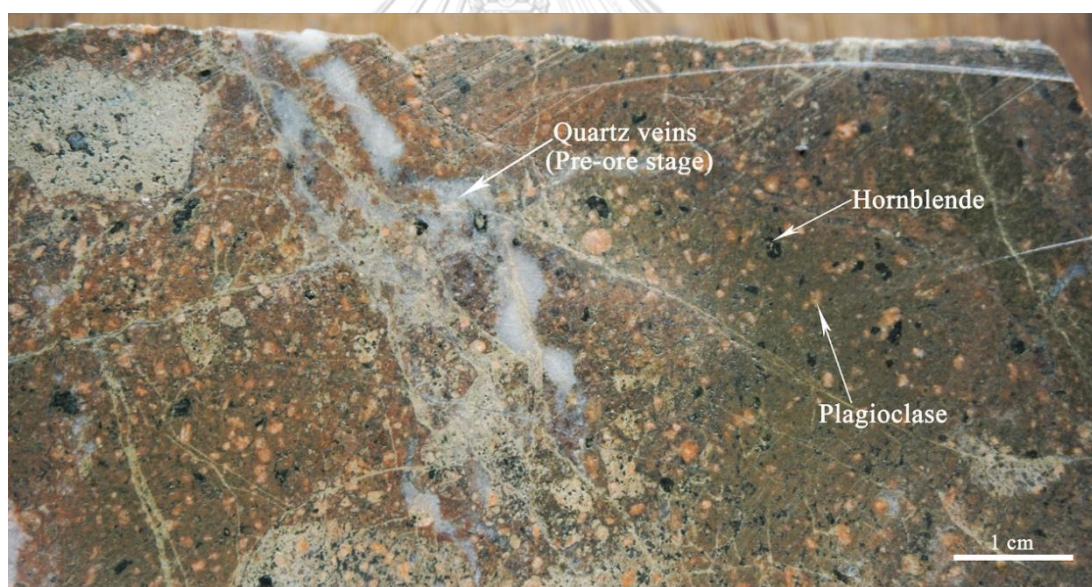
Fig. 4.1 Photograph showing quartz veins cross-cut monomictic plagioclase-hornblende-phyric andesite breccia (sample No. 4067-122.00 m).

4.3.2 Main-gold stage (gold mineralization stage)

The main gold stage occurs as breccia filling and veins/stockwork. The thickness is generally less than 5 cm, but orientation is not known because at the time of study, as diamond drill cores were already split. The veins of this stage are described as quartz-carbonate ±chlorite- sulfide-gold bended veins and stockworks. They are characterized by white to grayish green to pale green in diamond drill core (Fig. 4.2).

Stage 2 veins commonly display a typical epithermal low sulfidation quartz veins such as crustiform texture and colloform banding. The veins of this stage are commonly hosted in plagioclase-hornblende-phyric andesite (porphyritic unit) which is dominated with breccias facies (Fig. 4.2). The thickness of the gold bearing stage veins range from 1-5 cm and occasionally can be up to 10 cm width or more. Stage 2 mineralization often crosscut the pre-ore stage veins (Fig. 4.2). Veins of this stage are commonly characterized by subhedral to euhedral quartz at the contact with wall rocks and point out to center of veins (Fig. 4.2). It displays a typical open space filling fracture like texture observed in epithermal quartz veins.
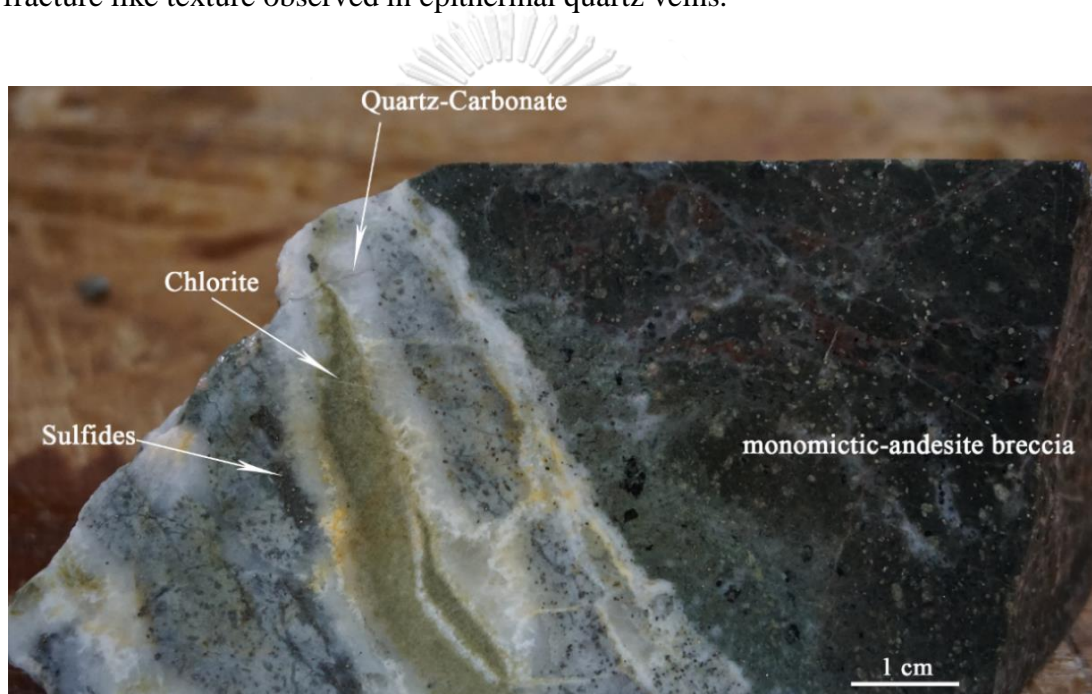
Fig. 4.2 Photograph of diamond drill core of ore sample showing quartz-carbonate-sulfide vein of Main-ore stage (Sample No. 4067-148.30 m.).

In drill core, disseminated sulfides are often observed in association with fine-grained quartz forming a band next to band of euhedral quartz. At the inner part of the stage 2 veins, sulfide-rich patches or layers are often found (Fig. 4.2). Major sulfide minerals of this stage consist of pyrite with subordinate amount of chalcopyrite, sphalerite and galena (Fig. 4.3). Sulfide mineral in sulfide disseminated quartz bands is dominated by pyrite. In contrast, sulfide minerals assemblage tends to be more complicated for sulfide-rich patches/layer. Hence, they are constituted mainly of subhedral to euhedral pyrite, closely associated with chalcopyrite, sphalerite, galena

(Fig. 4.3). Chalcopyrite, sphalerite and galena are also commonly formed as inclusions in pyrite. Gold is particularly common in association with sulfide minerals within sulfide-rich patches which are relatively more abundant in sulfide band or disseminated texture (Fig. 4.3).
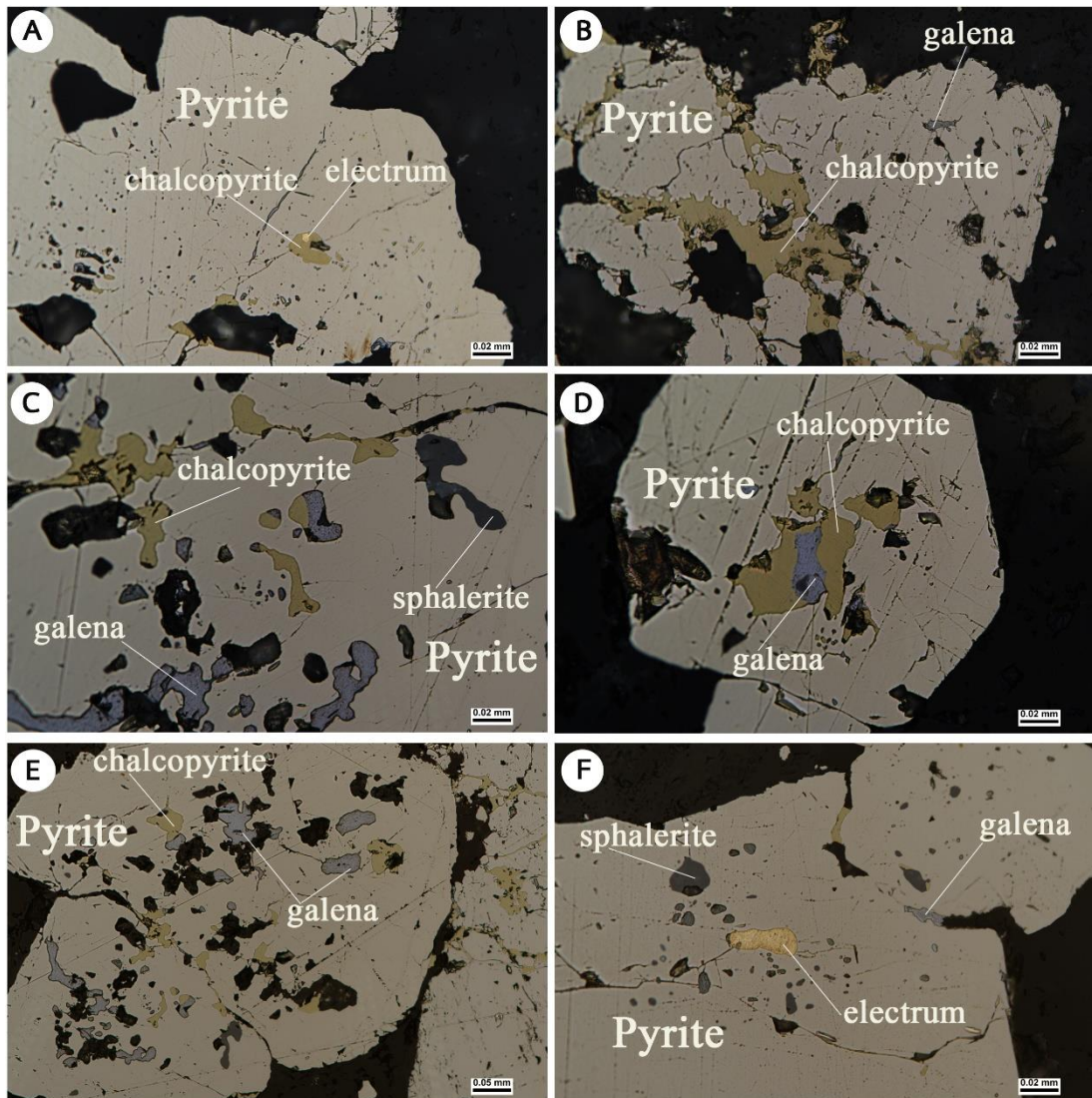
Fig. 4.3 **A.** Photomicrograph showing pyrite grain with inclusion of chalcopyrite and electrum. **B.** Massive chalcopyrite filling along the crack of pyrite grains. **C.** Chalcopyrite, galena and sphalerite filling into the porous texture of pyrite. **D.** and **E.** Chalcopyrite and galena filling into the porous texture of pyrite and **F.** Electrum inclusion in pyrite associated with sphalerite and galena.

4.3.3 Post-gold stage

This stage is characterized by small veins/veinlets of predominantly comprises of quartz with or without carbonate (Fig. 4.4). No sulfide minerals including gold

present in this stage. The carbonate minerals are commonly calcite. Cross cutting relationships suggest that at least two generations (stages) of quartz-carbonate veins/veinlets have been identified (Fig. 4.4). Both stages have similar mineral assemblages in which quartz and carbonate are the main component. Post-ore stage was characterized by carbonate ± quartz veins and rare pyrite with slightly altered host rocks. Late stage veins cross cutting all earlier stages are commonly barren and absence of sulfides.
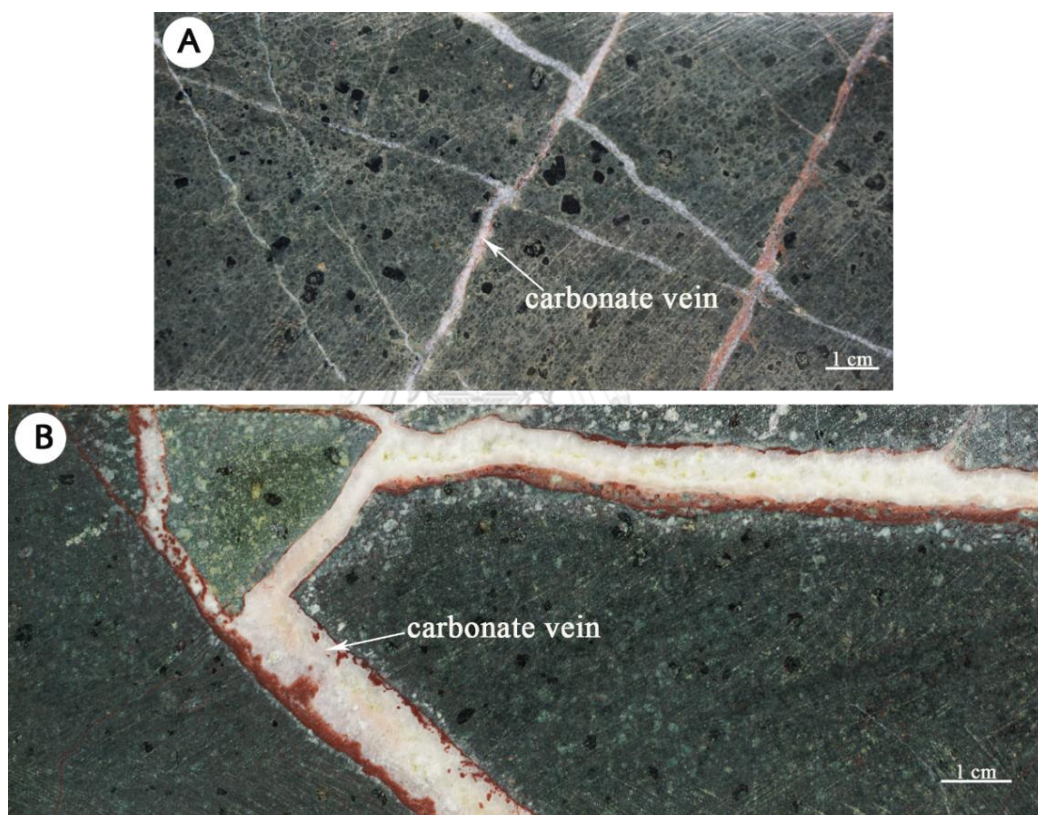
Fig. 4.4 **A.** Photograph showing carbonate veins (Post-gold stage (III), (Sample No. 4067-61.70 m) and **B.** Photograph showing carbonate veins (Post-gold stage (III), Sample No. 4080-97.00 m).

4.4 Mineralogy

The analyzes of concentration of minor elements were used EPMA instrument at the Department of Geology, Chulalongkorn University. These analyses provide some indication that concerns with the average concentration of minor elements of the ore body and the distribution of the different types of ores.

4.4.1 Sulfide mineralogy

Pyrite

Pyrites are the most common and abundant sulfide minerals in stage 2 (quartz-carbonate ± chlorite-sulfide-electrum) veins. Small amount of pyrite may also present in Stage 1 veins. Pyrite of Stage 2 veins occurs as isolated grains in association with quartz (Fig. 4.3A to F) and to some extend with carbonate and chlorite. It is also common to occur as aggregated grains or patches (Fig. 4.5A to D). Massive aggregated pyrite may occur as a continuous small veinlet.

Pyrite is also present with quartz-carbonate veins as the fragments which are associated with sphalerite, chalcopyrite and galena. Sphalerite, galena and chalcopyrite are replaced and contact with the pyrite grains. Some pyrites are recrystallized and damaged or presenting the micro-breccias (Fig. 4.6A and B). A small amount of pyrite fills cracks is replaced by chalcopyrite, sphalerite, galena and carbonate minerals with little silicates veinlet. In polished section pyrite is yellowish white, lighter than chalcopyrite, high reflectance, no bi-reflectance and is normally isotropic which occasionally presents anomalous weak anisotropy. The vein network or stockwork zone occurs mostly at contact boundary and the weakness of host rocks.

Pyrite is commonly present all mineralization stages at Suwan Prospect. Pyrite is normally associated with sulfide minerals and is abundant in all ore-forming stages, and is generally formed as euhedral to subhedral, cataclastic and aggregated grains. The grain size varies from less than 0.1 mm in diameter to greater than 0.3 mm. Locally pyrite textures are cataclastic and deformational processes which typically mechanisms affect ore minerals and wall rocks. In the photomicroscopes, they are typically euhedral coarser-grained pyrite grains (Fig. 4.5A or B). Pyrite textures are also associated with the main-ore stage, which is related to subhedral to euhedral pyrite and typically occurred with chalcopyrite, sphalerite, galena and electrum. This main stage is particularly abundant disseminated sulfide minerals in pyrite grains. For the other stages are rarely disseminated sulfide mineral in the pyrite that are mostly formed separating from pyrite grains.
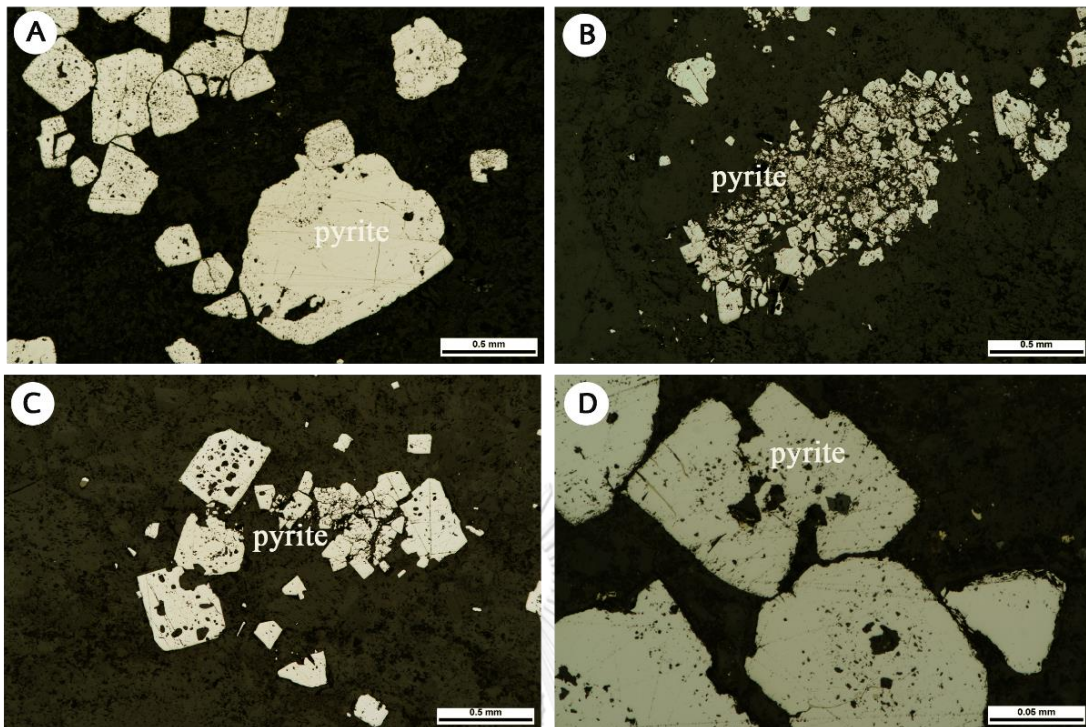
Fig. 4.5 Photomicrograph showing pyrite textures **A.** Euhedral to subhedral of pyrite grains with micro-crack and porous features of clast. **B.** Pyrite aggregate grained and destructive to finer clasts. **C.** Damage of euhedral pyrite grains and porous and micro-fracture of clasts and **D.** Euhedral to subhedral pyrite grains showing minor chalcopyrite and sphalerite fill in micro-crack and porous texture.

Chalcopyrite

Chalcopyrite forms in Stage 2 veins as fine grained (1-10 µm). It also occurs as aggregates infilled along grain boundaries of pyrite and as inclusions in pyrite, and sphalerite (Fig. 4.7). Chalcopyrite as a fracture filling in pyrite is the evidence for the main ore stage of micro-brecciation (Fig. 4.6). Chalcopyrite occurs as free grains in fracture and contact with sphalerite that is normally euhedral to subhedral and the most abundant sulfide mineral and has formed with sphalerite, chalcopyrite, galena and electrum. Locally, chalcopyrite is present as inclusion in sphalerite within the veins (Fig. 4.7). Selected chalcopyrite grains have been analyzed using EPMA method confirmed they are chalcopyrite (Table 4.2). An average of chalcopyrite composition are Fe 38%, S 33%, and Cu 28 % (Table 4.2). The analysis also reveals that chalcopyrite contains low concentrations of trace element, such as Ti, V and Sb (<0.1 weight%), As, Cd, Mo, Mn and Ni.
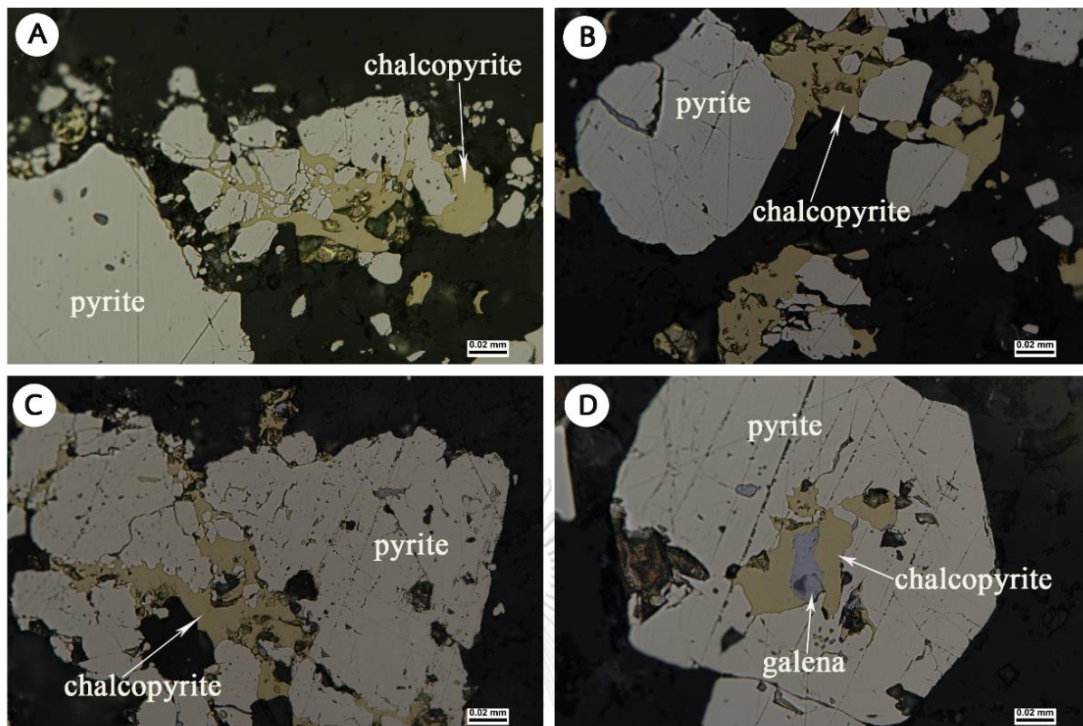
Fig. 4.6 Color reflected light photomicrograph illustrating simple grain boundary relationships between pyrite and chalcopyrite (yellow) (Sample No. 4067-61.50m).

Sphalerite

Sphalerite has been identified in Stage 2 which form fine-grained (0.01- 0.02 mm). It forms as free grains in association with quartz and disseminated or inclusions in pyrite (Figs. 4.7). Locally, sphalerite displays chalcopyrite disease (Fig. 4.7). Sphalerite composition obtained from EPMA analysis range from 26% to 71% Zn and average 63%, average of 5% Fe and average of 4% Cd (Table 4.3). The most common form of abundant sphalerite is in pyrite grains (Fig. 4.7). In rare area sphalerite is found as contacts with electrum, but it is a common relationship of the mineralization (Table 4.3).

Galena

Galena occurs in minor amount in Stage 2. It forms as inclusion in larger pyrite grains, and occasionally associatew with sphalerite and chalcopyrite (Figs. 4.3 and 4.6D). Galena is formed as anhedral to subhedral and occasionally infilled fracture in pyrite (Figs. 4.3C and F). The microscopic galena is usually found as intergranular filling along crack in pyrite (Fig. 4.7). Galena also forms as microscopic

blades accompanying sphalerite in chalcopyrite, between grains of sphalerite and pyrite, and between grains of sphalerite and as microscopic disseminates in pyrite grain. Galena and chalcopyrite often occur together with mutual contacts in fracture filling pyrite (Fig. 4.6D). Electron probe microanalysis (EPMA) of (n=21) galena shows concentration of Pb (~ 71%), S (~ 19%), Fe (~ 8 %) and trace of Cd (~ 0.17 %) (Table 4.4).
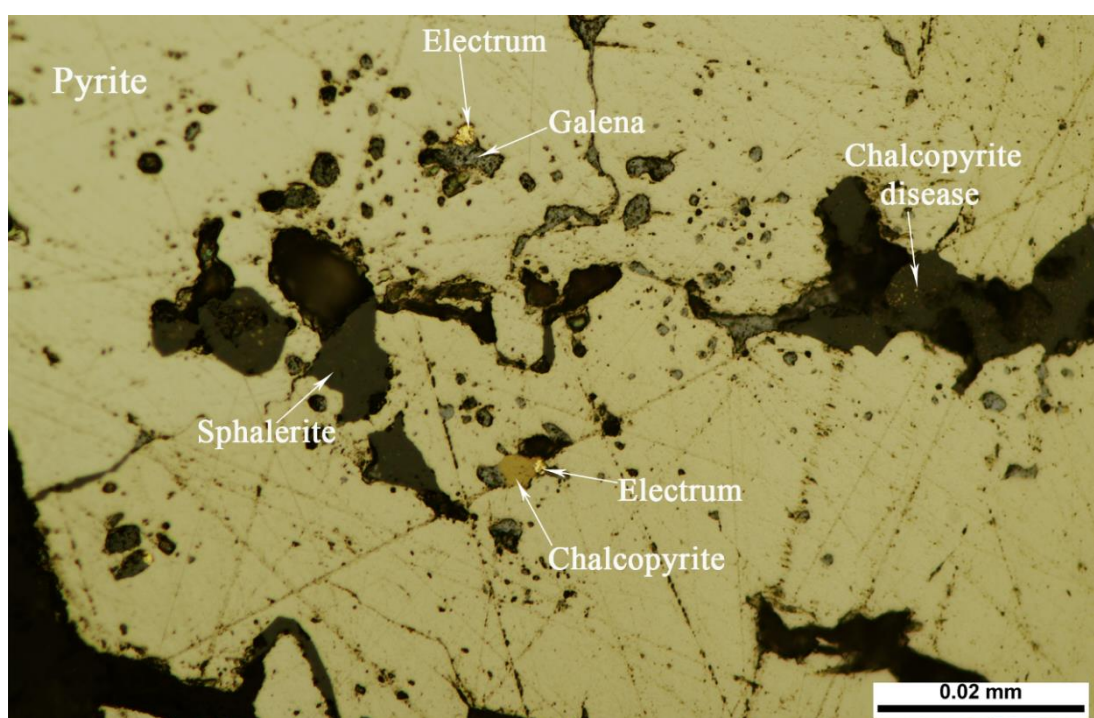
Fig. 4.7 Photomicrograph of polished mouth section showing sphalerite, chalcopyrite, galena and electrum filling in pyrite fracturing with chalcopyrite disease in dark sphalerite irregular shape (Sample No. 4067-38.00 m).

Electrum

Gold has been observed only in Stage 2 veins. It occurs mainly as inclusions in sulfide minerals especially in pyrite. Gold is often associated with chalcopyrite, sphalerite and galena and inclusion in subhedral pyrites (Figs. 4.7 and 4.8). The grain size of gold varies from less than 5 µm in diameter to greater than 20 µm. EPMA has been used to confirm petrographic identification of gold. EPMA results are given in Table 4.5. Total analyses of gold grain (n=9) revealed that it composes 47% Au and 37% Ag. EPMA data were also used to calculate fineness using the formula of (100xAu/(Au+Ag)); Morrison et al. (1991). Gold from Suwan Prospect has fineness

rage from 400 to 680. The average gold fineness of electrum at Suwan Prospect is 600. According to Morrison et al. (1991), fineness above 800 is classified as native gold and therefore gold at Suwan Prospect is concluded as electrum. EPMA mapping of sulfides and gold inclusions further support the present of electrum in Stage 2 mineralization stage (Fig. 4.9).
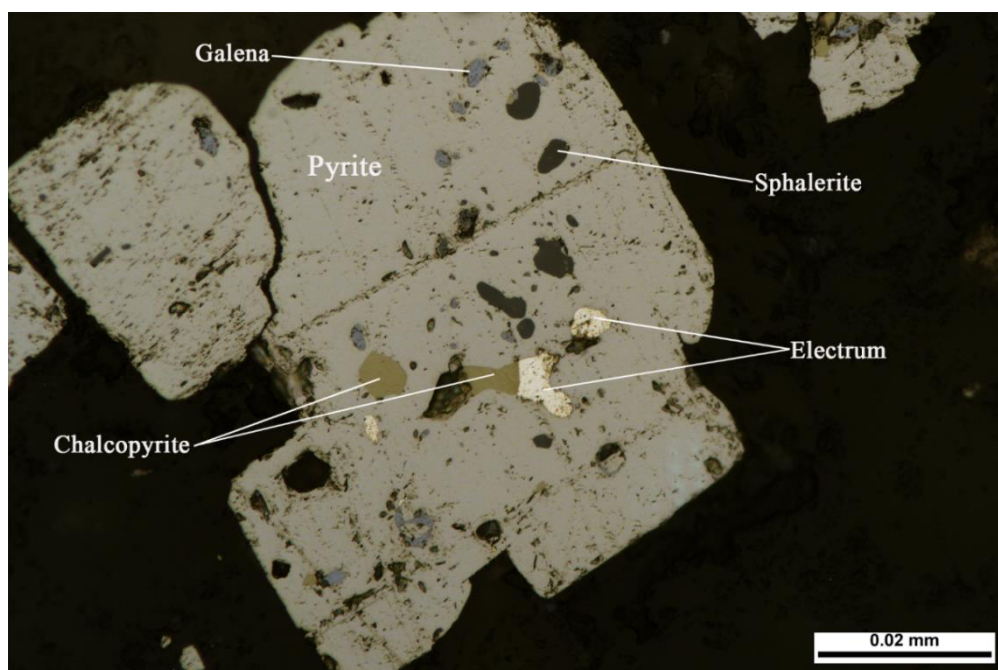
Fig. 4.8 Photomicrograph showing electrum, galena, sphalerite and chalcopyrite disseminations in pyrite grains (Sample No. 4067-110.20 m).
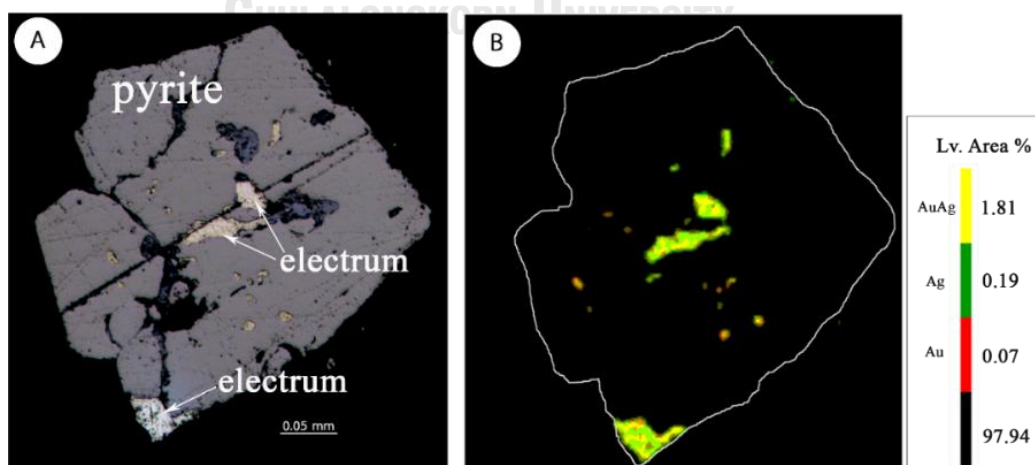
Fig. 4.9 Sulfide contains inclusions; **A** Photomicrograph of euhedral pyrite contains inclusions of electrum **B**. EPMA mapping showing Au and Ag concentration with color shading (Sample No. 4067-110.20 m).

Table 4.2 The EPMA pointing elements concentration of chalcopyrite grains

Elements/ Sample No.	S	As	Fe	Sb	Ag	Ni	Cu	Ti	Mo	Mn	V	Zn	Total (%)
T8-P1-2	29.424	0	31.591	0	0.1	0	37.71	0.035	0.319	0	0.025	0.16	99.364
T8-P1-3	29.202	0.011	32.078	0.002	0.006	0.051	38.388	0	0.234	0	0.023	0.005	100.000
T8-P2-4	42.977	0.086	43.068	0.083	0	0	13.542	0.002	0.239	0.002	0	0	99.999
T4-P1-1	25.252	0	34.548	0.026	0.037	0	39.686	0	0.452	0	0	0	100.001
T4-P1-5	25.406	0	34.384	0.119	0.042	0	39.504	0.01	0.435	0.008	0.031	0.06	99.999
T4-P1-10	25.962	0	34.232	0	0.063	0	39.197	0.011	0.445	0.027	0.015	0.047	99.999
M3-P1-7	32.024	0.078	35.773	0.175	0.284	0	30.612	0	0.371	0	0.025	0.046	99.388
M3-P3-19	38.564	0.039	42.579	0.098	0	0.028	17.721	0	0.268	0.015	0.03	0.077	99.419
M3-P3-20	41.481	0.01	45.566	0	0.015	0.04	12.138	0	0.436	0.04	0	0.139	99.865
Average (%)	32.990	0.030	38.405	0.070	0.063	0.010	27.779	0.004	0.375	0.013	0.015	0.054	99.806

Table 4.3 The EPMA pointing elements concentration of sphalerite grains.

Elements/ Sample No.	S	As	Fe	Sb	Cd	Ni	Cu	Mo	Mn	V	Zn	Total (%)
T6-P1-1-2	27.888	0	1.565	0.193	1.312	0.015	0.180	0.166	0.005	0.002	68.285	100.000
T6-P3-2	32.980	0.019	15.017	0.230	1.484	0	2.284	0.203	0	0.032	47.751	100.000
T6-P4-1	26.245	0	3.438	0	1.221	0	3.290	0.318	0	0.007	65.412	100.000
T8-P2-3	26.821	0	3.876	0.092	0.167	0	0.047	0.294	0.130	0	68.554	99.981
M1-P1-1	24.021	0	3.910	0.039	5.179	0	2.552	0.336	0.078	0	63.067	100.000
M1-P1-8	22.987	0.022	3.332	0	5.412	0	0.966	0.418	0	0.006	66.434	99.992
M1-P1-10	23.376	0.014	2.103	0	5.646	0.017	1.185	0.194	0.018	0.017	67.429	99.999
M1-P111	23.340	0	2.785	0	5.334	0	1.503	0.225	0	0.031	65.941	99.998
M1-P1-12	23.876	0.012	3.416	0	5.107	0.012	2.058	0.266	0.029	0	64.975	100.001
M1-P1-14	24.480	0.022	1.649	0	5.155	0.006	1.184	0.236	0	0	66.539	99.999
M1-P1-15	23.993	0	4.134	0	4.548	0.015	2.941	0.237	0.019	0.038	62.211	100.001
M1-P2-1	22.801	0	2.182	0	14.72	0	0	0.223	0.378	0.002	59.687	99.993
M1-P2-2	23.528	0	2.132	0	12.705	0	0.011	0.199	0.34	0.008	60.937	99.945
M1-P2-3	23.229	0	2.738	0	9.204	0.027	0.174	0.285	0.106	0.010	63.597	100.001
M1-P2-4	24.551	0.088	3.705	0.065	5.412	0.043	0.019	0.159	0	0.025	65.866	99.985
M2-P2-6	24.568	0	2.107	0	0.508	0	0.078	0.197	0.575	0.026	71.480	99.999
M3-P1-3	26.635	0.014	3.420	0.034	0.604	0	0.025	0.244	1.446	0.021	67.135	99.999
M3-P1-8	40.229	0.016	32.346	0.071	1.407	0	0.106	0.255	0.013	0.038	25.497	99.998
M3-P1-12	29.503	0	8.629	0.167	0.362	0	0	0.186	0.695	0.030	59.655	99.999
M3-P2-7	26.749	0	3.038	0.108	0.846	0	0.394	0.229	1.256	0	66.405	100.000
M3-P2-8	27.100	0	2.696	0	0.919	0.017	0.019	0.203	1.335	0.035	66.982	100.000
M3-P2-10	26.823	0.007	2.352	0	0.882	0	0.034	0.213	1.149	0.031	67.865	100.001
M3-P3-18	27.041	0	2.548	0	3.407	0.011	0.005	0.238	0.333	0.017	66.316	100.001
T6-P1-1-2	27.888	0	1.565	0.193	1.312	0.015	0.180	0.166	0.005	0.002	68.285	100.000
Average (%)	26.207	0.009	4.918	0.043	3.980	0.007	0.828	0.240	0.344	0.016	62.957	99.995

Table 4.4 The EPMA pointing elements concentration of galena grains.

Elements/ Sample No.	S	Fe	Sb	Cd	Ag	Pb	Ni	Cu	Mn	V	Total (%)
T6-P2-3	27.042	13.433	0	0.223	0	59.080	0	0.149	0.058	0.014	99.999
M1-P1-3	12.615	1.746	0	0.009	0	85.570	0.003	0	0	0.058	100.001
M1-P1-9	42.331	50.861	0	0	0.097	6.258	0	0	0.009	0	99.556
M2-P2-1	15.510	0.074	0.010	0.095	0	84.166	0.018	0.107	0	0.021	100.001
M2-P2-2	15.668	0.115	0	0.321	0	83.770	0	0	0	0.031	99.905
M2-P3-1	16.122	1.161	0	0.191	0	82.375	0.035	0	0	0	99.884
M2-P3-2	15.508	1.260	0	0.149	0	83.084	0	0	0	0	100.001
M2-P3-3	15.525	16.774	4.497	0.000	0.464	58.030	1.213	1.963	0	0.214	98.680
M2-P3-4	15.534	2.215	0	0.220	0	81.884	0.023	0.087	0.037	0	100.000
M2-P3-5	16.477	1.290	0	0.260	0	81.847	0.041	0.049	0	0.035	99.999
M2-P3-6	16.442	1.371	0	0.173	0.026	81.867	0.010	0.026	0.055	0.030	100.000
M2-P3-7	16.241	0.661	0	0.260	0	82.637	0	0	0	0.030	99.829
M2-P3-8	16.734	0.956	0	0.188	0	81.965	0	0.074	0.032	0.050	99.999
M2-P3-9	16.573	2.384	0	0.201	0	80.609	0	0.130	0	0.085	99.982
M3-P3-4	19.579	1.041	0	0.273	0	78.875	0	0.063	0.030	0.091	99.952
M3-P3-9	19.237	1.578	0.024	0.216	0	78.757	0.110	0.009	0.041	0.028	100.000
M3-P3-15	18.855	2.331	0	0.181	0	78.545	0	0	0	0	99.912
M3-P3-17	17.454	0.826	0	0.357	0	81.363	0	0	0	0	100.000
M3-P3-24	31.072	23.467	0	0.134	0.097	45.133	0.065	0	0	0.017	99.985
M5-P2-2	18.030	14.558	0	0.100	0.043	67.135	0.076	0.024	0	0.030	99.996
M5-P2-3	30.521	36.954	0	0.075	0	32.296	0	0	0	0	99.846
Average (%)	19.670	8.336	0.216	0.173	0.035	71.202	0.076	0.128	0.012	0.035	99.882

Table 4.5 The EPMA pointing elements concentration of electrum grains.

Elements/ Sample No.	S	As	Au	Fe	Cd	Ag	Ni	Cu	Mo	Mn	V	Zn	Total (%)
M1-P1-2	0.151	0.024	63.969	0.956	0.269	34.469	0.019	0.075	0	0	0.068	0	100.000
M1-P1-7	1.453	0	9.546	1.616	0.431	86.564	0.025	0.183	0.156	0	0	0.025	99.999
M1-P1-17	0.278	0	49.542	0.48	0.252	49.142	0.026	0	0	0.055	0.07	0	99.845
M3-P1-6	0.064	0	61.099	0.663	0.216	37.545	0	0.212	0.116	0	0.046	0.04	100.001
M3-P1-11	37.597	0	15.787	38.083	0.011	7.961	0	0.058	0.245	0.088	0.048	0.123	100.001
M3-P3-1	0.185	0	64.575	0.107	0.188	34.855	0	0.047	0.019	0	0.025	0	100.001
M3-P3-3	4.747	0	60.732	5.682	0.091	28.579	0.033	0.001	0.041	0.041	0.038	0	99.985
M3-P3-5	21.358	0.093	35.842	20.142	0.116	22.151	0.044	0	0.231	0	0.023	0	100.000
M3-P3-6	0.066	0	60.959	0.277	0.18	38.342	0.03	0	0.029	0.01	0.049	0.058	100.000
Average (%)	7.32	0.013	46.89	7.56	0.19	37.73	0.18	0.58	0.84	0.19	0.37	0.24	102.100

4.4.2 Gangue minerals

Gangue minerals identified in Stage1, 2 and 3 are mainly quartz and calcite. Small amount of gangue minerals including chlorite, adularia and chalcedonic quartz were also identified especially for Stage 2 mineralization. Adularia is particularly found in stage 2 (gold bearing veins). Chalcedonic quartz tends to occur as separated bands alternating with quartz, carbonate bands of Stage 2 veins. Some of these gangue minerals were also confirmed by XRD including adularia and carbonate.

Quartz and chalcedony quartz

Quartz in Stage 1 vein is commonly colorless to white or milky and occasionally associated with pyrite. In Stage 2, quartz occurs as anhedral to subhedral and often forms along the vein wall (Fig. 4.10) and closely associated with pyrite (Fig. 4.6A, 4.6B, 4.6C and 4.6D). Some euhedral quartz may associate with calcite in

center of veins in Stage 2 (Fig. 4.10). Chalcedony quartz particularly forms as separated bands alternating with quartz and occasionally with sulfide-rich band layers (Fig. 4.2).

Calcite

Calcite constitute second abundance after quartz in Stage 2 veins (Fig. 4.2). It often forms as major carbonate minerals in carbonate-rich bands of banded quartz-carbonate±chlorite-sulfide-electrum veins (Fig. 4.2). It is also common to associate with quartz in quartz-rich band/veins but tends to be finer grains and in minor amount veins (Fig. 4.10). Calcite is also found in Stage 3 and occasionally as major component (Fig. 4.4A and 4.4B)
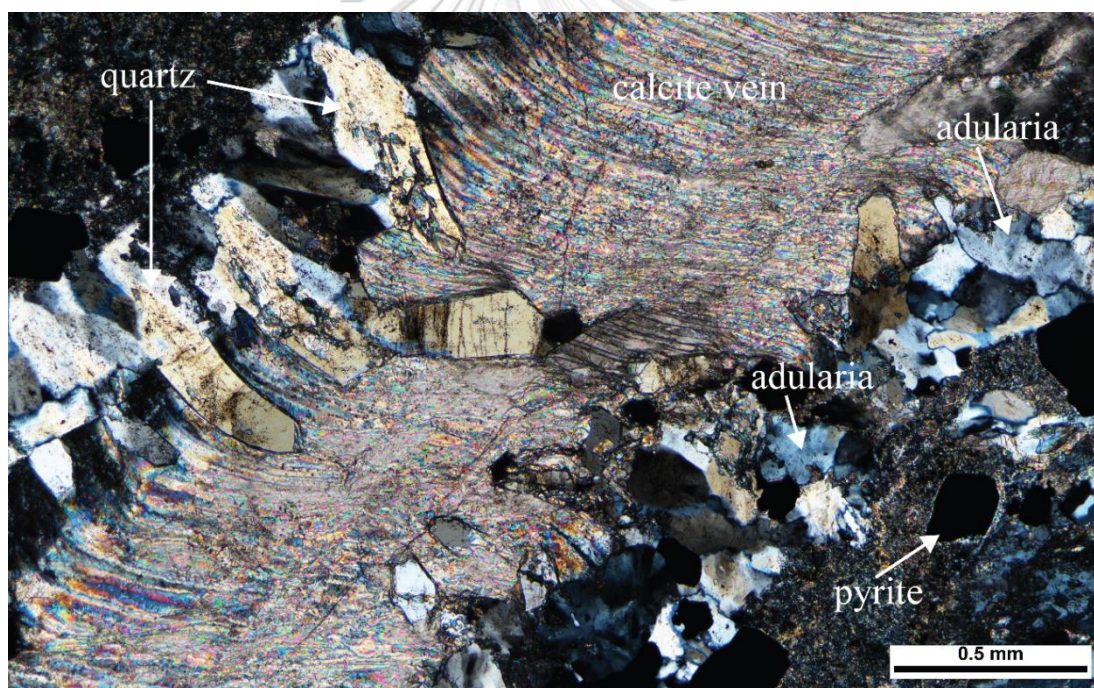
Fig. 4.10 Photomicrograph of stage 2 veins showing calcite-quartz-rich with adularia and pyrite. Note that anhedral to subhedral quartz occurs along vein wall and associates with adularia (Sample No. 4067-95.40 m).

Adularia (in veins)

Adularia has been identified in Stage 2 veins (quartz-carbonate±chlorite-sulfide-electrum veins). It occurs in minor amount as fine-grained of rhombohedral crystals commonly associated with quartz (Fig. 4.10). It occasionally found as euhedral grains in colloform-crustiform quartz veins.

Chlorite

Chlorite is typically green forming radiating, flaky or fibrous microscopic crystals or anhedral forms. It is commonly secondary mineral after primary mineral alteration (Fig. 4.11). Chlorite is associated with illite, smectite, quartz and calcite and fills dominantly vesicles and shows banded of alteration felsic volcanic rocks. For the XRD study, it was an unchanged peak for the glycolated and completely collapse after heated to 550 °C.
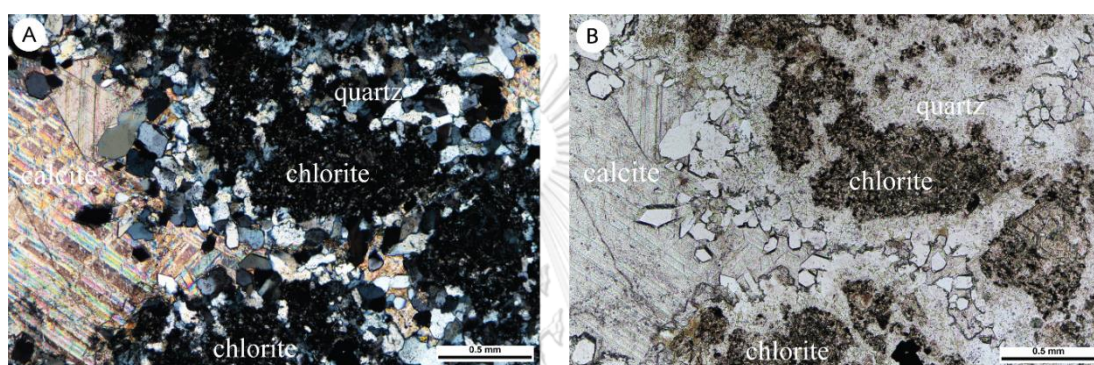
Fig. 4.11 Photomicrograph showing chlorite, calcite and quartz of the hydrothermal vein (Sample No. 4080-78.80m).

4.5 Hydrothermal alteration

Hydrothermal alteration study started from observation hydrothermal alteration features in diamond drill cores in term of apparent colors, alteration mineralogy and relationships to mineralized veins particularly emphasizing to gold bearing quartz carbonate ±chlorite-sulfides-electrum veins (Stage 2). Another two mineralization stages namely, 1) Stage 1 (pre-mineralization), and 2) Stage 3 (post-mineralization) are only contributed to very narrow zones of peripheral to veins/veinlets, which are only few millimeters wide and occur as silicification. Representative diamond drill core samples were collected for laboratory studies including careful reinvestigation of slabbed diamond drill cores, and petrographic study for each identified alteration types obtaining from drillcores observation. In addition, drillcore samples and some thin sections were stained to determine presence of adularia or fine-grained K-feldspar using sodium colbaltinitrite ($Na_3Co(NO_2)_6$). Total 12 samples have been undertaken for the staining. Representative samples were

also powdered to determine various clay minerals using X-ray diffraction (XRD) at Department of Geology, Faculty of Science, Chulalongkorn University.

4.5.1 K-feldspar staining

The study of K-feldspar staining aims at identifying the hydrothermal potassium feldspar (adularia) content in altered rock which is believed to be important alteration mineral in epithermal low sulfidation gold deposit. The presence of adularia in altered rocks could be used to support determination of style of mineralization at the Suwan Prospect. The staining technique was applied to diamond drill core samples, following the methodology presented by Norman (1974) . Total 12 rock slabs of diamond drill core samples were undertaken for staining.

Representative hydrothermal alteration samples from gold bearing quartz veins wallrocks at proximal and distal zones have been stained and results are shown in Figure 4.12 and 4.13. Stained rock slabs shown by different colors respond to minerals such as adularia, albite and illite-smectite (Figs. 4.12 and 4.13). Representative sample collected from proximal zone is shown in Figure 4.12. The study reveals that hydrothermal altered wallrocks at proximal and distal to gold bearing quartz-carbonate veins contain variable hydrothermally altered minerals and intensities (Figs. 4.12 and 4.13).   The same samples have been confirmed for the alteration mineral assemblages using X-ray diffraction analysis (XRD) (see section of clay mineralogy study).

Estimated mineral percentages of six minerals are shown in Table 4.6 including K-feldspar, albite, plagioclase, calcite, quartz and mafic and opaque minerals. The percentage of K-feldspar values are relatively highly particularly in plagioclase-hornblende phyric andesite (12-28%), and low in monomictic andesite breccia. The results indicated that the percentage of K-feldspar in plagioclase-hornblende-phyric andesite with quartz-carbonate veins and monomictic plagioclase-hornblende phyric andesite breccias are very low (4-11%).

🟨	K-feldspar (6%)	⬜	Calcite (11%)
🟡	Albite(53%)	🟩	Quartz (21%)
🟥	Plagioclase (8%)	⬛	Mafic minerals and opaque minerals (1%)
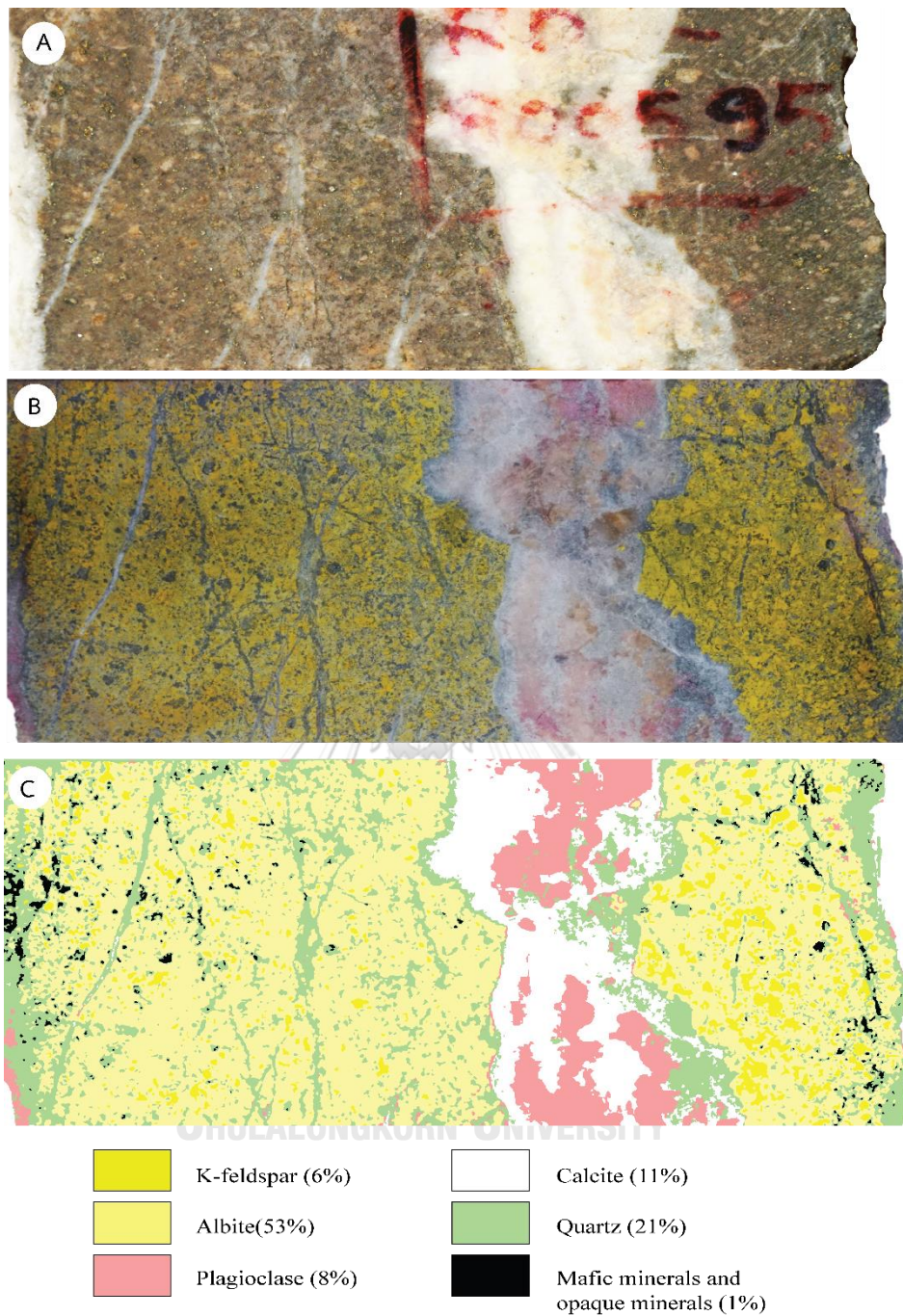
Fig. 4.12 Identification and quantification of hydrothermal K-feldspar abundance. **A.** Photograph of unstained rock slab showing gold bearing quartz-carbonate veins and veinlets cut through wallrock (proximal zone). **B.** Photograph of stained rock slab with $Na_3Co(NO_2)_6$ showing K-feldspar altered (yellow) and **C.** Image analysis showing quantification of six categories classified by ENVI 5.3 software, Six categories: 1) K-feldspar = dark yellow, 2) albite = light yellow, 3) plagioclase = pink, 4) calcite = white, 5) quartz = grayish green, and 6) mafic minerals and opaque minerals = black (Sample No. 4080-65.50 m).
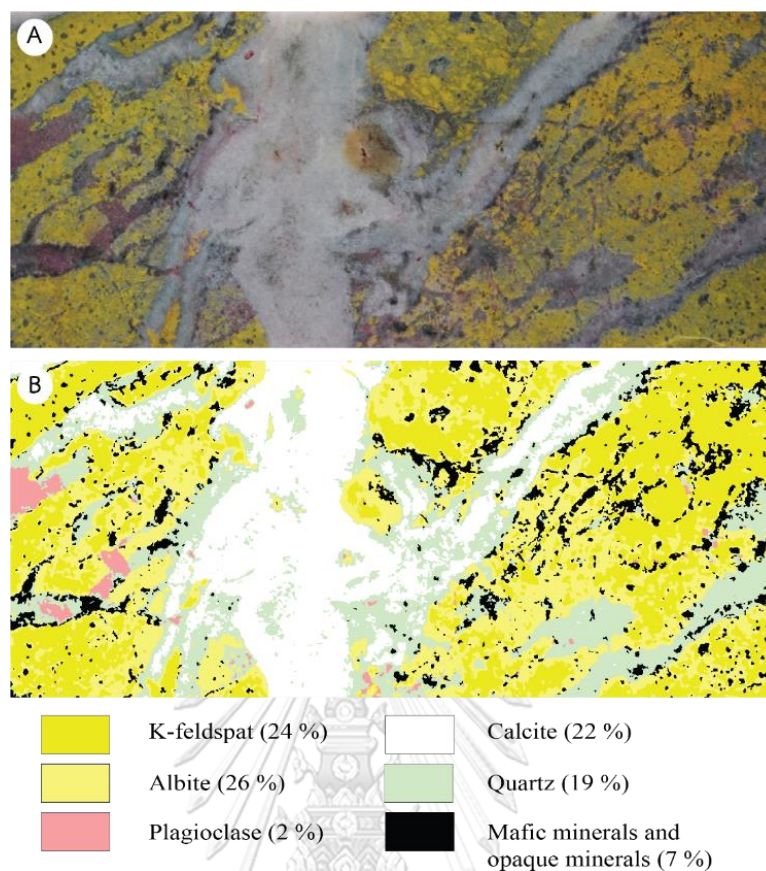
Fig. 4.13 Identification and quantification of secondary K-feldspar abundance. **A.** Photograph of stained rock slab surface with $Na_3Co(NO2)_6$ showing K-feldspar altered (yellow) and **B.** Image analysis showing quantification of six categories classified by ENVI 5.3 software, Six categories: 1) K-feldspar = dark yellow, 2) albite = light yellow, 3) plagioclase = pink, 4) calcite = white, 5) quartz = grayish green, and 6) mafic minerals and opaque minerals = black (Sample No. 4065-100.90 m).

Table 4.6 The quantitative results of mineral classification using K-feldspar staining technique

Element (%) Sample No.	K-feldspar	Albite	Plagioclase	Calcite	Quartz	Mafic and opaque	Rock type
4065-43.20	11	57	2	6	19	4	MPHA
4065-81.50	25	42	6	12	11	4	PHA
4065-100.90	24	26	2	22	19	7	PHA
4065-119.30	11	57	1	11	15	6	HAD
4067-54.70	22	45	3	4	22	3	MPHA
4067-94.50	12	47	1	19	12	8	PHA
4067-110.20	5	5	11	39	43	1	PHA (QCV)
4067-122.30	13	54	4	3	14	13	PHA
4067-128.00	28	26	21	3	6	16	PHA
4080-53.60	4	4	3	47	41	5	MPHA
4080-65.50	6	53	8	11	21	1	PHA
4080-79.80	7	52	8	10	19	4	MPHA

Abbreviation: HAD = Hornblende-phyric andesite, PHA = Plagioclase-hornblende-phyric andesite, PAD = Plagioclase-phyric andesite, QCV = Quartz-carbonate vein, MPHA = Plagioclase-hornblende-phyric andesite breccia.

4.5.2 Alteration study from whole-rock geochemistry

The purpose of this section is to conduct geochemical analysis of the altered rocks to interpret the relation of mineral assemblages. The fundamental method was calculate based of the chlorite-carbonate-pyrite index that measures the hydrothermal alteration of Na-plagioclase to illite-sericite and also chlorite mineral assemblages (CCPI = $100(MgO+FeO)/(MgO+K_2O+CaO+Na_2O)$), and was firstly proposed by (Large et al., 2001) for characterizing the alteration styles in volcanic massive sulfide deposits to epithermal systems. Then, in 2007, the CCPI was developed by Gemmell (2007) .

Alteration Index (AI = $100(MgO+K_2O)/(MgO+K_2O+CaO+Na_2O)$) defined by Ishikawa et al. (1976) was also applied to determine the plagioclase replacement by illite/sericite and chlorite in hydrothermal alteration of felsic volcanic rocks. This AI value is depended on the amount of mineralogical component (e.g., plagioclase, pyroxene, quartz and altered minerals in volcanic rocks).

Result of alteration study from whole-rock geochemistry

Rock slabs collected from the Suwan Prospect were analyzed for their geochemical composition using by X-ray fluorescence (XRF) at the Department of Mineral Resources. Consequently, based on geochemical composition obtained from XRF analysis, the whole-rock geochemical analysis including CCPI and AI methods was applied to all samples. Then, all CCPI and AI data were plotted in AI-CCPI alteration box plot diagram for interpretation of alteration assemblages (Fig. 4.14).

The XRF data of rock samples from the Suwan Prospect were calculated for major elements concentration that shown in scattering box plot of CCP Index with AI (Fig. 4.14) diagram. The result of altered box plot analysis has values ranging between 22-91 AI and CCPI ranges 28-75. The AI values are influenced by the mineralogical component, which is consisted of plagioclase, pyroxene, silica and altered minerals of volcanic rocks. The result of CCPI ranging from 58-61 and AI from 22-24 could be indicated that the altered primary minerals into secondary minerals such as: epidote, calcite, chlorite, pyrite and iron oxide.
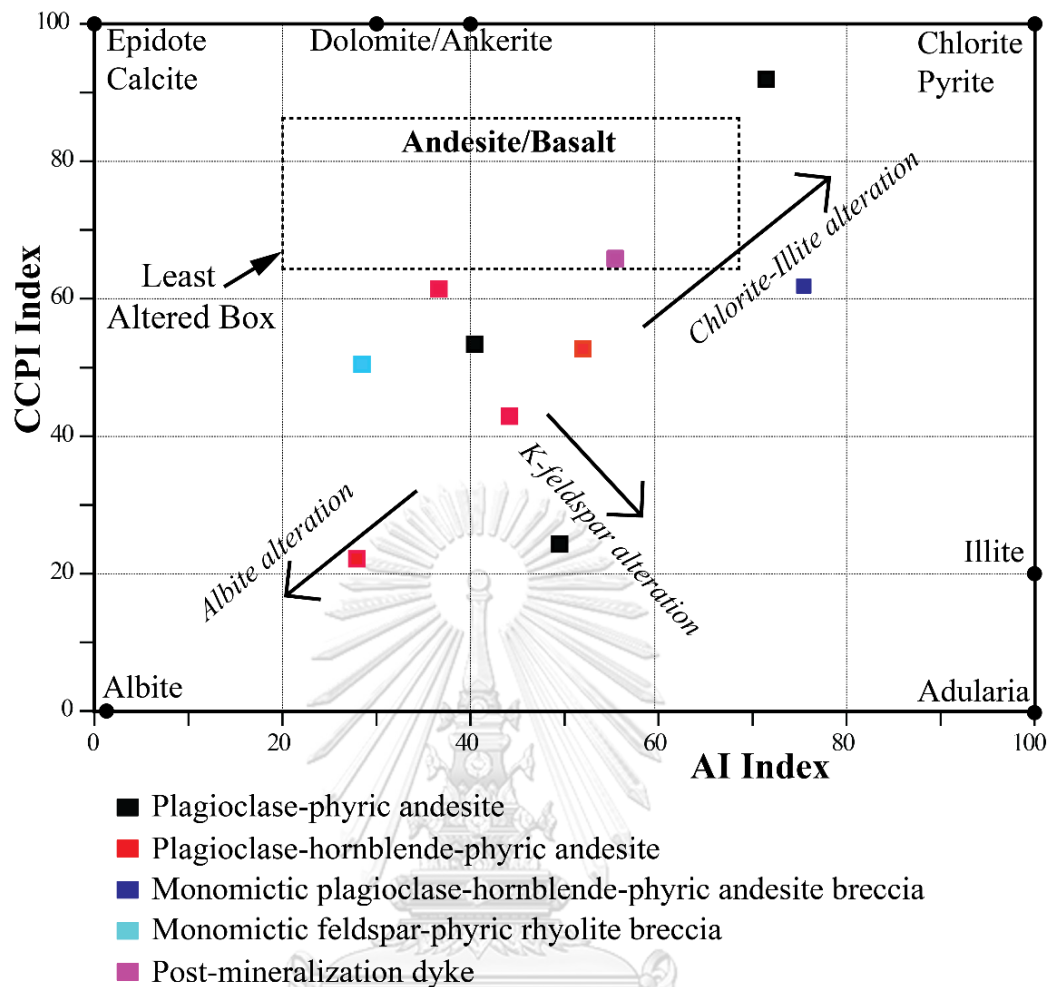
Fig. 4.14 Alteration box plot of the alteration index (AI) versus the chlorite-carbonate-pyrite index (CCPI) of the Suwan Prospect.

Several alteration types were identified including argillic (albite alteration), propylitic (chlorite-illite alteration), clay minerals (adularia alteration), and unaltered rocks (Fig. 4.14). The argillic alteration is typically associated with sericite ± K-feldspar ± adularia ± illite ± chlorite ± pyrite assemblage (Hedenquist et al., 2000) and plotted in the bottom right of diagram. The propylitic alteration is generally associated with epidote ± calcite ± chlorite ± pyrite assemblage and plotted in the area from the least altered rocks (rectangle in Fig. 4.14) towards the top left of diagram. Samples with CCPI values ranging from 20 to 51, and AI values ranging from 50 to 75 shown in Figure 4.14, are typically related to the chlorite-illite-adularia-albite assemblage of alteration zone. However, the post-mineralization dyke is plotted in the least altered area of andesite-basalt field (rectangle). Base on the results of whole-rock

geochemistry analysis of altered volcanic host rocks, these rocks contained varying elements that depend on location of hydrothermal veins.

4.5.3 Clay mineralogy study

Clay mineral study is essential for identifying hydrothermal alteration assemblage. Thus, XRD technique was applied to identify altered clay minerals. Ten samples have been analyzed using XRD method representing each altered zone (e.g. proximal to distal) to main mineralization zone. Samples were prepared as powder, air-dry, glycolate and heated at 550 °C. The XRD patterns obtained from the Diffract plus#1 software of the Bruker Analytical X-ray database to identify minerals and are later interpreted what type of clay minerals by the EVA software.

All clay minerals (illite, smectite and kaolinite) of mineralization zone and altered volcanic host rocks from the Suwan Prospect were firstly identified under microscope, and then analyzed by XRD for confirmation. XRD patterns for all samples were plotted with 2Ө angle shown in Figure 4.15.

Result of XRD study

The XRD results are given in Table 4.7. In addition, the results of XRD analysis of all samples of altered mineral concentrations (quartz, calcite, chlorite, illite, feldspar, adularia, kaolinite, and pyrite) are shown in Table 4.7. These chemical compositions of altered minerals (quartz, calcite, chlorite, illite, feldspar, adularia, kaolinite, and pyrite) from mineralization zone could be used to define style of alteration.

The concentrations of quartz are high in all sample. The concentrations of altered minerals include calcite, chlorite, illite, feldspar, adularia, pyrite, and kaolinite (Fig. 4.15 and Table 4.7). Some samples contain low illite/smectite concentration (see Fig. 4.15). They are typically interpreted to be mix-layered or interlayering of clay assemblage (Reynoles, 1992).

In case of high illite/smectite concentration (high intensity values shown in Fig. 4.15), there are a large amount of illitic minerals indicating the clay mineral alteration. Chlorite peaks were also presented at ~12.6 2Ө, as there are moderate intensity and strong relief. In addition, the intensities of kaolinite and smectite are also

recorded at 12.4 and 25.1 of 2Ө. However, the intensities of chlorite, kaolinite and smectite are obviously decreased for glycolated and heated samples (Fig. 4.15).
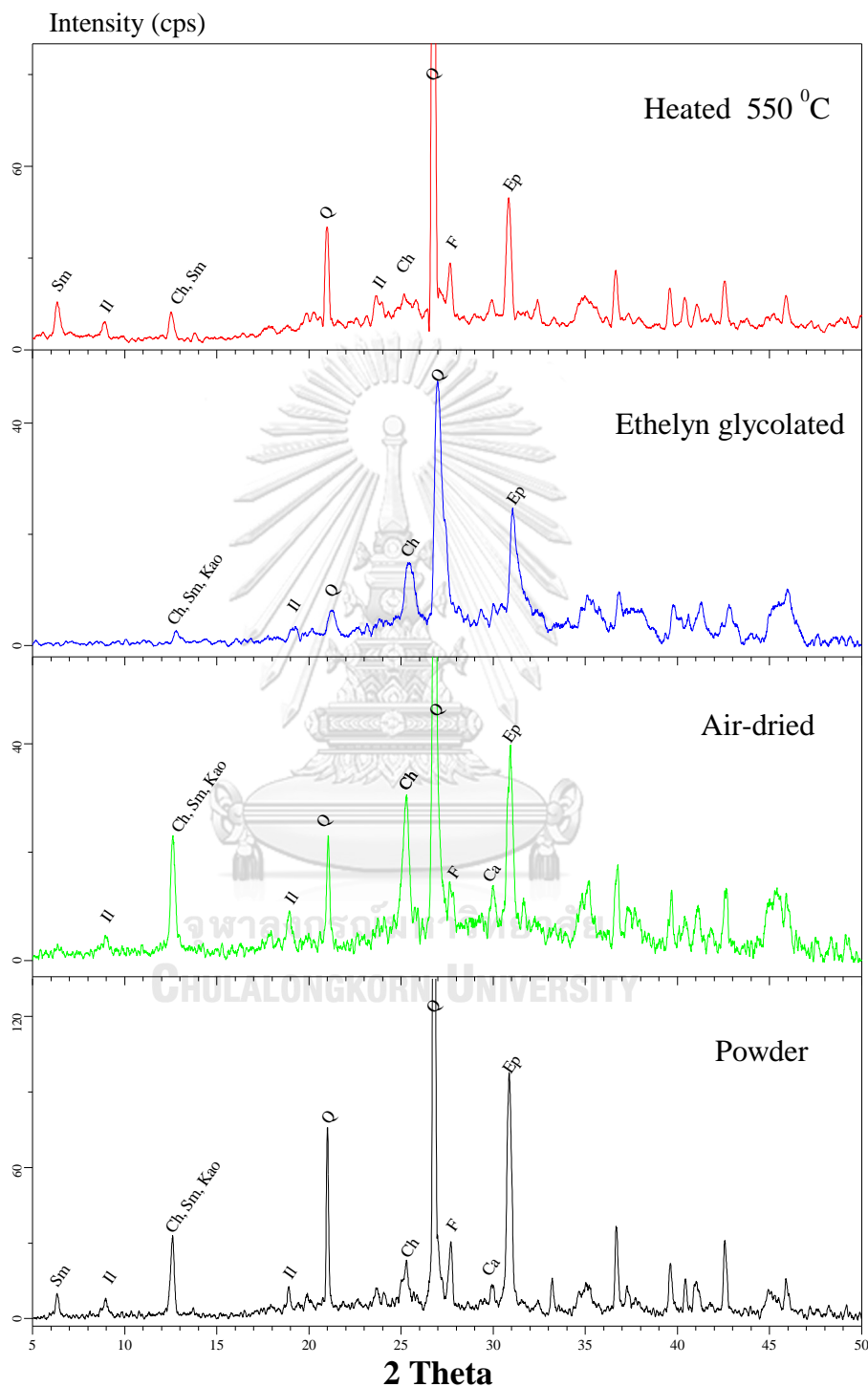
Fig. 4.15 XRD patterns of 4 types of clay mineral sample (powder, air-dried, glycolatec and heated samples) showing obvious peaks of mineral assemblages (Sample No. 4067-39.50 m; Sm=Smectite, Il=Illite, Ch=Chlorite, Kao=Kaolinite, Q=Quartz, F=Feldspar, Ep=Epidote, Ca=Calcite).

Increasing in intensity is possibly caused by smectite swelling after glycolation of sample. Feldspars are also found from XRD analysis; peak patterns are quite similar to those of chlorite and smectite. To clarify signals among chlorite, smectite and feldspar, glycolated samples are selected to fade the feldspar signal. Based on this technique, peak patterns of feldspar are eliminated. Thus, it is concluded that the glycolation and heat treatment affect to fade the XRD intensity of chlorite, kaolinite and smectite and feldspar. Most of samples from drill holes show illite-smectite content ranging from 0.11 to 2.4 % (Table 4.7). A summary of results from the XRD analysis of clay mineral is consistent with mineralogy related to illite to illite-smectite-chlorite because there are very high content (> 7%) of those minerals.

Table 4.7 The average percentage of mineral concentration calculated by powder X-ray diffraction analysis.

Sample No.	4066-87.30	4067-37.60	4067-39.50	4067-71.50	4067-75.60	4067-128.00	4080-53.60	4080-57.80	4080-88.50	4138-68.80
quartz	55.02	17.80	87.34	37.14	30.66	62.32	57.02	52.44	69.79	94.50
calcite	20.88	2.06	3.20	38.82	32.37	22.40	19.05	4.07	8.27	0.56
chlorite	0.30	3.66	5.14	2.39	4.22	3.74	1.99	1.77	2.44	1.31
illite/smectite	1.79	0.54	0.39	0.11	11.88	1.33	2.47	14.13	7.76	1.16
feldspar	11.60	52.03	0.18	0.46	0.99	0.41	0.89	3.23	2.30	0.76
adularia	0.20	1.13	0.43	8.41	0.50	1.89	3.28	1.39	0.58	0.73
kaolinite	2.68	21.87	0.02	10.38	10.51	3.87	10.33	7.41	8.76	0.57
pyrite	7.53	0.91	3.30	2.28	8.86	4.03	4.97	15.57	0.10	0.41
Total (%)	100.00	100.00	100.00	100.00	100.00	100.00	100.00	100.00	100.00	100.00

4.6 Alteration styles

The alteration of clay minerals was typically used to interpret alteration styles such as quartz-adularia (silicic alteration), kaolinite-smectite (argillic alteration), chlorite-calcite (propylitic alteration) and illite-smectite (clay alteration) assemblages.

Interpretations of alteration styles are based on petrographic study, K-feldspar staining, XRD and EPMA results. According to White and Hedenquist (1995) and Hedenquist et al. (2000), the hydrothermal alteration assemblages are associated with temperature and pH of hydrothermal system which produces altered minerals and zoning; there are silicic, argillic, propylitic and clay alteration types. The mineralogical association of low sulfidation epithermal deposits is typically associated with clay minerals such as illite-smectite of the interstratify layers by near-

neutral condition (Henley & Ellis, 1983). In addition, the gangue minerals including quartz, calcite and adularia are principally produced from low sulfidation systems (White & Hedenquist, 1995).

Based on results of petrographic study, K-feldspar staining, XRD and EPMA data, at least four types of hydrothermal alteration have been identified namely, 1) silicic, 2) argillic, 3) propylitic and 4) clay alteration types. Details of each individual alteration are described below.

4.6.1 Silicic alteration

The silicic alteration or silicification is mainly identified in peripheral to the gold bearing quartz-carbonate veins/veinlets. It constitutes mainly quartz, and minor adularia, illite and pyrite. Quartz occurs as cryptocrystalline and microcrystalline infilled vugs and replaced in some minerals such as feldspar and mafic minerals (Fig. 4.16). Adularia typically forms in minor amount as fine-grained crystals often displaying rhombohedral crystal shape (Fig. 4.16). In this study, adularia forms as sub-rhombic to rhombic shaped crystals, patchy twinning, anhedral to euhedral forms, and small grains enclosed in quartz. Under microscope, hydrothermal quartz that associated with adularia has replaced plagioclase and K-feldspar (Fig. 4.17). EPMA analysis has confirmed the present of adularia in silicic alteration zone.

4.6.2 Argillic alteration

The clay minerals in argillic alteration zone consists of kaolinite, illite/sericite, smectite, quartz with pyrite. Alteration zone is strongly destructive of original texture and produces weak weathered zone. Argillic alteration zone is mapped using petrological and geochemical results in which mineral compositions are carefully identified and analyzed for confirming alteration styles. This alteration is commonly associated with overprinted, and high weathered leaching zones, which are also found in clay mineral zones. Gold-Silver deposit at Suwan Prospect is typically high grade in deposition zones with the overprinted alterations.
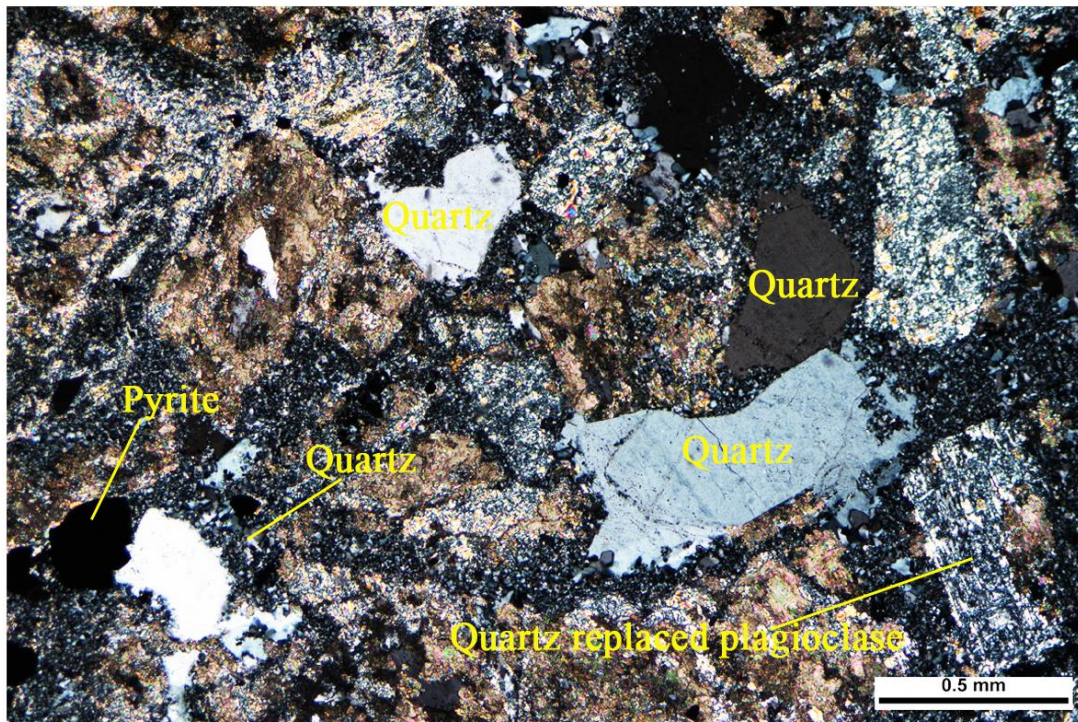
Fig. 4.16 Photomicrograph of silicic alteration zone showing cryptocrystalline quartz replacing feldspar (Sample No. 4066-106.00 m).

4.6.3 Propylitic alteration

The propylitic alteration is generally widely distributed and distal from the ore zones or vein zones. This alteration style is represented by predominant chlorite, epidote, and minor calcite (Fig. 4.17). The rocks undergone propylitic alteration tend to be pale to dark green. At Suwan Prospect, it appears to confine to coherent andesite unit. In volcanogenic-sedimentary rock unit, this alteration is locally developed and commonly represented by chlorite and calcite with some pyrite. Chlorite is mainly confined to groundmass and some mafic phenocrysts. While, epidote prefers to occur in phenocrysts.
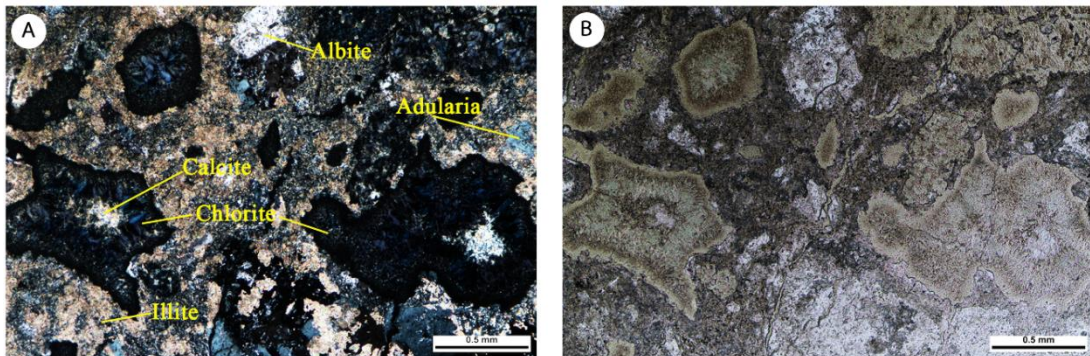
Fig. 4.17 Photomicrographs showing altered minerals (sample No. 4065-43.20 m). **A.** Photomicrograph showing adularia, chlorite, albite, illite and calcite (cross nicol) and **B.** Photomicrograph showing green color of chlorite, albite (colorless) and calcite (PPL).

4.6.4 Clay alteration

The clay alteration type is dominated by illite/smectite ± albite ± chlorite ± pyrite with minor quartz and calcite. These clay minerals (e.g. illite and smectite) are mainly identified using XRD analysis as they are very difficult to distinguish under microscope. The typical peak patterns of illite from XRD are represented at peak at 10 of 2Ɵ (Fig. 4.15). Clay alteration is mostly appeared in close to the silicic alteration zones that are particularly hosted in plagioclase-phyric andesite and monomictic andesite.

CHAPTER 5
DISCUSSION AND CONCLUSION

5.1 Introduction

The objective of this project was investigated the geological setting and characterize of epithermal systems in the Suwan Prospect of Phitsanulok province. The general aims of the research include hosted rocks, mineral assemblage, mineralization and paragenesis, which have been suggested to characterize of gold and silver deposits.

5.2 Discussion

The characteristics of epithermal deposits are often complexed geological environments. Thus understanding the geological environments within the study area is important to characterize model of the epithermal system.

5.2.1 Geological setting of Suwan Prospect

Volcanogenic environments commonly have complex and diverse facies associations and stratigraphic relationships. The depositional environment has been proposed from volcanic facies associations at the Suwan Prospect that comprise three compositionally different volcanic units. These are porphyritic andesite unit, volcanogenic sedimentary rock unit and felsic volcanic unit. The porphyritic andesite unit is deposited at the bottom of their stratigraphic sequences and presents deposition of monomictic andesite breccia. The porphyritic andesite unit is comparable with Chatree deposit (Table 5.1) that was the earliest depositional event at Chatree are. This event was followed by the deposition of the volcanic sedimentary unit which are siltstone, sandstone, mudstone and breccias. These processes include subaqueous deposition from subaerial pyroclastic flows that entered water, and subaqueous resedimentation of unconsolidated aggregates (Jutzeler et al., 2014). The volcanogenic sedimentary rock unit is presented at the middle of stratigraphic sequences in the study area. This sequence is very thick, laterally continuous layer

(e.g. laminated siltstone) and graded bedding and may have been accumulated during periods of relatively minor volcanic activity (Salam, 2013). The latest event represented by the uppermost of sequence that occurs as felsic volcanic facies association (rhyolite dominated facies). It comprises feldspar-phyric rhyolite, quartz-rich fiamme breccia, lithic-rich fiamme breccia and volcanic sandstone.

Table 5.1 Characteristics of host rocks of Chatree deposits compared with Suwan Prospect.

Chatree deposit (Salam, 2013)	Suwan Prospect
Fiamme breccia unit Lithic-rich fiamme breccia, laminated siltstone and carbonaceous mudstone, quartz-rich fiamme breccia and stone.	**Felsic volcanic unit** Lithic-rich fiamme breccia, quartz-rich fiamme breccia, sandstone, feldspar-phyric rhyolite breccia, monomictic feldspar-phyric rhyolite breccia.
Volcanogenic sedimentary unit Siltstone, carbonaceous mudstone, sandstone and limestone and sand-matrix polymictic breccia, feldspar-phyric rhyolite, monomictic feldspar-phyric rhyolite breccia, polymictic intermediate-felsic breccia and sand-matrix rhyolitic breccia.	**Volcanogenic sedimentary unit** Siltstone, sandstone (cross-laminated), mudstone and limestone, polymictic intermediate-felsic breccia and sand-matrix polymictic breccia.
Polymictic mafic-intermediate breccia unit Polymictic mafic-intermediate breccia, clast-supported and matrix-supported polymictic breccia.	**Porphyritic andesite unit** Plagioclase-phyric andesite, monomictic plagioclase-phyric andesite breccia, plagioclase-hornblende-phyric andesite and monomictic plagioclase-hornblende-phyric andesite.
Porphyritic andesite unit Coherent plagioclase-phyric andesite and monomictic plagioclase-phyric andesite breccia, fiamme breccia, carbonaceous mudstone, coherent plagioclase-hornblende-phyric andesite and monomictic plagioclase-hornblende-phyric andesite breccia.	

At Suwan Prospect, occurrence of gold-silver mineralization is controlled not only by structures but also by lithology and stratigraphy. The bottom volcanic sequence (mainly porphyritic andesite and monomictic andesite breccia) hosts minor mineralization in the study area. It mainly occurs as small veins, veinlets and stockworks. However, vein density is higher in the lower facie associations (e.g. monomictic andesite breccia facie). The Suwan Prospect rarely hosts ore lenses where the mineralization is hosted in coherent plagioclase-hornblende-phyric andesite facies. This is a small resource, although the small veins, veinlets and stockworks typically have high Au grade (see Chapter 4). In contrast, the major ore zones of the Chatree deposits are hosted in volcanic breccia facies (monomictic andesite breccia and polymictic mafic-intermediate breccia facies) and are thick veins accompanied by stockworks.

The host volcanic sequences are mostly andesitic in composition, sometimes basaltic or rhyolitic rocks. The magmatic source established relationship for the oceanic and continental margin volcanic arcs was described for Permian-Triassic volcanic rocks in the study area (Salam et al., 2014). The suggested evolutionary sequence in oceanic arc from island arc tholeiite erupted at early stage of arc development has been confirmed for only a study area. The volcanic islands in the study area are rarely preserved, because of undergo rapidly erosion as well as subsidence or subaerial erupted of the volcanic rocks and weathering processes. In simple volcanic arc (Mitchell & Garson, 1981), facies are either basaltic lavas or andesite lava flow breccias formed by autobrecciation of submarine andesitic flows. These are commonly overlain by or interbedded with thick very coarse submarine sediment and mud flow deposits formed by erosion of subaerial volcanoes. Laterally equivalent rocks further from the volcanic arc are turbidites and mudstone; toward the volcanoes the marine volcanogenic rocks are locally interbedded with reef talus, fringing or barrier reef limestone, and lagoonal, fluviatile and conglomerate deposits surrounding subaerial eruptive centers. In complex oceanic volcanic arcs, the volcanogenic successions are similar to those of continental margin arcs although the composition of the clastic material reflects the highly variable nature of the volcanic rocks, with tholeiite basalts and calc-alkaline andesites, dacites and rhyolites both occurring in parallel belt as a result of subduction controlled in type of the magmatism

(Mitchell & Garson, 1981). For the Suwan Prospect (Fig. 5.1), the volcanogenic succession can be described to the result of arc collision by tectonic setting. It is difficult to determine whether these arcs developed on a continental margin, or were oceanic, although an oceanic setting may be indicated by the presence of abundant submarine volcanic rocks (e.g. andesite and basalt).

5.2.2 Mineralization

In general, the epithermal Au-Ag deposits are the shallow and relatively distal part of ore forming environments that form above high-temperature hydrothermal systems (Simmon et al., 2005). The most local of ore forms, beneath, and the deepest part is represented by intrusion centered of the ore mineralization (Simmon et al., 2005) such as Cu-Mo mineralization in the southern part of the Chatree deposits. This porphyry Cu-Mo mineralization has been relationship between Chatree epithermal of N-Prospect, and is hosted in the altered granodiorite porphyry and the altered andesite lava (Tangwattananukul & Ishiyama, 2017). According to the previous exploration and mining history along LFB from Lao PDR extended to the south eastern part of Thailand (see Chapter 2), there are many well-known mineralization systems including Cu-Au skarn, Cu skarn, Au skarn and Au-Ag epithermal of the deposit styles. Especially, the Chatree deposit is Au-Ag low sulfidation epithermal system (Table 5.2). It is defined as the association of quartz-calcite-adularia±illite and sericite. These associations indicate a near neutral hydrothermal fluid condition and contain high Au-Ag-Zn at the top of the sequence and increasing Pb and Cu in deeper levels. Gold mineralization at the Chatree deposit is mostly in the form of electrum inclusions or complex inclusion in arsenopyrite-pyrite and free grains of electrum between quartz grains and carbonate or chlorite grains. The simple sulfide assemblages are composed of pyrite, marcasite, chalcopyrite, sphalerite and galena. The Chatree deposit consists of 5 km strike length of mineralized lode, hosted in fault-collapsed crater structure and alternating volcanic breccia and volcanic sedimentary sequence. The deposit is well preserved from the upper most level to deepest level by normal fault movement and a thick covering of rhyolitic eruptive sequence (Lunwongsa et al., 2010; Salam, 2013). The Suwan Prospect has similarities to the Chatree deposit in scope of the host rocks, mineralization and alteration styles.

The continuity of structure controls has been extended from the Chatree deposit with the broad hydrothermal alteration halo within the potential ore zone for gold discovery in the future.

Fig. 5.1 Summary of depositional environments interpreted for the Suwan Prospect.

Table 5.2 Characterize depositional of Chatree deposits compare with Suwan Prospect

	Chatree Deposits (Salam, 2013)	Suwan Prospect
Vein texture	crustiform-colloform banded, cockade, comb, breccia, vuggy, massive vein	crustiform - banded, breccia, vuggy?
Gangue	quartz, calcite, dolomite, jasper, illite, sericite, smectite, ankerite, rhodochrosite, hematite, adularia, chlorite, epidote, chalcedony, prehnite, laumontite, montmorillonite	quartz, calcite, illite, sericite, smectite, adularia, chlorite, epidote, chalcedony, kaolinite
Ore mineral	pyrite, chalcopyrite, sphalerite, galena, tetrahedrite, native silver, electrum, argentite, acanthite, tetrahedrite, boulangerite, pyrargyrite, arsenopyrite, tetrahedrite-tennantite	pyrite, chalcopyrite, sphalerite, galena, electrum, arsenopyrite

5.2.3 Hydrothermal alteration

Base on the overall results of alteration study (see Chapter 4) at the Suwan Prospect, a schematic model for alteration mineral zonation can be established on the bases of quartz, adularia, illite, smectite, chlorite, pyrite and clay minerals. The alteration styles well-defined on the drill-core samples by geochemical laboratory analyses are displayed and point to the low sulfidation epithermal system (Fig. 5.2). The four alteration assemblages of the Suwan Prospect have been clearly identified. However, interpretation for individual prospect needs to be aware because there is a limitation for study on nine drill holes. Nevertheless, the distribution of alteration assemblage at the Suwan Prospect has similarities to alteration styles at Chatree. There are four mains alteration assemblages at Chatree that based on distinctive alteration mineral assemblages including; 1) Silicic (quartz-illite-adularia-pyrite), 2) Argillic (illite-quartz-adularia-chlorite-pyrite), 3) Propylitic (chlorite-calcite-pyrite-epidote), and 4) Clay (kaolinite-montmorillonite-illite). Multiple phases of alteration are evident in the volcanic sequence with alteration intensity being greatest near veins and breccias. Quartz is the most abundant alteration mineral and is widely distribution in all alteration types which presented as chalcedony and fine-grained silica and in veins has crustiform, colloform and cockade textures. Each major Au-Ag

mineralization event is characterized by quart-carbonate-adularia-chlorite-sulfide-electrum (Diemar et al., 2000; Salam, 2013). There are at least five vein stages of the mineralization at the Chatree deposit. Early vein mineralogy was dominated by quartz, calcite, adularia and pyrite, followed by quartz, calcite, chlorite, dolomite, illite-smectite, pyrite and then quartz, calcite and pyrite. Post-ore vein stage was comprised of calcite, epidote and adularia.
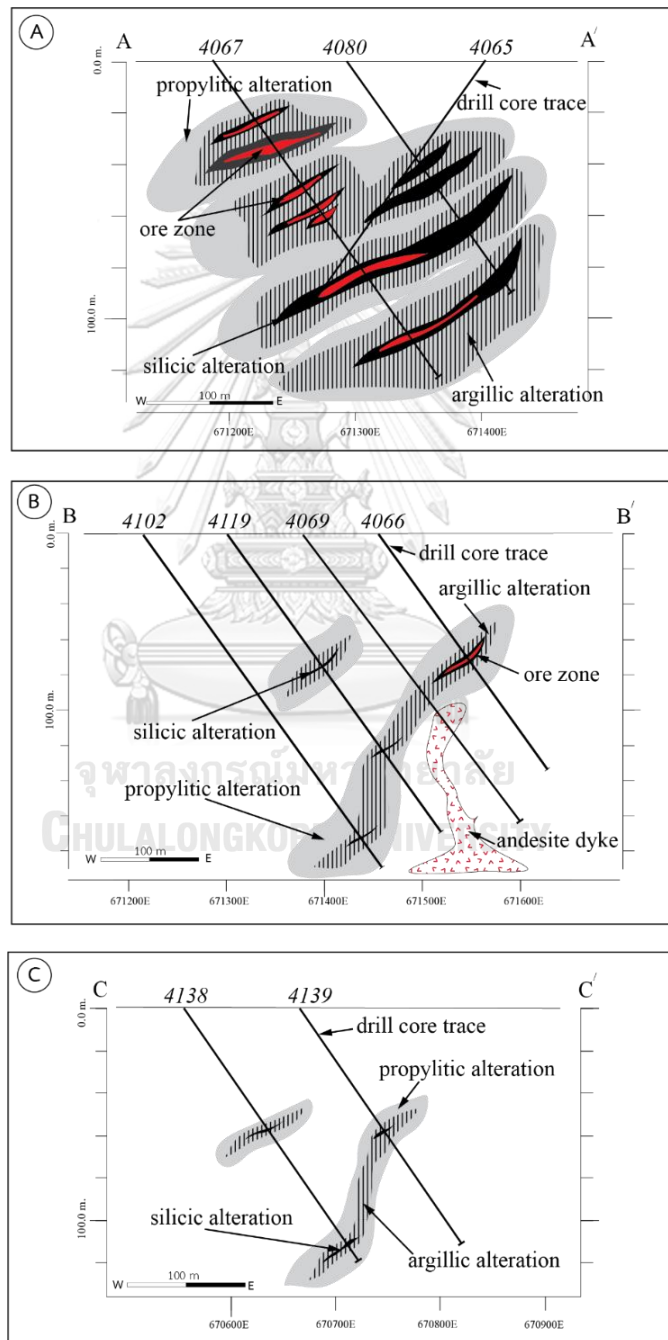

Fig. 5.2 The schematic model of ore zone and alteration styles at the Suwan Prospect.

5.3 Conclusion

    The main summary derived from the research of the Suwan Prospect low sulfidation epithermal gold and silver deposit are as follow:

- The Suwan Prospect is located at the Northwestern part of Chatree deposit, Phitsanulok province, Central Thailand, which is hosted by sequences of volcanic units of Permian to Triassic age.

- Three major rock units in Suwan Prospect are interpreted by depositional relationship that consist of 1) Porphyritic andesite (plagioclase-hornblende-phyric andesite, plagioclase-phyric andesite, hornblende-phyric andesite and monomictic andesite breccia,); 2) Volcanogenic sedimentary rocks (mudstone, siltstone, sandstone, polymictic intermediate-felsic breccia and sand-matrix polymictic breccias) and 3) Felsic volcanic rock (lithic-rich fiamme breccia, quartz-rich fiamme breccia feldspar-phyric rhyolite and monomictic-feldspar-phyric rhyolite breccia). These rock units have been significantly proximal zone of the volcanic depositional environments.

- Suwan Prospect is hosted by mainly direction NNE-SSW and NE-SW trending of structures. These trending are provided the host for mineralization.

- Hydrothermal vein textures include crustiform banded of chalcedonic-quartz-carbonate-sulfide veins, stockwork, crystalline calcite veins and microcrystalline quartz silicification.

- Hydrothermal veins of main ore stage (Stage 2) are intersected in drill holes DDH4066, DDH4067 and DDH4080.

- Ore minerals are commonly shown as dissemination and inclusion with pyrite grains. Gold occurs as electrum which have fineness 400 – 680. The mineral assemblages are electrum, chalcopyrite, sphalerite, galena and pyrite.

- Gangue mineral assemblages are commonly microcrystalline, crystalline and cryptocrystalline quartz, adularia, chlorite, illite-smectite and calcite. Gangue mineral assemblages rich in chalcedonic quartz were primarily formed during hydrothermal process.

- Alteration styles classified in this study include silicic, argillic, propylitic and clay minerals, which consist of mineral assemblages of quartz, adularia, illite/sericite, smectite, chlorite, epidote, calcite, kaolinite and pyrite.

- Geochemical association of mineralizing events at Suwan Prospect is variable relating to the alteration styles. The geochemical compositions have been relatively to the ore stages within the veins. These are composed of major oxides components of alteration such as 1) high values of K_2O, Na_2O, Al_2O_3 and SiO_2 are presenting in silicic, argillic and clay alteration. 2) high values of MgO, FeO, Fe_2O_3, Al_2O_3, CaO and SiO_2 are presenting in propylitic alteration which is classified by alteration box plot and confirmed by EPMA and XRD analyses.

- Precious and base metals at Suwan Prospect have been presented minor of ores concentrations which are composed of Au, Ag, Cu, Pb, Zn, Mo, Ni, S, As, Fe, Sb, Cd, Ti, Mn and V.

- All geological characteristics at Suwan Prospect are proposed to be a part of the low sulfidation epithermal deposit. They contain many similarities to the Chatree deposits.

จุฬาลงกรณ์มหาวิทยาลัย

CHULALONGKORN UNIVERSITY

REFERENCES

Andrianarimanana, M. (2016). Mineralogy and petrography of skarn at Khao Lek, Amphoe Nong Bua, Changwat Nakhon Sawan. *Unpublished MS. Thesis, Chulalongkorn University*, 87 p.

Backhouse, D. (2004). Geological setting, alteration and nature of mineralization at the Phu Kham copper-gold deposit, Lao PDR. *BSc (Hons) thesis, University of Tasmania, Hobart, Australia.*

Barr, S. M., & MacDonald, A. S. (1991). Toward a late Paleozoic - ealy Mesozoic tectonic model for Thailand. *Journal of Thai Geosciences, v. 1*, p. 11-22.

Boynton, W. V. (1984). Cosmochemistry of the Rare Earth Elements; Meteorite. *Science Publishing Company, Amsterdam.*

Bunopas, S. (1981). Paleogeographic history of western Thailand and adjacent parts of South-East Asia: A plate tectonics interpretation. *PHD. Dissertation, Victoria University of Wellington, Wellington, New Zealand, eological Survey Division, Department of Mineral Resources, Bangkok, Thailand, reprinted 1982, Geological Survey paper No. 5*, 810 pp.

Bunopas, S. (1994). Regional Stratigraphy, Paleogeographic and Techtonic Event of Thailand and Continenttal Southeast Asia. *Proceeding of the International Symposium on: Stratigraphic Correlation of Southeast Asia, 15-22 November 1994, Bangkok, Thailand*, P. 2-24.

Bunopas, S., & Vella, P. (1983). Techtonic and Geologic Evolution of Thailand. *Workshop on Stratigraphic Correlation of Thailand and Malaysia, Haad Yai, Thailand, 8-10 September 1983*, P.307-322.

Charusiri, P., Daorerk, V., Archibald, D., Hisada, K., & Ampaiwan, T. (2002). *Geotectonic evolution of Thailand: A new synthesis, Journal of Geological Society of Thailand* (Vol. 1).

Chonglakmani, C., Fontaine, H., & Vachard, D. (1983). A Carboniferous - Lower Permian (?) Section in Chon Daen Area, Central Thailand. *Conference on Geology and Mineral Resources of Thailand, Bangkok, 19-28 November 1983*, p. 16-20.

Chonglakmani, C., & Sattayarak, N. (1978). Stratigraphy of the Huai Hin Lat Formation (Upper Triassic) in Northeastern Thailand, in Nutalaya, P.(ed.), Proc.3 rd. *Regional Conference on Geology, and Mineral Resources of Southeast Asia, Bangkok, Thailand.*, P. 739-762.

Crow, M. J., & Khin Zaw. (2011). Metalliferous Minerals, The Geology of Thailand. *The Geological Society, London*, p. 459-492.

Cumming, G. V., James, R., Salam, A., Zaw, K., Meffre, S., Lunwongsa, W., & Nuanla-Ong, S. (2008). *Geology and mineralization of the Chatree epithermal gold-silver deposit, Phetchabun Province, Central Thailand.*

Department of Mineral Resource. (1989). Magnetic Anomaly Map of Thailand (Residual Total Field). *Scale 1:1,000,000, Department of Mineral Resources, Bangkok, Thailand.*

Department of Mineral Resource. (1999). Geological map of Thailand, 1:1,000,000. *Geological Survey Division, Department of Mineral Resources, Bangkok, Thailand.*

Department of Mineral Resource. (2013). Geological Map of Thailand, 1:250,000.

Department of Mineral Resource, Ministry of Natural Resources and Environment, Bangkok, Thailand., http//.www.dmr.go.th.

Department of Mineral Resources. (2014). Geology of Thailand: Department of Mineral Resources, Ministry of Natural Resources and Environmental, Bangkok, Thailand,. 508.

Diemar, M. G., & Diemar, V. A. (1999). *Geology of the Chatree epithermal gold deposit, Thailand*.

Diemar, M. G., Diemar, V. A., & Udompornwirat, S. (2000). The Chatree Epithermal Gold-Silver Deposit, Phichit-Phetchabun Provinces, Thailand. *Symposium on Mineral, Energy and Water Resources of Thailand : Towards the year 200, October 28-29, 1999, Bangkok, Thailand*(p. 423-428).

Gemmell, J. B. (2007). Hydrothermal Alteration Associated with the Gosowong Epithermal Au-Ag Deposit, Halmahera, Indonesia: Mineralogy, Geochemistry, and Exploration Implications. *Economic Geology, Society of Economic Geology Inc., Vol. 102*, p. 893-922.

Gifkins, C., McPhie, J., & Allen, R. (2002). Pumiceous rhyolite paperite in ancient submarine volcanic succession. *Journal of Volcanology and Geothermal Research, V.114*, p. 181-203.

Gifkins, C. C. (2001). Submarine volcanism and alteration in the Cambrian, Northern Central Volcanic Complex, Wesern Tasmania. *PhD. thesis, (unpublished), University of Tasmania*, 335 p.

Gifkins, C. C., Allen, R. L., & McPhie, J. (2005). Apparent welding textures in altered pumice-rich rocks. *Volcanology and Geothermal Research, 142*, P.29-47.

Hahn, L. (1982). Stratigraphy and marine ingressions of the Mesozoic Khorat Group in Northeastern Thailand. *Geologisches Jahrbuch, Reihe B, 43*, p. 7-35.

Hara, H., Kon, Y., Usuki, T., Y., L. C., Kamata, Y., Hisada, K., . . . Charusiri, P. (2013). U-Pb ages of detrital zircons within the Inthanon Zone of the Paleo-Tethyan subduction zone, northern Thailand: new constraints on accretionary age and arc activity. *Journal of Asian Earth Science, V. 74*, p. 50-61.

Hedenquist, J., Arribas, A., & Gonzalez-Urien, E. (2000). Exploration for Epithermal Gold Deposits. *Reviews in Economic Geology, 13*, 245-277.

Heggemann, H., Helmcke, D., & Tietze, K. W. (1994). Sedimentary Evolution of the Mezosoic Khorat Basin in Thailand. *Zbl. Geol. Palaont, V. 1*, p. 1267-1285.

Henley, R. W., & Ellis, A. J. (1983). Geothermal Systems Ancient and Modern: A Geochemical Review. *Earth Science Review, V. 19*, p. 1-50.

Hinthong, C. (1981). Geology and Mineral Resources of Changwat Phranakhon Si Ayutthaya (ND47-8), Scale 1:250,000. *Department of Mineral Resource, Ministry of Natural Resources and Environment, Bangkok, Thailand.*

Irvine, T. N., & Baragar, W. R. A. (1971). A guide to the chemical classification of the common volcanic rocks. *Canadian Journal of Earth Science, V. 8*, p. 523-548.

Ishikawa, Y., Sawagushi, T., Iwaya, S., & Horiuchi, M. (1976). Delineation of prospectiong targets fo Kuroko deposits based on modes of volcanism of underlying dacite and alteration halos. *Mining Geology, Vol. 26*, p. 105-117.

James, R., & Cumming, G. V. (2007). Geology and Mineralization of the Chatree Epithermal Au-Ag deposit, Phetchabun Province, Central Thailand. *International Conference on Geology of Thailand: Towards Sustainable Development and Sufficiency Economy (GEOTHAI'07)*, P. 378-390.

Janousek, V., Farraw, C., Erban, V., & Moyen, J.-F. (2019). A program for recalculation of geochemical data from igneous and metamorphic rocks. *Geochemical Data Toolkit for Windows, http://www.gcdkit.org, Version 6.0.*

JANOUŠEK, V., FARROW, C. M., & ERBAN, V. (2006). Interpretation of Whole-rock Geochemical Data in Igneous Geochemistry: Introducing Geochemical Data Toolkit (GCDkit). *Journal of Petrology, 47*(6), 1255-1259. doi:10.1093/petrology/egl013

Jungyusuk, N., & Khositanont, S. (1992). Volcanic rocks and associated mineralization in Thailand. *National Conference on "Geologic Resources of Thailand: Potential for Future Development", Department of Mineral Resources, Rama VI Rd., Bangkok, Thailand*, P. 522-538.

Jutzeler, M., McPhie, J., & Allen, S. R. (2014). Facies architecture of a continental, below-wave-base volcaniclastic basin: TheOhanapecosh Formation, Ancestral Cascades arc (Washigton, USA). *GSA Bulletin; March/April 2014, V. 126; No. 3/4*, p. 352-376. doi:doi: 10.1130/B30763.1

Kamvong, T., Charusiri, P., & Intasopa, S. B. (2006). Petrochemical Characteristics of Igneous Rocks from the Wong Pong Area, Phetchabun, North Central Thailand: Implications for Tectonic Setting. *Journal of Geological Society of Thailand, No. 1.*, P. 9-26.

Kamvong, T., Khin Zaw, & Harris, A. (2006). Geology and geochemistry of the Phu Lon copper-gold skarn deposit at the northern Loei Fold Belt, Northeast Thailand. *AESC2006, Melbourne, Australia*, p.1-9.

Khin Zaw, Kamvong, T., Khositanont, S., & Mernagh, T. P. (2011). Oxidized vs. Reduced Cu-Au Skarn Formation and Implication for Exploration, Loei and Troung Son Fold Belt, SE Asia. *International Conference on Geology, Geotechnology and Mineral Resources of Indochina (GEOINDO 2011), 1-3 December 2011, Khon Kean, Thailand*, p. 97-100.

Khin Zaw, Kamvong, T., Khositanont, S., Stein, H., Vasconcelos, P., & Goldding, S. (2009). Proceedings of the Tenth Biennial SGA Meeting, Townsville, August, 2009, Townsville, Australia.

Khin Zaw, Meffre, S., Kamvong, T., Khositanont, S., Stein, H., Vasconcelos, P., & Goldding, S. (2009). Geochronological and metallogenic framework of Cu-Au skarn deposits along Loei Fold Belt, Thailand and Lao PDR. *Proceeding of the 10th Biennial SGA meeting, Townsville, Australia, 17-20 Aug*, p.309-311.

Khin Zaw, Meffre, S., Lai, C. K., Burrett, C., Santosh, M., Graham, I., . . . Cromie, P. (2014). Tectonic and metallogeny of mainland Southeast Asia - A review and contribution. *Gondwana Research, 26*, p. 5-30.

Khin Zaw, Rodmanee, T., Khositanont, S., Thanasuthipitak, T., & Ruamkid, S. (2007). Geology and genesis of Phu Thap Fah gold skarn deposit, Northeastern Thailand: Implications for reduced gold skarn formation and mineral exploration. *GEOTHAI'07 International Conferance on Geology of Thailand: Towards Sustainable Development and Sufficiency Economy*, p. 93-95.

Khositanont, S., Zaw, K., Meffre, S., Panjasawatwong, Y., Ounchanum, P., & Thanasuthipitak, T. (2013). Geotectonic and geochonology of volcano-plutonic rocks in the Loei-Phetchabun Fold Belt. *The 2nd Lao-Thai Technical Conferance on Geology and Mineral Resources, January 17-18, 2013*, p. 81-95.

Large, R. R., Gemmell, J. B., Paulick, H., & Huston, D. L. (2001). The Alteration Box

Plot: A simple approach to under standing the relationship between alteration mineralogy and lithogeochemistry associated with volcanic-hosted massive sulfide deposits. *Economic Geology, Vol. 96*, p. 957-971.

Le Bas, M. J., Le Meitre, R. W., & Streckeisen, A. (1989). A chemical classification of volcanic rocks base on the total alkaline-silica diagram. *Journal of Petrology 27*, p. 745-750.

Madeisky. (1996). A lithogeochemical and radiometric study of hydrothermal alteration and metal zoning at the Cinola epithermal gold deposit. *Geology and ore deposits of the American Cordillera, Queen Charlotte Islands, British Columbia. In: Coyner, A.R., Fahey, P.L. (Eds.), V. 3*, 1153-1185.

Madeisky, & Stanley, C. R. (1993). Lithogeochemical Exploration of Metasomatic Zones Associated with Volcanic-Hosted Massive Sulfide Deposits Using Pearce Element Ratio Analysis. *International Geology Review, 35:12*, p. 1121-1148. doi:DOI: 10.1080/00206819309465580

Manaka, T., Khin Zaw, Meffre, S., Vasconcelos, P., & Golding, S. (2014). *The Ban Houayxai epithermal Au–Ag deposit in the Northern Lao PDR: Mineralization related to the Early Permian arc magmatism of the Truong Son Fold Belt* (Vol. 26).

McDonough, W. F., & Sun, S. S. (1995). The composition of the Earth. *Chemical Geology, v. 120*, p. 223-253.

McPhie, J., & Allen, R. (2003). Facies architecture of mineralised submarine volcanic sequences: Cambrian Mount Read volcanics, West Tasmania. *Economic Geology, V. 87*(p. 587-596).

McPhie, J., Doyle, M., & Allen, R. (1993). Volcanic textures : A guide to the interpretation of textures in volcanic rocks. *Centre for Ore Deposit and Exploration Studies, University of Tasmania*, 198 P.

Meesook, A., Suteethorn, V., Chaodumrong, P., Teerungsigul, N., Sardsud, A., & Wongprayon, T. (2002). Mesozoic rock of Thailand: A Summary. *The Symposium on Geology of Thailand, 26-31 August 2002, Bangkok, Thailand*, p. 82-94.

Metcalfe, I. (1984). Stratigraphy, palaeontology and palaeogeography of the Carboniferous of Southeast Asia. *Memoirs of the Geological Society of France, 147*, 107-118.

Mitchell, A. H. G., & Garson, M. S. (1981). Mineral deposits and global tectonic settings. *Academic Press, A Subsidiary of Harcourt Brace Jovanovich, Publishers, London, New York, Sydney, Sanfracisco*, 405 p.

Morrison, G., J. Rose, W., & Jaireth, S. (1991). *Geological and geochemical controls on the silver content (fineness) of gold in gold-silver deposits* (Vol. 6).

Norman, M. B. (1974). Improved techniques for selective staining of feldspar and other minerals using amaranth. *Journal of Research of the U.S. Geological Survey, V.2*, P.73-79.

Paipana, S. (2014). Geology and mineralization characteristics of Bo Thong Antimony ± Gold deposit, Chonburi Province, eastern Thailand (BSc (Hons) Thesis). *ARC Center of excelence in ore deposits (CODES), University of Tasmania, Hobert, Australia*, 100 p.

Panjasawatwong, Y., Khin Zaw, Chantaramee, S., Limtrakun, P., & Pirarai, K. (2006). *Geochemistry and tectonic setting of the Central Loei volcanic rocks, Pak Chom*

area, Loei, northeastern Thailand (Vol. 26).

Pearce, J. A., & Norry, M. J. (1979). Petrogenetic implication of Ti, Zr, Y and Nb variations in volcanic rocks. *Contributions to Mineralogy and Petrology, v. 69*, p. 33-47.

Poppe, L. J., Paskevich, V. F., Hathaway, J. C., & Blackwood, D. S. (2002). A Laboratory Manual for X-ray Powder Diffraction. *U.S. Geological Survey Open-File Report 01-041, U.S. Geological Survey, Coastal and Marine Geology Program*, 88 P.

Racey, A., Goodall, J. G. S., Love, M. A., Polachan, S., & Jones, P. D. (1994). New age data for the Mesozoic Khorat Group of Northeast Thailand. *Proceedings of the International Symposium on: Stratigraphic Correlation of Southeast Asia, Bangkok, Thailand*, p. 245-252.

Reynoles, J. (1992). X-ray diffraction studies of Illite/Smectite from rock, <1 micron rondomly oriented powders, and <1 micrron oriented powder aggreegates: The absence of laboratory-induced artifacts. *Clay and Clay minerals, V. 40, No.4*, p. 387-396.

Salam, A. (2013). A Geological, Geology and Metallogenic Study of The Chatree Epithermal Deposit, Phetchabun Province, Central Thailand. *PhD. thesis, (unpublished), University of Tasmania.*, 365 P.

Salam, A., Khin Zaw, Meffre, S., McPhie, J., & Lai, K. (2014). *Geochemistry and geochronology of the Chatree epithermal gold–silver deposit: Implications for the tectonic setting of the Loei Fold Belt, central Thailand*.

Sattayarak, N. (1983). Review of the continental Mesozoic stratigraphy of Thailand. *Workshop on Stratigraphic Correlation of Thailand and Malaysia, Haad Yai, Thailand, Haad Yai, Thailand*, p. 127-148.

Sattayarak, N., Srikulwong, S., & Pum-Im, S. (1989). Petroleum Potential of the Triassic Pre-Khorat Intermontane Basin in Northeastern Thailand. *Proceeding International Symposium on Intermontane Basins, Chiang Mai, Thailand.*, P. 43-58.

Simmons, S. F., White, N. C., & John, D. A. (2005). Geological Characteristics of Epithermal Precious and Base Metal Deposits. *Economic Geology, 100th Anniversary Volume*(Society of Economic Geology, Inc), p. 485-522.

Sun, S. S., & McDonough, W. F. (1989). Chemical and Isotopic systematics of oceanic basalt: Implication for mantle composition and processes. In: Saunders, A.D., Norry, M.J. (Eds.), Magmatism in the Ocean Basin. *Geological Society of London Special Publication*, p. 313-345.

Tangwattananukul, L., & Ishiyama, D. (2017). *Characteristics of Cu-Mo Mineralization in the Chatree Mining Area, Central Thailand: Cu-Mo mineralization in Chatree deposit, Thailand* (Vol. 68).

Tate, N. M. (2005). Discovery, geology and mineralization of the Phu Kam copper-gold deposit Lao People's Democratic Replublic. *In: Mao JW, and Bieerlein F.p., (eds), Mineral Deposit Reserch: Meeting the Global Challenge: Proceedings of the Eighth Biennial SGA Meeting, Beijing, China, 18-21 August 2005, Vol. 2*, p. 1077-1080.

Thompson, R. N. (1982). British Tertiary Volcanic Province. *Scottish Journal of Geology, v. 18*, p. 49-107. doi:https://doi.org/10.1144/sjg18010049

Tulyatid, J. (2001). Application of Airborne Geophysical Data on the Mapping of

Suture Zones and Mellogenic Provinces of Thailand. *Technical report (unpublished), Economic Geology Division, Department of Mineral Resources, Thailand, No. EGD 12/2001*, 42 pp.

Warren, I., Simmons, S. F., & Mauk, J. L. (2007). Whole-rock Geochemistry Techniques for Evolution Hydrothermal Alteration, Mass Changes and Compositional Gradients Associated with Epithermal Au-Ag Mineralization. *Society of Economic Geologists, Economic Geology, V. 102*(p. 923-948).

White, N. C., & Hedenquist, J. W. (1995). Epithermal gold deposits. Styles, characteristics and exploration. *Society of Economic Geology, Newsletter, No. 23*, p.1-9.

Winchester, J. A., & Floyd, P. A. (1977). Geochemical discrimination of different magma series and their differentiation products using immobile elements. *Chemical Geology, V. 20*, p. 325-343.

Wisedsind, W., Kiatwongchai, T., & Hatch, D. (1994). Airborne geophysical survey interpretation of Phetchabun study area: Changwat Phetchabun, Phichit, Lopburi and Nakorn Sawan, Thailand. *Economic Geology report (Unpublished), Economic Geology Division, Department of Mineral Resources, No. 6/1994*, 199 pp.

VITA

NAME   TANAD SOISA

DATE OF BIRTH   19 Jan 1980

PLACE OF BIRTH   Buriram Province

**INSTITUTIONS
ATTENDED**   Bachelor Degree, Khon Kaen University

HOME ADDRESS   103/53 M.7, Thanyaluck Village, Clongloung District,
                             Phathumthani, Thailand 12120.